Evaluation of Sleep and Sleep Disorders using Non-contact Technologies

Thesis submitted in partial fulfillment
of the requirements for the degree of
"DOCTOR OF PHILOSOPHY"

by

Eliran Dafna

Submitted to the Senate of Ben-Gurion University
of the Negev

תאריך לועזי

09.03.2017

Beer-Sheva

Evaluation of Sleep and Sleep Disorders using Non-contact Technologies

Thesis submitted in partial fulfillment
of the requirements for the degree of
"DOCTOR OF PHILOSOPHY"

by

Eliran Dafna

Submitted to the Senate of Ben-Gurion University
of the Negev

Approved by the advisor: Dr. Yaniv Zigel, , 9/3/2017
Approved by the Dean of the Kreitman School of Advanced Graduate Studies

תאריך לועזי

09.03.2017

Beer-Sheva

This work was carried out under the supervision of

Dr. Yaniv Zigel

In the Department of Biomedical Engineering

Faculty of Engineering Sciences

Research-Student's Affidavit when Submitting the Doctoral Thesis for Judgment

I___**Eliran Dafna**__, whose signature appears below, hereby declare that
(Please mark the appropriate statements):

_**X**_ I have written this Thesis by myself, except for the help and guidance offered by my Thesis Advisors.

_**X**_ The scientific materials included in this Thesis are products of my own research, culled from the period during which I was a research student.

_**X**_ This Thesis incorporates research materials produced in cooperation with others, excluding the technical help commonly received during experimental work. Therefore, I am attaching another affidavit stating the contributions made by myself and the other participants in this research, which has been approved by them and submitted with their approval.

Date: _09.03.2017___ Student's name: ___Eliran Dafna__ Signature: ____________

Affidavit

The paper entitled "Breathing and Snoring Sound Characteristics during Sleep in Adults" was written equally by me and my colleague Asaf Levartovsky from the Faculty of Health Sciences, Ben-Gurion University of the Negev, and with the help of our academic advisors Dr. Yaniv Zigel and Prof. Ariel Tarasiuk. In this paper, we showed that using a breathing/snore detector, we were able to examine objectively the characteristics of breathing/snoring sounds during sleep. Moreover, we explored the effect of patients' gender, age, and body mass index on breathing parameters, and the variation of those parameters across sleeping time.

My share in this paper was: Collection of data and establishment of the sleep/respiratory database used in this study. I developed the breathing/snoring sound detector (Paper I) as the ground stage of the thesis. Using this detector, I extracted thousands of snoring and breathing events from hundreds of patients. From each snoring event, I formulated and computed several snoring properties to be later compared and analyzed to better understand the influence of anthropometric parameters as well as sleep pattern on snoring properties. I was also involved in the statistical analysis of the data, figure graphical design, and writing the paper.

Asaf's share in this paper was: Database management, statistical analysis of the data, tables and figure graphical design, and writing the paper.

Yaniv Zigel and Ariel Tarasiuk: As our academic advisors, they led and supported us through the entire study process. Their knowledge, experience, and insights definitely improved the research's hypothesis and objectives to produce significant findings. In addition, they participated in writing the paper.

Abstract

Polysomnography (PSG) is the gold standard for sleep evaluation. This method requires a full night laboratory stay and subjects are connected to numerous electrodes and sensors, which are attached on the patient's body. PSG is time-consuming, tedious, and costly due to signals complexity and the need for technical expertise. In recent years, extensive effort has been devoted to seeking alternative simple cost-effective technologies for objective sleep-wake evaluation to increase accessibility in sleep disorders diagnosis.

We hypothesize that sleep-wake activity can be estimated using audio signal analysis of breathing sounds, which are altered by changes in ventilation and upper airway patency. The objectives of our work are: 1) to develop a breathing sound analysis algorithm for distinguishing between sleep and wake phases using non-contact technology; 2) to reliably estimate sleep quality parameters such as total sleep time, sleep latency, sleep efficiency, wake after sleep onset time, and arousal index; and 3) to validate the proposed algorithms in comparison to PSG.

Overall, 150 patients were prospectively recorded at the Sleep-Wake Disorder Unit at Soroka University Medical Center. Nocturnal respiratory sounds were acquired during routine PSG study; an ambient microphone (RODE NTG1) was installed 1 meter above the patient's head.

This study presents a pioneering approach for determining sleep-wake pattern using non-contact audio-based signals. We developed a breathing sound (snoring) detector that was trained and validated on a comprehensive database. Based on acoustic features calculated from both time and spectra domains, an accuracy rate of above 98% was registered.

We explored the relation between breathing acoustics and a variety of anthropometric parameters and sleeping conditions, to develop a robust sleep evaluation system. We found that by analyzing breathing sounds a reliable estimation of sleep quality parameters can be achieved. Epoch-by-epoch accuracy rate for the validation study was 83.3% with sensitivity of 92.2% (sleep as sleep), specificity of 56.6% (awake as awake). Comparing sleep quality parameters of the proposed system and PSG demonstrates average error of sleep latency, total sleep time, wake after sleep onset, and sleep efficiency of 16.6 min, 35.8 min, and 29.6 min, and 8%, respectively. This study highlights the potential of breathing sound analysis to measure sleep in research and clinical situations.

Keywords: sound analysis, breathing, sleep, machine learning, signal processing.

Acknowledgements

I would like to show my appreciation to Dr. Yaniv Zigel, whose being my supervisor through the entire process; his expertise ideas and knowledge were a significant factor to the success of our research.

To Prof. Ariel Tarasiuk, for his time, patience, guidance and help throughout this study and his contribution in the making process of papers published as part of my thesis work, it has been a huge honor working with him.

Additional thanks to Bruria Friedman, an important contact at the 'Sleep-Wake Disorder Unit' of Soroka university medical centre, for her collaboration, great help, and understanding.

I would would like to thank Matan Halevi and Dvir Ben Or and Tal Rosenwine for their knowledge, assistance and time spent in the lab on this research.

And finally, I wish to express my gratitude and my love to my wife Hofit for her tremendous support and understanding.

Table of contents

Introduction

Polysomnography (PSG) is currently considered the gold standard for sleep evaluation [1]. This method requires a full night laboratory stay and subjects are connected to numerous electrodes and sensors that are attached on the patient's body. Time series data are aggregated, processed, and visually examined or mathematically transformed in order to reveal insights about sleep-wake states and many aspects of physiology. Moreover, in routine sleep diagnostic procedures, sleep scoring is done manually by applying complex and visual scoring rules simultaneously on multiple signals acquired by applying contact sensors, e.g., electroencephalography (EEG), electrooculography (EOG), electromyography (EMG), electrocardiography (ECG), and respiratory activity [1, 2]. PSG is time-consuming, tedious, and costly due to complexity and the need for technical expertise.

Currently, the biomedical engineering field of sleep disorders evaluation is on a "fast track" towards ambulatory sleep medicine [3-5]. In recent years, extensive effort has been devoted to seeking alternative simple cost-effective technologies for objective sleep-wake evaluation and even rapid eye movement (REM) detection to increase accessibility in sleep disorders diagnosis. These new technologies are based on reduced-channels and sensors, and sophisticated computer-based algorithms [3, 4, 6-9]. Under the assumption that movement is associated with wake phase and lack of movement implies a sleep phase, clinicians and researchers have attempted to measure the binary presence of sleep or wake phases by measuring wrist movements using actigraphy [5, 10, 11]. Field-based activity monitoring devices are increasingly used as simple and cheap accelerometer-based devices [12-14]. Montgomery-Downs et al. [13] recently reported that this new technology has specificity limitations similar to those of a traditional actigraphy device. These devices consistently misidentify wake as sleep and thus overestimate both sleep time and quality.

It was long-established that central control of ventilation and upper airway patency are strongly affected by transitions from sleep to wake and vice versa [4, 15, 16]. During sleep, there is a considerable increase of upper airway resistance [4, 17, 18] due to decreased activity of the pharyngeal dilator muscles [19, 20]. This elevated resistance is reflected by amplification of air-pressure oscillations in the upper airways during breathing. These air-pressure oscillations are perceived as breathing sounds during sleep [21]. In contrast, during wakefulness, there is an increase in activity of the upper airway dilating muscles, hence decreased upper airway resistance and airway oscillations. Another interesting phenomenon occurs during REM which is associated with limbs paralysis during sleep in order to prevent us from harming ourselves during dreams. REM, also known as paradoxical sleep, is where the body is sleeping while the brain keeps running as if in a wake state.

We hypothesize that sleep-wake activity can be estimated using audio signal analysis of breathing sounds, which are altered by changes in ventilation and upper airway patency. The main objective of this work is to present a new concept and to develop a non-contact audio-based system for sleep evaluation. In order to do so, three milestones must be achieved in the following order: 1) whole night breathing and body movement detection, 2) exploring the relations between breathing sounds to the sleep-wake phases and regarding anthropometric parameters, and 3) training a learning machine to be able to differentiate between the sleep and wake episodes based on the acoustic contents and the properties of the sounds generated during the night. To the best of our knowledge, there is no technology available to estimate sleep-wake pattern using a non-contact inexpensive sensor. This study describes a pioneering attempt to estimate sleep using only audio signal analysis recorded by a non-contact microphone and a digital audio recorder.

Experimental setup

For the objectives mentioned above, data acquisition took place at the Sleep Wake Disorder Unit at Soroka University Medical Center. In addition to the routine PSG test, we installed an ambient microphone in the patient's bedroom, attached to the ceiling and hanging about one meter above the patient's head. The audio signals and the PSG signals along with the sleep expert's manual sleep scoring, are stored and aggregated to establish the database used for this study. Figure 1 presents the setting in the Sleep Wake Disorder Unit at Soroka University Medical Center. Overall, 150 patients referred for routine PSG test were recorded. See Table 1 for subjects' characteristics, and Table 2 for subjects' sleep quality parameters.

Figure 1. The setting in the sleep-wake disorder unit at Soroka University Medical Center. On the left, the patient's bedroom and the additional microphone. On the right, the digital audio recorder located in the technician’s control room.

Table 1. Subject anthropometric parameters.

Gender (M/F)	Age (yr)	BMI (kg/m^2)	ESS (score)	AHI (events/hr)
97/53	53.8±15.1 (19–86)	31.5±5.6 (16.8–52.1)	9.9±6.0 (0–24)	18.4±17.4 (0.0–84.1)

BMI – body mass index, ESS – Epworth sleepiness scale, AHI – apnea hypopnea index. All values are mean ± SD (range).

Table 2. Subjects' sleep quality parameters.

TIB (min)	TST (min)	SL (min)	SE (%)	WASO (min)	AwI (events/hr)
424.5±53.1	336.5±57.0	33.3±26.8	78.0±13.3	49.1±43.2	1.3±1.0
(285.0–503.0)	(148.5–432.0)	(0.5–125.0)	(30.9–97.7)	(3.0–253.0)	(0.0–6.2)

TIB – Time in bed; TST – Total sleep time; SL – Sleep latency; SE – Sleep efficiency; WASO – Wake time after sleep onset; AwI – Awakening index. Values are mean ± SD (range) between subjects.

Publications derived from this study

During my PhD. studies, seven conference papers [22-28] and three journal papers [29-31] have been published during 2013–2016. Each paper concludes one of the above milestones and relies on accomplishment of the previous milestones.

1) Dafna Eliran, Tarasiuk Ariel, and Zigel Yaniv. "Automatic detection of whole night snoring events using non-contact microphone." *PloS one* 8.12 (2013): e84139.

In this paper [29], we showed that during sleep, airways resistance increases and therefore breathing sounds become more noticeable. Using a microphone pointed toward a patient's head from one meter above, a wide variety of breathing sound intensities can be captured including very quiet breathing (~20 dB) and very loud snores (>80 dB). This study showed that using audio signal processing and a novel algorithm, a high reliability of breathing detection is achieved (>98% detection rate). A typical example of the detector on one subject is presented in Figure 2.

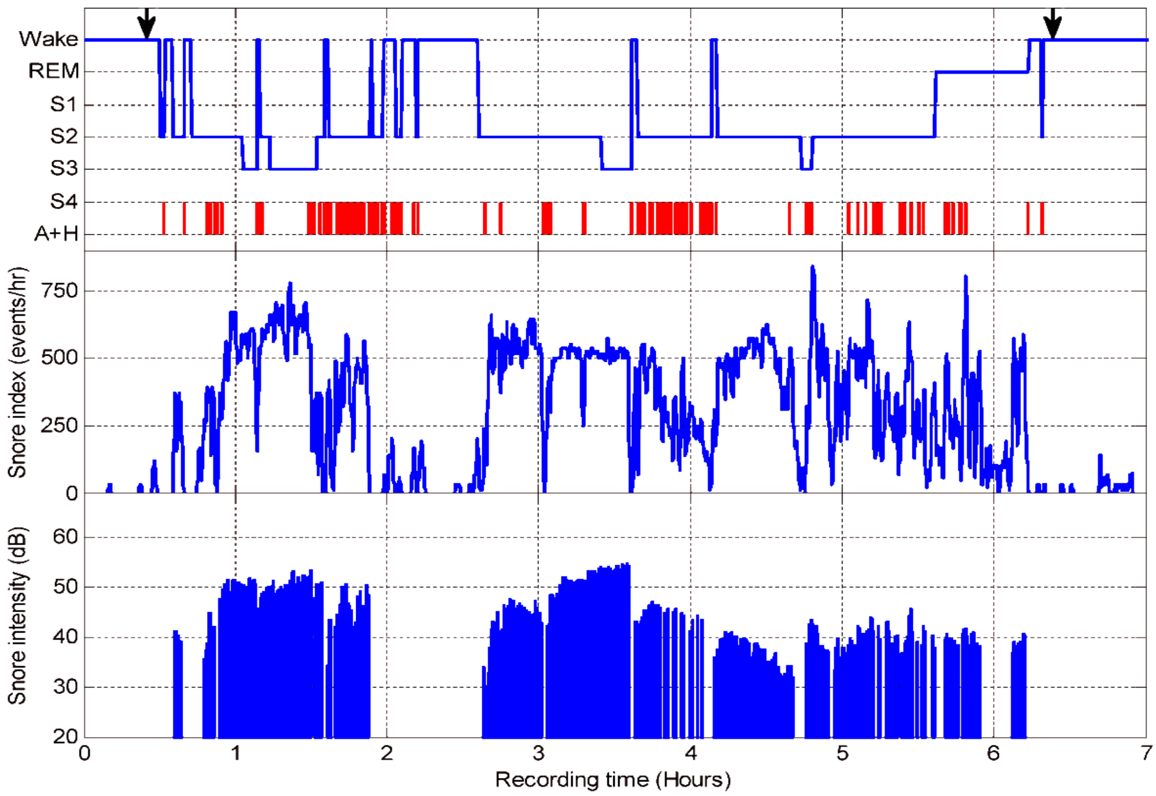

Figure 2. Example of whole-night snore index and snore intensity.
Upper panel – sleep stages throughout the night and apnea/hypopnea events (A+H) based on the PSG test. Middle panel – automatically detected and calculated snoring index (events/hr) per 30 second epoch. Lower panel – snore intensity (dB). Arrows indicate lights off and lights on, respectively. Data was collected from a 63-year-old woman (BMI=31, AHI=14). For this subject only, a snoring index of >240 events/hr is displayed [29].

<u>Methods:</u> Figure 3 shows the block diagram of the proposed breathing detector. The input of this detector is a whole night audio signal. This signal is first enhanced (in signal-to-noise ratio (SNR) manner) using an adaptive noise reduction algorithm to be able to detect very faint breathing sounds. This filter was specifically designed for this purpose of breathing sound enhancement based on several aspects and properties associated with breathing sounds. The next step is to detect suspected breathing events based on energy contents. Then, from each suspected event, acoustic features are extracted and fed into a classifier to discriminate between breathing and non-breathing events. Additional information can be found in the Appendix section.

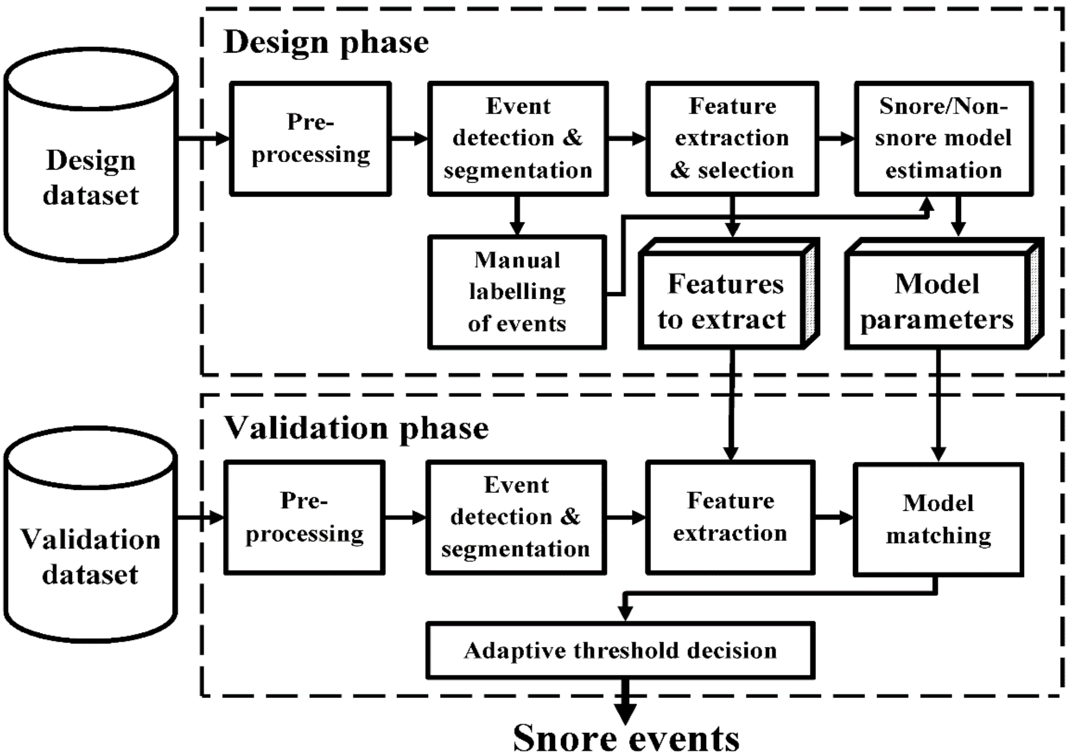

Figure 3. block diagram of the proposed breathing (snoring) detector [29].

2) Levartovsky Asaf, Dafna Eliran, Zigel Yaniv, and Tarasiuk Ariel. "Breathing and Snoring Sound Characteristics during Sleep in Adults." *Journal of Clinical Sleep Medicine: JCSM: official publication of the American Academy of Sleep Medicine* 12.3 (2016): 375-384.

In this paper [30], we showed that using the breathing/snoring detector mentioned above, we were able to examine objectively the characteristics of breathing/snoring sounds during sleep. Moreover, we explored the effect of patients' gender, age, and body mass index on breathing parameters, and the variation of those parameters across sleeping time. Analyses were performed on 121 patients who were referred to routine polysomnography test.

This unique approach is in contrast to earlier reports that used a sound level meter without an algorithm that can discriminate between relevant respiratory sounds and other noises. In both sexes snoring index and % snoring was higher in slow wave sleep (SWS), and men have a significantly higher snoring index and % snoring than women at all sleep stages. This finding is compatible with other reports, which described that snoring index was most prominent in SWS. However, our findings do not support earlier studies claiming that snoring intensity is higher in SWS. For more details, please see [30]. Figure 4 shows one of our findings regarding breathing and snoring index based on patient gender across sleeping time.

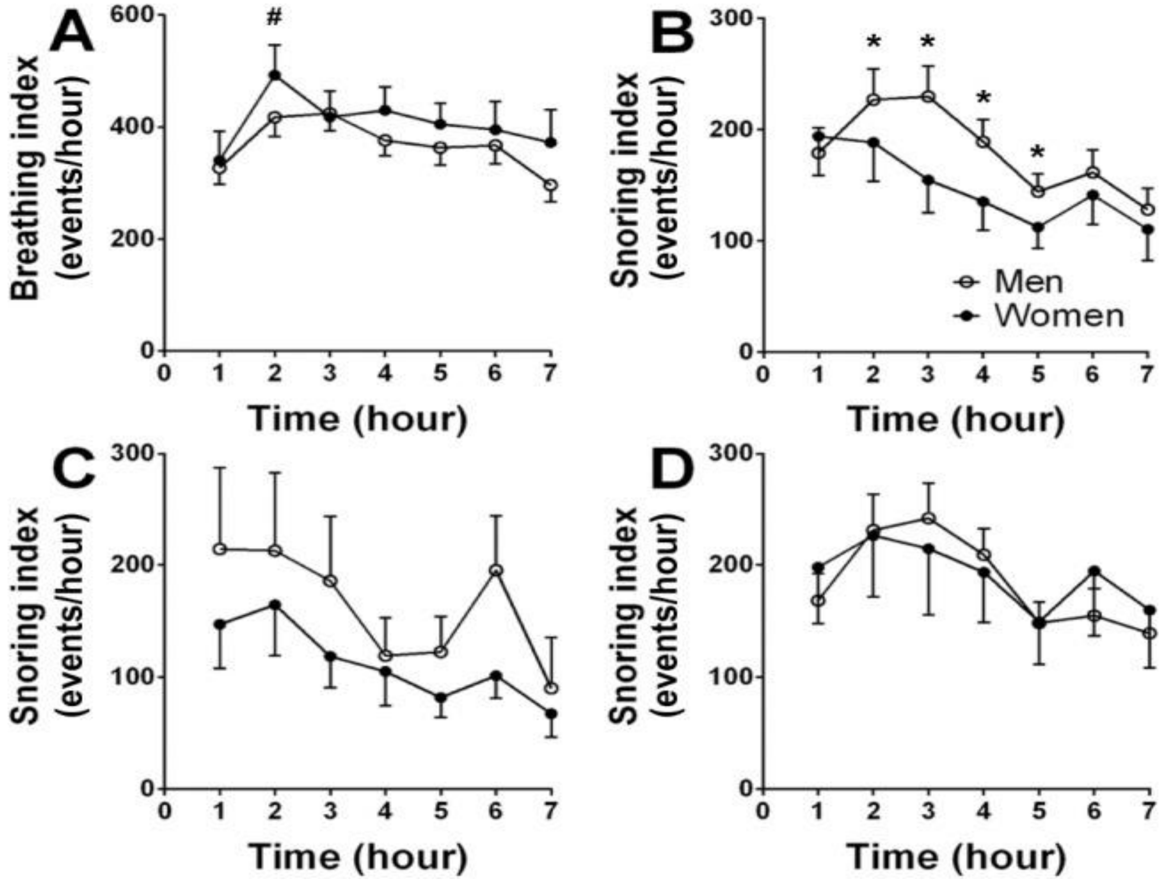

Figure 4. Breathing and snoring index for each hour of sleep.

(A) Breathing sound (> 20 dB) index of all subjects. (B) Snoring (> 50 dB) index of all subjects. (C) Snoring index of the comparison group. (D) Snoring index of the OSA group.

#significant change of breathing sound index between second and first hour of sleep in both sexes ($p = 0.04$); *significant sex differences ($p = 0.01$). Snoring index (B) significantly declined during sleep ($p < 0.01$). Significant differences were determined by two-way analysis of variance. Values are mean ± standard error of the mean [30].

This paper was equally written by me and my colleague Asaf Levartovsky from the Faculty of Health Sciences, Ben-Gurion University of the Negev.

Methods: Figure 5 shows the block diagram of the process to explore the effect of different parameters on snoring acoustics. Based on the detected breathing events, we divided our data into several subsets and ran statistical tests to determine if snoring is different in the divided subsets.

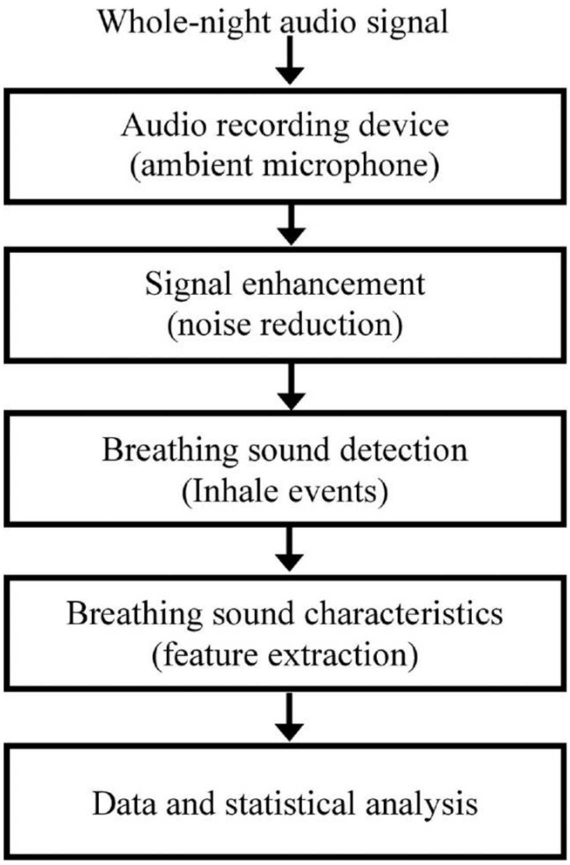

Figure 5. Block diagram of audio data handling and analysis [30].

3) Dafna Eliran, Tarasiuk Ariel, and Zigel Yaniv. "Sleep-wake evaluation from whole-night non-contact audio recordings of breathing sounds." *PloS one* 10.2 (2015): e0117382.

This paper [31] presents the desired objective of this Ph.D. thesis. Here, we showed that using the breathing/snoring sound analysis, a binary decision of sleep and wake states across the night can be reliably estimated. Using the sleep and wake pattern (sequence), an important clinical sleeping quality diagnosis (parameters) is achieved. These sleeping quality parameters include: total sleep time, sleep latency; the wakening duration during "sleeping time"; the sleep efficiency, which is ratio of sleep time and total time in bed; and the awakening counts during sleeping time. This paper generated a great impact on the sleep medicine society and was reviewed worldwide on the media as a "groundbreaking approach" and was recommended by the Faculty F1000Prime. Figure 6 shows a typical example of the sleep-wake likelihood score curve.

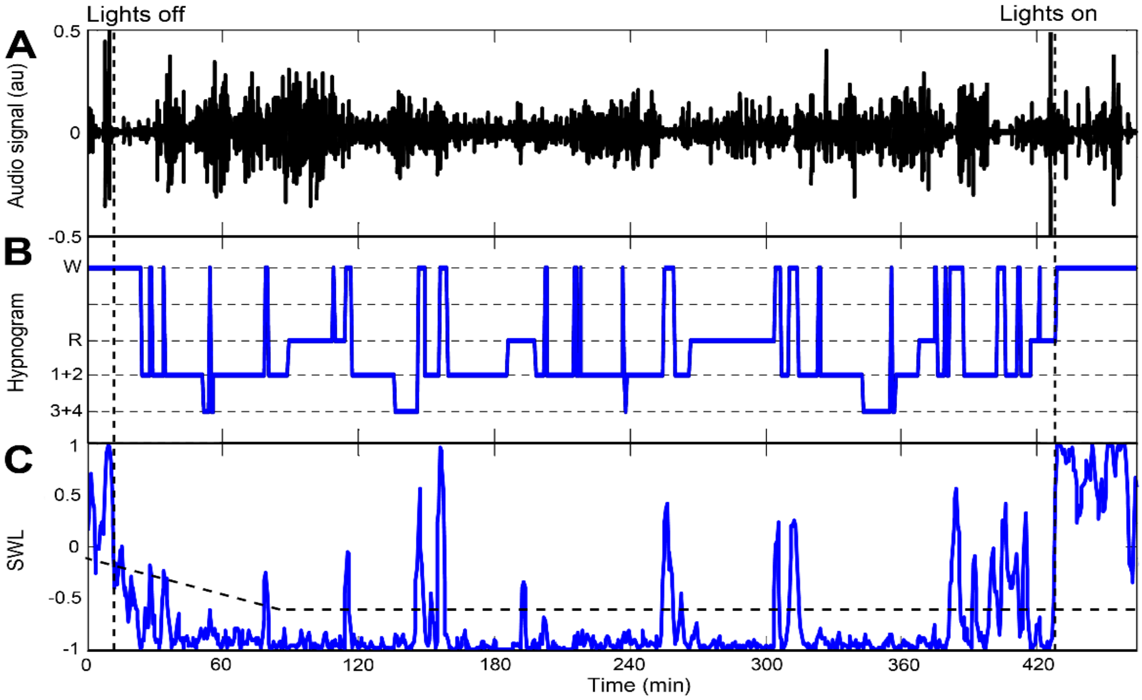

Figure 6. Example of sleep-wake likelihood (SWL) score curve.

(A) Audio signal of whole-night recording. (B) Hypnogram. (C) The estimated whole-night SWL score curve. SWL was calculated using the eight acoustic features fed into AdaBoost classifier. Higher values of SWL indicate increased likelihood towards wake state. When focusing on sleep and wake phases, note the similarity between the hypnogram (B) and the SWL (C). The horizontal dashed line represents the corresponding individual decision threshold over time. Data was collected from 52-year-old male, BMI 31 [31].

Methods: Figure 7 shows the block diagram of the proposed sleep-wake estimation. The input of this system is a whole night audio signal. This signal is first enhanced and breathing (snoring) events are located. From the detected breathing events acoustic features are extracted and fed into a time-series classifier (with two feedback delays). The output of the classifier is a "sleeping" likelihood score (curve for the entire night). This curve is then post-processed to produce a more realistic sleeping curve with individual adaptations. The outcome of the system is a sleep quality assessment clinical report. System design and validation were performed on 150 patients who were referred to routine polysomnography test. Additional information can be found in the Appendix section.

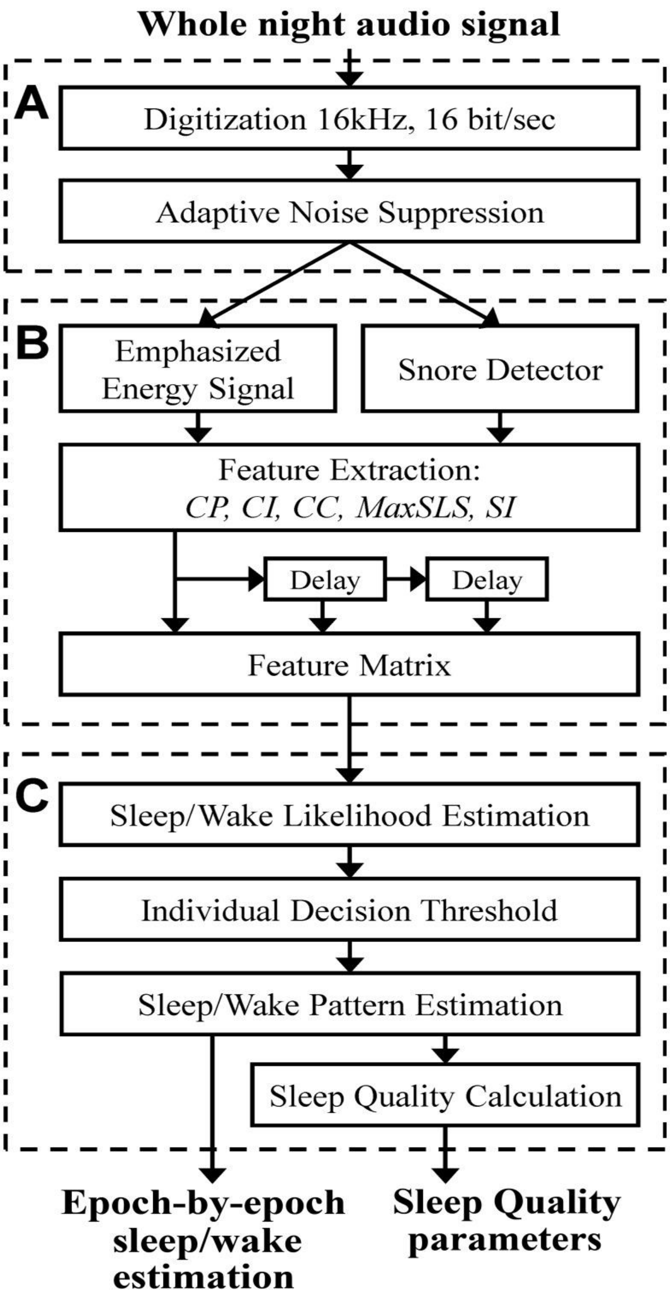

Figure 7. Block diagram of the proposed sleep-wake system [31].

Although these three papers conclude the entire Ph.D. thesis objectives, in a recent conference paper [22] at the IEEE EMBC 2016, we showed preliminary results that using audio analysis, the sleep and wake estimation can be extended into three **macro sleep stages (MSS)** including wake, REM, and non-REM phases with decent detection performances, presenting even a bigger impact approach. In this study, audio signals of 35 patients referred to a sleep laboratory were recorded and analyzed. An additional 178 subjects were used to train a probabilistic time-series model for MSS staging across the night.

The nine features extracted are designed to discriminate between the three classes of MSS: Wake, REM, and NREM. These features can be categorized into two types: breathing characteristics and noise characteristics.

Breathing characteristics features – Six breathing-related features were empirically designed in order to test our hypotheses regarding the differences in MSS. We applied the breathing detector described in paper [29] to effectively detect the events of interests.

1) Respiratory cycle duty – this feature measures the time proportion of breathing effort relative to the respiratory cycle duration. 2) Respiratory cycle period [31] – this feature measures the average respiratory cycle duration based on autocorrelation approach. 3) Respiratory cycle intensity [31] feature is determined by the value of the autocorrelation first peak. 4) Respiratory cycle consistency [31] – measures the homogeneity of the respiratory cycles. 5) Respiratory mean SNR feature – measures the average signal-to-noise ratio (dB scale) of all respiratory events detection. 6) Respiratory Frequency centroid – is the average frequency centroid of all breathing detected.

Non-breathing characteristics features – The hypothesis is that body movement is associated with wakefulness, i.e., the same assumption used in actigraphy devices. Moreover, REM is characterized by a paralyzed-limbs phenomenon, which prevents the patient from harming himself during dreaming; therefore, we hypothesize that REM epochs will contain fewer body movements. Three non-breathing-related features were empirically developed:

1) Non-breathing percentage feature is calculated as the ratio between all non-breathing detected durations combined relative to the 30s epoch duration. 2) Non-breathing 90% SNR feature represents the SNR value of the 10% upper percentile of all non-breathing detected. 3) Non-breathing frequency centroid feature is calculated in the same way as for the breathing frequency centroid.

The audio-based system was validated on 20 of the 35 subjects. System accuracy for estimating (detecting) epoch-by-epoch wake/REM/NREM states for a given subject is 74% (69% for wake, 54% for REM, and 79% NREM). Mean error (absolute difference) was 36±34 min for detecting total sleep time, 17±21 min for sleep latency, 5±5% for sleep efficiency, and 7±5% for REM percentage. These encouraging results are matched and even superior to other reduced channels technologies (contact sensors) [3, 5, 31-33]. This indicates that audio-based analysis can provide a simple and comfortable alternative method for ambulatory evaluation of sleep and its disorders.

In the following year I plan to elaborate these findings with a larger database including recording with at-home conditions and to statistically strengthen the results and to publish in a prestigious journal.

Papers

Automatic detection of whole night snoring events using non-contact microphone.

Dafna Eliran, Tarasiuk Ariel, and Zigel Yaniv.

PloS one 8.12 (2013): e84139.

Automatic Detection of Whole Night Snoring Events Using Non-Contact Microphone

Eliran Dafna[1], Ariel Tarasiuk[2], Yaniv Zigel[1]*

1 Department of Biomedical Engineering, Ben-Gurion University of the Negev, Beer–Sheva, Israel, 2 Sleep-Wake Disorders Unit, Soroka University Medical Center, and Department of Physiology, Faculty of Health Sciences, Ben-Gurion University of the Negev, Israel

Abstract

Objective: Although awareness of sleep disorders is increasing, limited information is available on whole night detection of snoring. Our study aimed to develop and validate a robust, high performance, and sensitive whole-night snore detector based on non-contact technology.

Design: Sounds during polysomnography (PSG) were recorded using a directional condenser microphone placed 1 m above the bed. An AdaBoost classifier was trained and validated on manually labeled snoring and non-snoring acoustic events.

Patients: Sixty-seven subjects (age 52.5±13.5 years, BMI 30.8±4.7 kg/m^2, m/f 40/27) referred for PSG for obstructive sleep apnea diagnoses were prospectively and consecutively recruited. Twenty-five subjects were used for the design study; the validation study was blindly performed on the remaining forty-two subjects.

Measurements and Results: To train the proposed sound detector, >76,600 acoustic episodes collected in the design study were manually classified by three scorers into snore and non-snore episodes (e.g., bedding noise, coughing, environmental). A feature selection process was applied to select the most discriminative features extracted from time and spectral domains. The average snore/non-snore detection rate (accuracy) for the design group was 98.4% based on a ten-fold cross-validation technique. When tested on the validation group, the average detection rate was 98.2% with sensitivity of 98.0% (snore as a snore) and specificity of 98.3% (noise as noise).

Conclusions: Audio-based features extracted from time and spectral domains can accurately discriminate between snore and non-snore acoustic events. This audio analysis approach enables detection and analysis of snoring sounds from a full night in order to produce quantified measures for objective follow-up of patients.

Citation: Dafna E, Tarasiuk A, Zigel Y (2013) Automatic Detection of Whole Night Snoring Events Using Non-Contact Microphone. PLoS ONE 8(12): e84139. doi:10.1371/journal.pone.0084139

Editor: Muhammad Khurram Khan, King Saud University, Saudi Arabia

Received April 10, 2013; **Accepted** November 12, 2013; **Published** December 31, 2013

Funding: This work was supported by the Israel Ministry of Industry, Trade and Labor - the Kamin Program, award no. 46168 to YZ and AT. These funders had no role in study design, data collection and analysis, decision to publish, or preparation of the manuscript.

Competing Interests: The authors have declared that no competing interests exist.

* E-mail: yaniv@bgu.ac.il

Introduction

Partial or complete collapse of the upper airway during sleep has different effects on the human body, ranging from noisy breathing (simple snoring) [1] to obstructive sleep apnea (OSA), which can lead to considerable cardiovascular morbidity [2,3]. Snoring is the most common symptom of sleep-disordered breathing. By age 60, snoring adversely affects 60% of men and 40% of women [4]. It is caused by the vibration of soft tissue in the upper airways involving anatomical structures such as the soft palate, uvula, and pharynx [5,6].

The most common method for evaluating snoring history uses self-report questionnaires [4,7,8]. The estimated prevalence of self-reported snoring in the general population extends over a wide range from 16% to 89% [9–13]. This prevalence depends on awareness, age, culture, and partner complaints [4,7,14]. Early work has shown a poor correlation between measured loudness of snoring and subjective appreciation by different observers. It was concluded that to a large extent snoring is "in the ear of the beholder" [4]. Thus, reliable snoring reporting cannot be made based solely on a patient's (or partner's) history of noisy respiration during sleep [8,11,15], or with sleep laboratory technician reports [4]. An additional limitation of questionnaires is that a large portion of the subjects respond that they "do not know" if they snore [10]. To overcome these limitations, some clinicians ask the patient to supply an audio recording of their snoring, for example, prior to snore reduction surgery or to avoid operating on a "snorer" when in fact the problem lies with the bed partner being disturbed by essentially normal nocturnal breathing noise [1].

One of the main goals of sleep medicine today is to improve accessibility to sleep-disordered breathing diagnosis and treatment. The gold standard for evaluating sleep-disordered breathing is the multichannel polysomnography (PSG) study [16]. PSG on snorers, with no additional complaints suggestive of sleep-disordered breathing, will be normal in up to 80% of studies [7,15]. However, due to difficulties associated with PSG, such as its long waiting list and costs, there is an urgent need for simple and reliable technology for snore detection and analysis. Audio signal analysis of snore sounds can be deployed in different tasks, such as assessment of the outcome of surgical treatment [17,18]. Recently several papers have proposed OSA detection systems [19] and apnea-hypopnea index (AHI) estimation based on whole-night audio recording of snoring [20,21]. Furthermore, in order to reliably evaluate the severity and variability of an individual's snore, the recording of an entire night is required. Hence, developing an automatic snore detection method to analyze full-night recordings in a timely and accurate manner would be advantageous.

A limited number of studies have addressed this issue of automatic detection and classification of snore signals, and even less is known about snore detection using ambient (non-contact) microphone technology. Several snore/non-snore classification methods have been suggested using different techniques to analyze snore sound events. These include pitch and formants, features regarding spectrum modeling such as Mel-frequency cepstral coefficients (MFCC), linear predictive coding (LPC) [22], and standard acoustic measures such as sound intensity [13]. Most of these studies were conducted without separate groups of subjects for their design and validation studies. Duckitt et al. [23] recorded sound with an ambient microphone from 6 subjects that was segmented into snoring episodes, breathing, duvet noise, and silence periods using hidden Markov models and spectral-based features. Cavusoglu et al. [24] proposed a method for snore detection involving 15 subjects for both design and validation study using a linear regression fed by sub-band spectral energy distributions processed by principal component analysis. Karunajeewa et al. [25] proposed a method for classifying snores and breathing sounds using the mean and covariance of four features extracted from time and spectral domains. Azarbarzin et al. [26] proposed an unsupervised snore sound extractor based on a fuzzy C-means clustering algorithm and achieved higher accuracy using a tracheal microphone, due to a higher signal-to-noise ratio (SNR) [27].

The need for an agreed upon approach to extract and analyze whole-night snoring sounds is of major importance to the field of sleep-disordered breathing. Snore sounds vary significantly; in some cases the snore sound may be soft, but in others it can be very loud [1,4,28–34]. Our study aimed to develop and validate a novel robust snore detection system (algorithm) using a non-contact technology. This detector is based on signal enhancement and features extracted from different domains as they have complementary information about snore/non-snore discrimination. The snore detection algorithm is based on three major steps: 1) Signal enhancement and segmentation, 2) Feature extraction that included specially designed novel features for characterizing snore events; the final features were selected using a comprehensive feature selection technique that automatically revealed the most prominent features, and 3) Detection of snore events using an AdaBoost classifier [35] that was trained using thousands of snore and non-snore events. The novelty of our proposed method is its automatic detection of every snore event from the whole-night audio recording using non-contact technology. Moreover, this approach includes comprehensive sets of features involving time and spectral domains, which were selected using a feature selection algorithm. In addition, we propose an objective score for quantifying snore intensity.

Methods

This article has online Methods Supporting File S1.

Setting

A university affiliated sleep–wake disorder center and biomedical signal processing laboratory. The Institutional Review Committee of the Soroka University Medical Center approved the study: protocol number 10621. Informed consent was obtained from all subjects.

Subjects

We prospectively recruited 67 consecutive adults (aged 19 to 87 years, 27/40 women/men) referred to the Sleep–Wake Unit at Soroka University Medical Center in Beer Sheva, Israel for routine polysomnographic (PSG) sleep-disordered breathing diagnosis, starting in February 2008. We selected the first 25 subjects (patients) for the system design (training) study. The remaining 42 subjects (beginning in May 2009) were included in the blind validation study.

PSG study

Prior to nocturnal in-laboratory PSG, all subjects completed a validated self-administered sleep questionnaire [3,36–38]. The Epworth Sleepiness Scale (ESS) was used to evaluate daytime sleepiness [39]. Overnight PSG was performed according to previously described methods [3,40]. Subjects reported to the laboratory at 20:30 and were discharged at 06:00 the following morning. They were encouraged to maintain their usual daily routine and to avoid any caffeine and/or alcohol intake on the day of the study. Shift workers did not perform the PSG study in the week following their shift duty. The PSG study included electroencephalography, electrooculography, and electromyography applied over the submental muscles and bilateral anterior tibialis muscles for detection of periodic limb movements, electrocardiography, respiratory activity (abdomen and chest efforts belt), oxygen saturation, and snore level intensity (Quest Technology 2700, Orlando, FL, USA). PSG scoring was done by a trained technician and underwent a second scoring by one of the investigators (AT). Apneas and hypopneas were scored according to the American Academy of Sleep Medicine criteria [16].

The experimental system

We have developed a system for snore detection that utilizes a non-contact microphone for audio signal recordings taken from a full night at a sleep laboratory. The acquired audio signals were further used to develop the snore detection algorithm. A digital audio recorder (Edirol R-4 Pro, Bellingham, WA, USA) with a directional microphone (RØDE, NTG-1, Silverwater, NSW, Australia) placed at a distance of 1 meter above head level was used for audio recording. An additional audio recorder (handy *Olympus LS-5*) was placed on the dresser beside the patient's head in the laboratory and used to validate the system in a non-laboratory setting. The audio signals were stored along with the PSG signals for later analysis. Each audio signal was synchronized with the PSG study at 15 ms resolution. The synchronization was performed via a cross-correlation technique between the PSG snore intensity level channel and the digital audio signal (after energy extraction). The main purpose was to synchronize all PSG channels to the digital audio signal, including hypnogram and respiratory effort channels, to support and assist the manual labeling of snore events. Fig. 1 shows the block diagram of the proposed snore detection algorithm for the design and validation phases of the study. In the snore detection algorithm, an adaptive noise reduction algorithm was applied for signal enhancement in a pre-processing stage. For system design, snore and non-snore events (see below) were manually labeled and used to train an

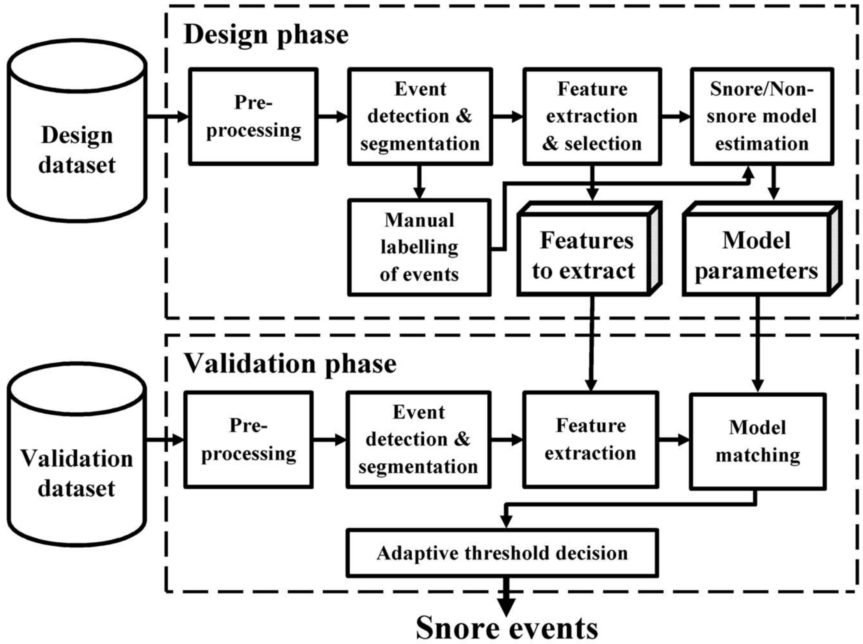

Figure 1. Block diagram of the study protocol. Upper panel – design phase ($n = 25$). Lower panel – validation phase ($n = 42$).
doi:10.1371/journal.pone.0084139.g001

AdaBoost classifier (see below) fed by acoustic features from time and spectral domains. Using a feature selection algorithm on the design group, the best features were selected and used in the validation phase as well.

The Snore Detection Algorithm

Pre-processing (Fig. 1). For design and validation phases, the acquired audio signals recorded in the sleep lab were digitized at a sampling frequency of 44.1 kHz, PCM, and 16 bits per sample, which is the minimum sampling rate of the audio recorder. All audio signals were down-sampled to 16 kHz, and each audio signal underwent an adaptive noise suppression (spectral subtraction) process based on the Wiener-filter. This process relies on automatically tracking background noise segments in order to estimate their spectra and subtracting them from the audio signal [41]. In this study, a noise spectral template was subtracted from each audio frame (40 ms). This template was initially estimated from the lowest energy frame of the first 10 sec of the audio signal and was updated during the adaptive noise suppression process. Each frame's frequency component was suppressed by a specific value (suppression factor) derived from the noise spectral template, and it was limited to the range [0, −25 dB] in order to prevent a major distortion when low SNR was present (see a detailed description in the online supporting File S1).

Event detection and segmentation (Fig. 1). Audio events (snore and non-snore events) were automatically detected and segmented using an adaptive energy threshold. These audio events were segments with higher energy compared to the remaining (diminished) background noise in the audio signal. A detailed block diagram of the event detection and segmentation module is presented in the online supplement (Fig. S1 in File S1). Initially, the full-night audio signal was divided into one-minute sections, and for every section, an energy vector was calculated using energy frames (frame size: 60 ms with 75% overlap). A section-related energy threshold (adaptive threshold) e_{th} was calculated using a histogram of the energy vector $hist_{energy}(e)$. Since the prevalence of the (remaining) background noise frames was greater relative to the audio events (snore/non-snore), the energy value related to the peak of the histogram e_{max}, was located on the low energy scale:

$$e_{\max} = \arg\max_{e}\{hist_{energy}(e)\}. \tag{1}$$

The energy threshold ($e_{th} > e_{max}$) was set to the energy value corresponding to one-tenth of the peak amplitude:

$$hist_{energy}(e_{th}) = 0.1 \times hist_{energy}(e_{\max}) \tag{2}$$

A five-order median filter was applied to the threshold values (vector) to smooth outliers. *Event detection* – Energetic audio events were detected as a group of consecutive energy frames that surpassed the section-related threshold. *Event segmentation* – In order to find the exact event boundaries (edges), the time edges of each audio event were calculated using an estimated slope technique. An illustration of the segmentation process is shown in Fig. 2. This technique included the estimation of a slope from ten consecutive energy frames (150 ms window) – a linear regression fitting line was calculated from the consecutive energy frames in order to estimate its slope. This process was repeated and progressed outside the event boundaries one frame at a time for as long as the slope did not change its sign. Next, a *fragmentation test* was applied. In case the detected audio events were too close to each other (<200 ms), they were suspected to be one fragmented event (such as split snores). This fragmentation test involved a spectral similarity measure for the 100 ms adjacent windows of the suspected events (the ending part from the first event and the initiating part from the following event). In case of similarity, the events were merged to form one event. Finally, an *event duration test* was applied – only 200 ms to 3500 ms events were used in this study since we noticed that the duration of >99% of the manually labeled events fell in this range. Fig. 3 shows snore statistics based on manual labeling of snoring events. For more information and

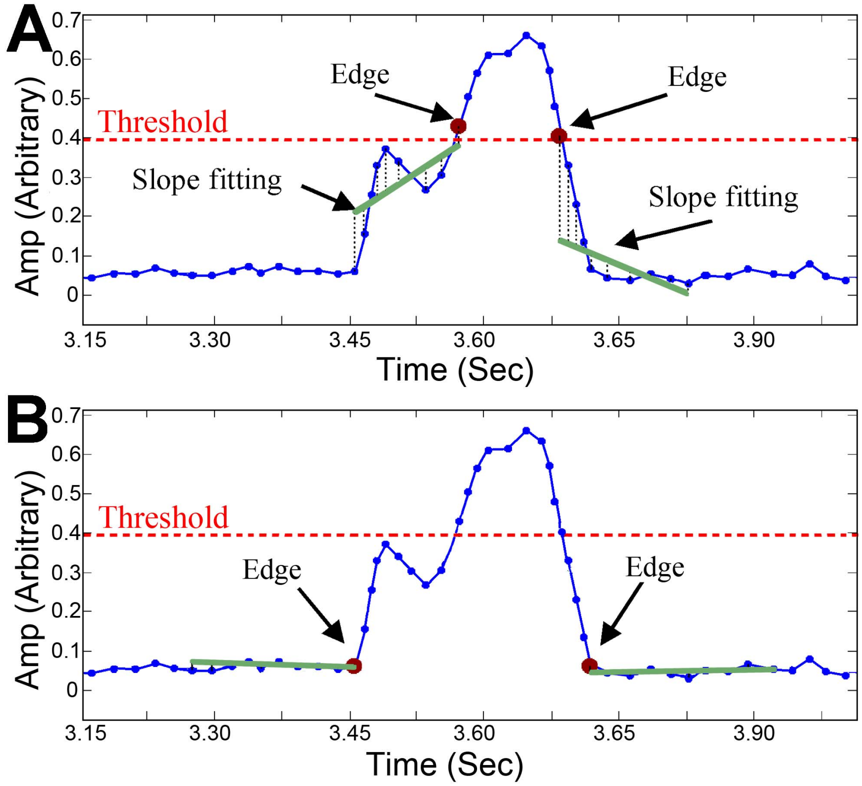

Figure 2. Audio event (snore/non-snore) segmentation. A) The initial segmentation edges of the audio event. B) The modified segmentation edges when applying the segmentation procedure. The green solid line represents the slope fitting of ten consecutive frames from both sides of the event. This process is repeated and progressed outside the event boundaries one frame at the time for as long as the fitted slope did not change its sign (±).
doi:10.1371/journal.pone.0084139.g002

demonstration of the event detection process see Fig. S1 and S2 in File S1.

Manual labeling of events (Fig. 1). This stage was essential for designing and evaluating the snore detection algorithm. Therefore, an ad hoc graphical user interface (GUI) for manual event classification based on visual and acoustic perception of the event itself and its surrounding context was designed. In this GUI, audio signals were presented in the time and frequency domains accompanying the synchronized PSG's respiratory effort signals. Using these signals, we were able to label each audio event as an

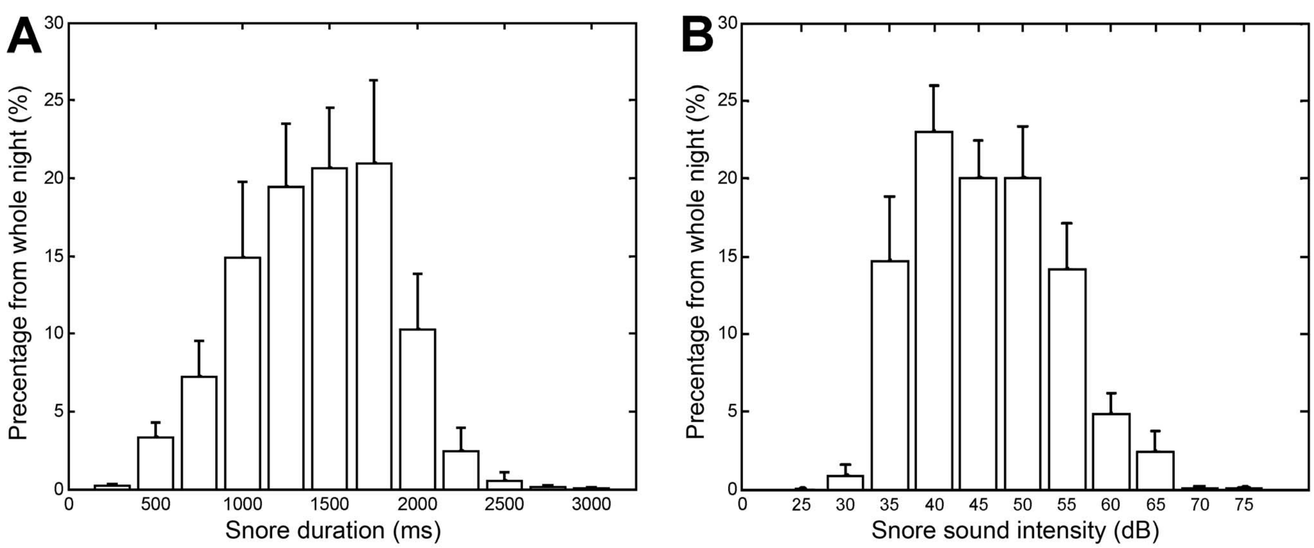

Figure 3. Snore characteristics. A) Snore duration, B) Snore intensity. Data was collected during design phase ($n = 25$). 99.9% of snoring event durations were in the range of 200 to 3500 ms. 99.2% of the snore intensity was in the range of 25 dB to 75 dB.
doi:10.1371/journal.pone.0084139.g003

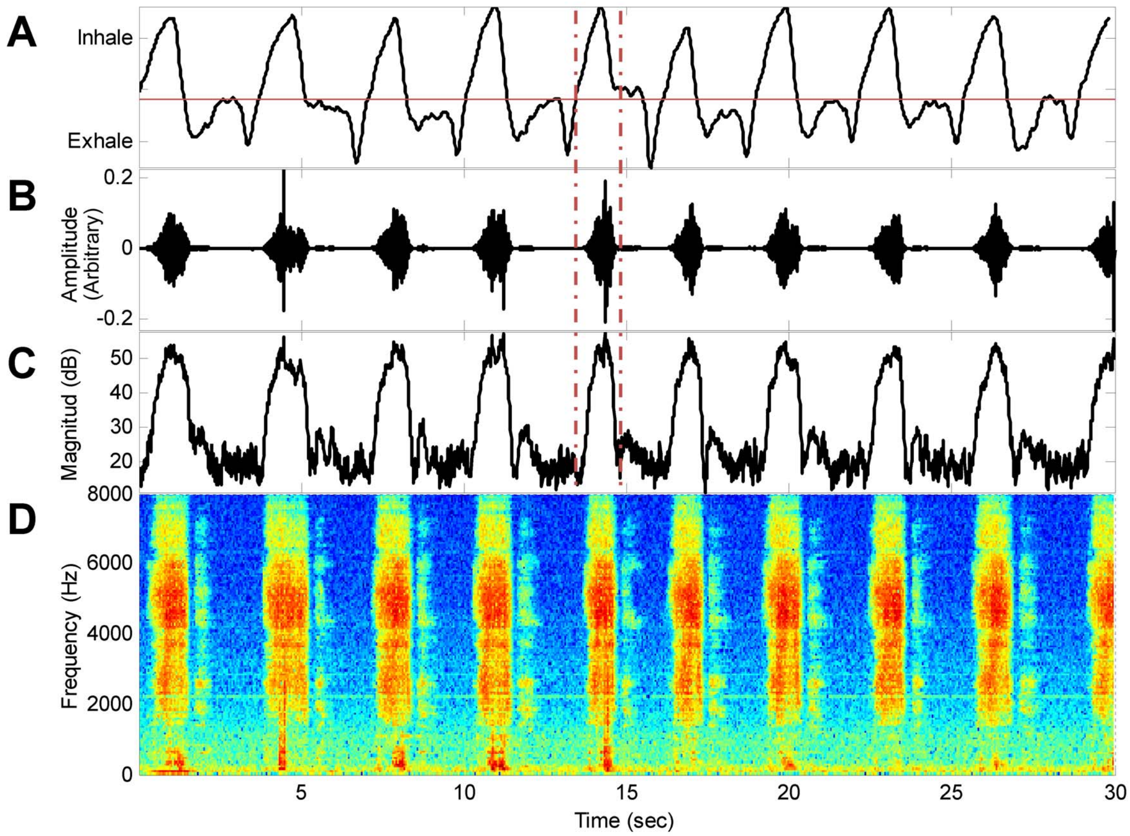

Figure 4. Example of snoring pattern during 30 sec epoch. A) Air flow, B) Audio signal, C) Energy signal, D) Spectrogram. Dashed vertical lines highlight one inspiratory event. Note that snore events are predominantly apparent during the inspiratory phase of the respiratory cycle. Data was collected from a 57-year-old man (BMI = 31, AHI = 16, during sleep stage 2).
doi:10.1371/journal.pone.0084139.g004

inspiratory sound (snore) or non-inspiratory sound (exhale sound or noise). Fig. 4 shows an example of signals from a 57-year-old man; note that the prominent audio events (Fig. 4B) were inspiratory episodes.

Three research assistants (including one of the authors, ED) performed manual annotation of the audio signals in order to train and evaluate the snore detection system. All assistants were guided by a sleep expert (AT) in the annotation protocol in order to make sure that the definition of snore/non-snore was clear.

Two classes of audio events were defined in the annotation protocol: snoring and non-snoring. Snoring was defined as a breathing sound that occurred during an inspiration (that was visualized by the PSG's respiratory belt movements in the GUI) with an intensity >20 dB (the minimum sound detection sensitivity of our audio recording setup). Nevertheless, breathing sounds may occur during inspiratory and/or expiratory episodes. However, in the current study, the inspiratory sounds were chosen as snores since we found that 97.5±2.2% (mean ± SD) of noisy breathing cycles during sleep were composed of an inspiratory sound that was much louder than the expiratory sound. Moreover, often expiratory sounds were not observed at all (Fig. 4). Non-snore events were defined as events that did not follow the snore definition, such as bedding noise, coughing, talking, and other environmental noises.

According to the manual snore/noise annotation protocol, agreement measurements (Cohen's kappa [42]) between the three scorers were calculated. $\kappa_{12} = 97.4\%$, $\kappa_{13} = 97.9\%$, and $\kappa_{23} = 97.0\%$ are the agreement scores between scorers 1 and 2, scorers 1 and 3, and scorers 2 and 3, respectively. Discrepancies were resolved by additional revision by the scorers. The majority of these proved to be human error (>98% – accidently pressing the wrong classification button), and the rest (<2%) were resolved by a majority vote of the three scorers.

Feature extraction (Fig. 1). We established a pool of 127 features relevant for distinguishing snore events from non-snore events. Table 1 summarizes these feature categories based on time- and spectral-related domains using intra/inter-event properties. A detailed description of the entire set of features is available in the online supporting File S1.

A brief description of the feature categories:

I. ***The time-domain set*** – constructed from features that quantify parameters regarding the event's timing and their location relative to adjacent events. Twenty-five features, separated into three sub-categories, are included in this set:

a) ***The periodicity features*** seek a snoring pattern (repeated events) calculated via autocorrelation, R, of an energy signal interval (with a pre-defined duration), which includes the event surroundings (Fig. 5). The first peak of the estimated autocorrelation function within the range of 1 sec to 10 sec was selected because it holds information about the basic rhythm period (i.e., location of the peak τ_p) and its power (its amplitude relative to the zero-lag autocorrelation R_0). The *rhythm period* feature was calculated as τ_p and the *period's intensity feature* R_I was calculated as the product of the first peak amplitude value $R(\tau_p)$ and the initial correlation area *Area*.

Table 1. The entire (127) feature categories.

Feature categories	Number of features	Selected features
I. Time-related features	25	10
a) Periodicity features (Inter-events)	10	6
b) Duration and sample scattering (Intra-events)	4	1
c) Energy features (Intra-events)	11	3
II. Spectral-related features	102	24
a) Spectral parameterization (Intra-events)	68	16
b) Bio-characteristic frequencies (Intra-events)	10	4
c) Dynamic frequencies features (Intra-events)	24	4

The entire set of features is divided into time- and spectral-related domains. Note that in parentheses are the inter/intra characteristics of the feature category. A detailed description of the entire set of features is available in the online supporting File S1.
doi:10.1371/journal.pone.0084139.t001

$$R_I = R(\tau_p) \times Area \tag{3}$$

where *Area* is actually the normalized square area between the $R(\tau)$ curve and the $a\tau+1$ linear line from $R(0)$ to $R(\tau_p)$ calculated as:

$$Area = \frac{1}{\tau_p}\sum_{\tau=0}^{\tau_p}(a\tau + 1 - R(\tau))^2 \tag{4}$$

where a is the estimated linear slope. The more periodic the energy pattern, the greater the *period's intensity feature* (Fig. 5).

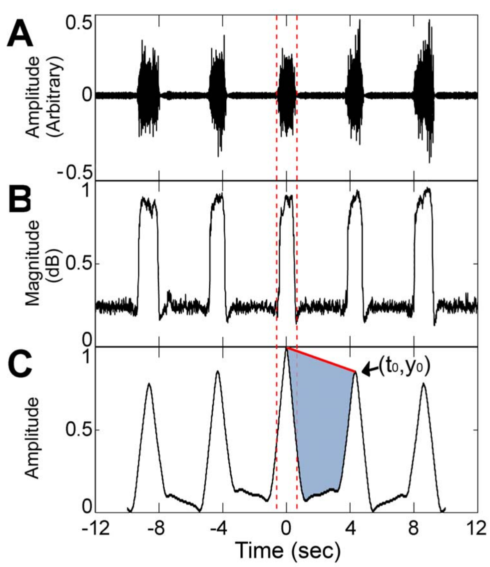

Figure 5. Demonstration of the major periodicity features. A) Audio signal containing snore pattern. B) The energy signal – achieved by a logistic transformation over the standard energy signal to emphasize the rhythm pattern. C) Smoothed autocorrelation R(τ) of the segment. In this example, the rhythm period was equal to $t_0 = 4.1$ seconds with intensity of $y_0 = 0.8$. Note that the tested event is aligned at $t = 0$ and $t = 12$ seconds for each side being tested. The shaded area in C represents the period's intensity feature. A more periodic energy pattern will result in a greater area and, hence, a greater period intensity value. The features were calculated for each tested event (between dashed vertical lines) by exploring the event's surroundings.
doi:10.1371/journal.pone.0084139.g005

Another important feature is *relative energy prior to event* E_P, which was calculated as:

$$E_p = \sum_{m=m_i-10Fr}^{m_i} e_m \Bigg/ \sum_{m=m_i}^{m_f} e_m \tag{5}$$

where e_m represents the energy signal at frame index m, and m_i and m_f represent the initial and final frame index of the tested event, respectively. Fr represents the frame rate ($10Fr$ is the 10 sec interval prior to the tested event). This feature uses additional statistical information about snoring template/rhythm. During snoring episodes, the energy signal interval that comes prior to the tested snore event includes a certain number of snores corresponding to the breathing period; normalizing the total energy of this interval [the nominator of Eq. (5)] with the total energy of the tested event [the denominator of Eq. (5)], yields a value that is an estimation of the number of similar events in this prior interval, resulting in a relatively low value and a narrow dynamic range of E_P (4.6 ± 2.0). In noisy environments (non-snores), E_P usually receives high values (27.0 ± 20.0).

b) ***The duration features*** include parameters such as the *whole event's duration* (in seconds) and its *95% energy duration* (in seconds). In some cases (especially in OSA snores), the difference between these two can be significant.

c) ***The energy features*** involve two major sub-sets: event-based and frame-based features. Event-based energy features are those regarding an event's total energy such as the event's intensity and SNR on the dB scale. Frame-based energy features include those that quantify and parameterize the shape and the formation of the event's energy over time.

II. ***The spectral-domain set*** – consists of features extracted from the signal frequencies' components. This set includes 102 features spread among three sub-categories: parameterization of the models describing the signal spectrum, bio-characteristic frequencies regarding vocal tract parameterization (modeling), and the dynamics of the frequencies' components: a) *The Spectral parameterization* consists of several spectral models such as linear prediction coding (LPC), Mel-frequency cepstral coefficients (MFCC) [22], and sub-band frequency distribution. For each model, we also included the first four statistical moments (1-mean, 2-variance, 3-skewness, and 4-kurtosis). b) *Bio-characteristic frequencies* include features

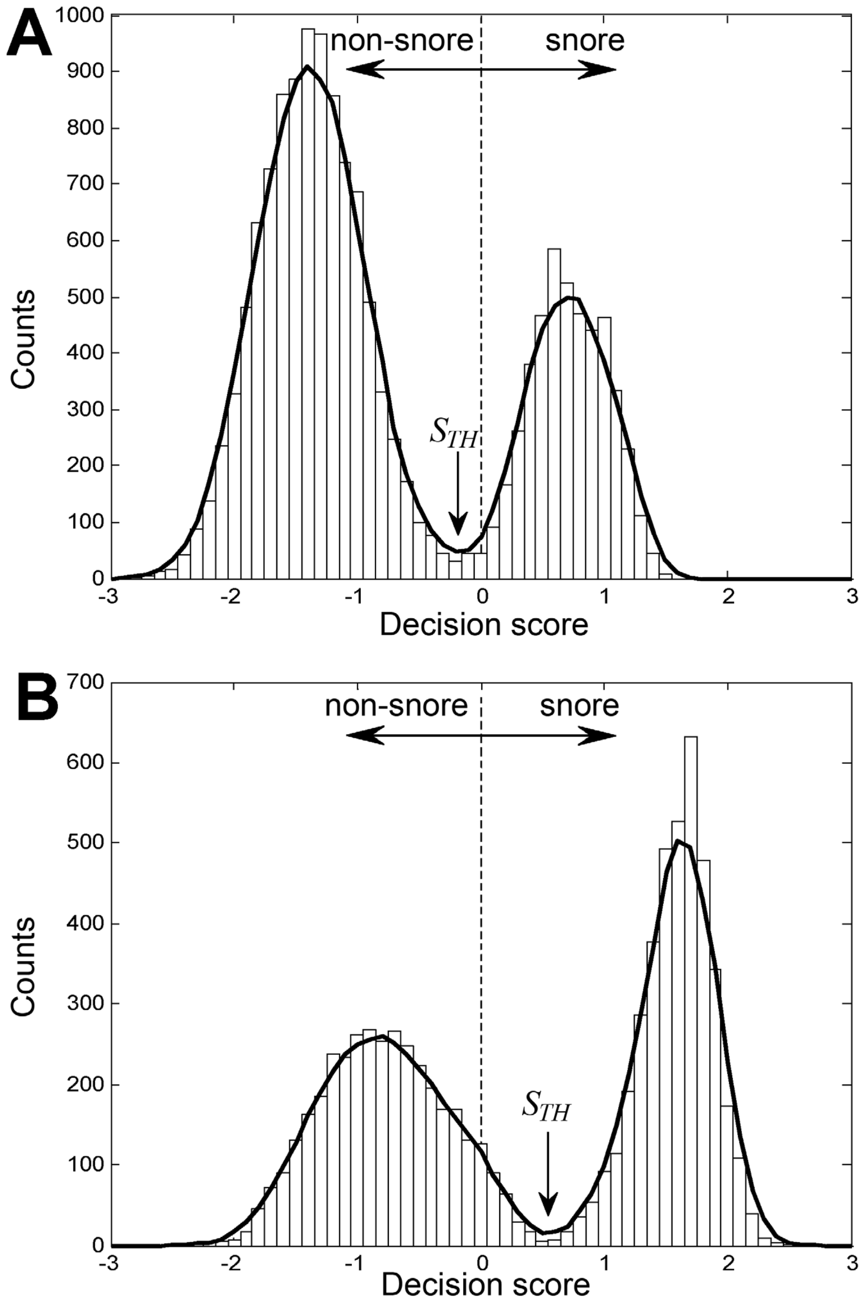

Figure 6. Individual decision score threshold for snore/non-snore events from two subjects. A) Example of subject with scores slightly shifted to the left (i.e., prone to noise detection). B) Example of subject with scores slightly shifted to the right (i.e., prone to snore detection). To avoid a false decision, the search of the minimum point was limited to a narrow region around zero. When only one type of event is present or no significant "valley" was found, a zero threshold was selected. Columns represent the histograms of the overall event scores. Bold lines represent a smoothed five-order moving average low-pass filter. The dashed line represents the default decision threshold, and S_{TH}, represents the calculated score threshold.

doi:10.1371/journal.pone.0084139.g006

that estimate the vocal tract formation such as *formants*, *pitch*, and pitch-related features [43,44]. c) *Dynamic frequencies* aim to measure changes in event frequency components. Usually, a snore's spectrum is more stationary in comparison to other noises (when spectral subtraction has already been performed).

Feature selection. A feature selection algorithm [45] was applied (Fig. 1). This was performed in order to reduce the complexity of the snore detection algorithm, to improve its performance, and to avoid over-fitting. A forward feature selection (FS) was conducted on the complete set of 127 features. The criterion that was chosen for the feature selection algorithm was the detection accuracy (snore as snore and non-snore as non-snore) that was accomplished using the AdaBoost classifier decision (see below) compared with the manual labeling of the events. We used the 10-fold cross-validation method [45] on the design dataset in order to determine the optimal number of features and the corresponding feature subset, and the resubstitution method in order to estimate the upper bound of the system's accuracy (detection rate). The optimal selected features were used in the validation phase of the study.

Classifier parameters estimation. An AdaBoost classifier [35] was used. Generally, a k-order AdaBoost classifier involves binary discrimination of k-weak learners, meaning k simple rules (thresholds) in a d-dimensional feature space (in our case $d = 34$) based on the true labeling of the events. Classification decision (pattern matching) was made using a decision score that is calculated via weighted summation of the k-weak learners. In the design phase, the classifier parameters were estimated (Fig. 1) to discriminate between two classes: snore and non-snore events. In order to estimate the classifier's parameters, the aforementioned manually labeled events were used. As mentioned above, the AdaBoost decision was also used for the feature selection criterion. For this purpose, the order was set to $k = 100$, which was found to be efficient yielding reliable results and a reasonable time-consuming feature selection process. For the purpose of snore detection (the overall system), the optimal order was found to be $k = 300$. This order was determined using the selected features ($d = 34$) yielding the best results for the design dataset and avoiding over-fitting.

Pattern matching (Fig.1). The classification decision was made using a decision score, S, calculated via weighted summation of the k-weak learners. Hence, the tested events were given a detection score, measuring their similarity to the (trained) snore/non-snore properties. During the design phase, snores were assigned the value "+1" and non-snores "-1," producing a linear estimation within that range, i.e., a snore event is likely to have a more positive score than a non-snore event. During the validation phase, a detection score was calculated for each detected audio event (for each of the 42 subjects).

Individual decision score threshold (Fig. 1). Since snoring properties can vary between subjects, we found that applying an individual decision score threshold improved system performance. Accordingly, for each subject, a score threshold (S_{TH}) was calculated using the scores of the subject's detected events. This score histogram was considered to behave as a bi-modal distribution since it is composed of snore and non-snore scores. The threshold was determined as the score value (index) of the minimum ("valley") point in the histogram (Fig. 6).

Data and Statistical Analyses

Audio signal processing and statistical analyses were performed using MATLAB (R-2010b, The MathWorks, Inc., Natick, MA, USA). Both the system design study ($n = 25$) and the validation study ($n = 42$) had similar data handling protocols. Statistical power ($\alpha = 0.05$) was calculated for the validation set based on event score values extracted from the system design data set. A sample size of 40 subjects was calculated to provide a statistical power of 0.88 in order to achieve a system accuracy rate of >97%. Therefore, 42 subjects were recruited for the validation study. PSG, demographic, and audio data were compared between design and validation study groups using unpaired student t-tests or χ^2 tests. The relationship between the subjective impression of subjects (questionnaires) and the objective measure of snoring was assessed with the help of Spearman correlations. The snore/non-snore classification performances of the design study involved resubstitution and ten-fold cross-validation methods. The snore/non-snore classification performances of the validation study involved a hold-out method, in which the system training was performed using the design dataset, and system validation was performed on the validation dataset. Detection performances were calculated using sensitivity, specificity, and accuracy:

$$Sensitivity = \frac{N_{TP}}{N_{TP} + N_{FN}} \tag{6}$$

where N_{TP} represents the number of detected snores as snores (true positive), and N_{FN} is the number of events corresponding to the false detection of snores as non-snores (false negative).

$$Specificity = \frac{N_{TN}}{N_{TN} + N_{FP}} \tag{7}$$

where N_{TN} represents the number of detected non-snores as non-snores (true negative), and N_{FP} is the number of events corresponding to the false detection of non-snores as snores (false positive).

$$Accuracy = \frac{N_{TP} + N_{TN}}{N_{TP} + N_{TN} + N_{FP} + N_{FN}} \tag{8}$$

By observing the intensity of patients' snores, we arbitrarily divided the intensity into three levels: <40 dB, ≥40 dB ≤55 dB, and >55 dB, according to the distribution of the snoring intensity. This data can be presented using histogram bars and, hence, provides useful information about an individual's snore intensity. Moreover, a snore intensity score was calculated for each subject, namely *objective snore intensity* (OSI). This score was calculated as the mean of a whole-night's snore intensity (in dBs) of an individual subject based on his/her detected snores. Finally, performances for different working points were obtained from a receiver-operating curve (ROC) and the area under this curve (AUC). Data are presented as mean ± SD.

Results

No significant differences were found between system design ($n = 25$, m/f 14/11) and validation ($n = 42$, m/f 26/16) groups in subjects' demographic characteristics, age, BMI, snoring, ESS, or AHI (Table 2). During the PSG study, an average of 7.5±1.1 hours of audio signals were recorded from each subject with no significant differences between the design and validation studies. A total of 180.3 hours and 324.2 hours were analyzed in these studies, respectively, and a total of 39,025 and 68,367 snore events were identified from the audio signals in them, respectively. Additionally, a total of 37,712 and 136,849 non-snore events were identified in each study, respectively. The non-snore events consisted of: 1) biological sources such as breathing (exhale), talking, murmurs, groaning, moaning, and coughing; and 2) other sources such as bedding noises, noise from electric devices, and slamming doors.

Preprocessing

Background noise removal proved to be beneficial in enhancing the signal and emphasizing faint and hidden acoustic events. On average, the enhancement of each acoustic event was improved by +6 dB, supporting earlier studies [41,46]. While the time and spectra domains seemed to be dramatically improved in the entire audio signal, some small distortion was registered (can be detected by ear) on the lower SNR events. Nevertheless, the enhancement contribution was unquestionable throughout the entire process described in Fig. 1.

The event detection process proved to be very sensitive, followed by a high detection rate. Compared with manually

Table 2. Subject Characteristics.

	System Design (n = 25)	System Validation (n = 42)	*p*
Gender (M/F)	14/11	26/16	0.633
Age (yr)	53.1±11.7 (29–82)	52.2±14.5 (23–81)	0.793
AHI (events/hr)	18.9±18.0 (2.0–64.9)	20.3±16.2 (0.5–74.4)	0.743
BMI (kg/m^2)	31.1±3.3 (26.7–38)	30.6±5.3 (16.8–39.3)	0.672
ESS (score)	10.3±6.4 (0–19)	13.7±6.5 (0–23)	0.573
Total labeled snoring events (×1000) (M/F)	23.0/16.0	46.3/22.0	0.366
Labeled snoring index (events/hr)	395.2±241.3	412.9±256.2	0.780
Total labeled noise events (×1000) (M/F)	23.4/14.3	87.0/50.1	0.880

AHI – apnea hypopnea index, BMI – body mass index, ESS – Epworth sleepiness scale. All values are mean ± SD (range).
doi:10.1371/journal.pone.0084139.t002

marked detectable events, the positive detection rate (*PD*) was 100%, and the positive predictive value (*PPV*) of 23% was achieved – meaning false-alarm detection was four times that of true detection. Nevertheless, the high false alarm events were easily eliminated by the duration test (200 ms to 3500 ms) and the snore/non-snore classifier itself.

Feature selection

We used the proposed AdaBoost-based method for the snore/non-snore detection algorithm. Fig. 7 shows the performance of the forward feature selection process conducted for the design study. The optimal performances were achieved using 34 features extracted from the complete set of 127 features (Table 1).

The 34 selected features contained representatives from two feature domains: time and frequency. The three most significant selected features (descending priority) derived from the forward feature selection process were: *(1) Relative energy prior to event (E_P), (2) Rhythm intensity of ±12 seconds (R_I), and (3) The first formant frequency*. Note that the first three significant features were extracted from the two domains explored (time and spectra). The most discriminative feature that was selected is E_P. The second complementary feature was the rhythm intensity related to the ±12 sec surrounding the events. The information from this feature emphasizes the first feature in the absence of a rhythmic pattern

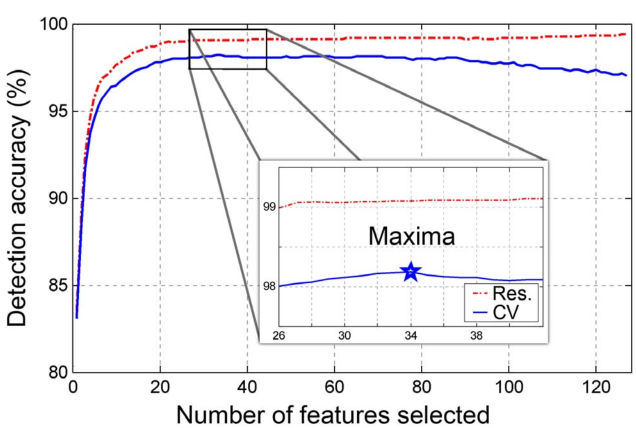

Figure 7. Criterion curve of the feature selection algorithm. The inner window is a zoom in at the maximal value. Thirty-four features were selected. The dashed-dotted line (red) represents the resubstitution (Res) method performances, and the solid line (blue) represents the 10-fold CV performances (CV).
doi:10.1371/journal.pone.0084139.g007

such as snoring episodes. Even though OSA patients disrupt this rhythm during apneic events, they still have some consecutive snores prior to such an event. For detailed selected features, see online supporting information Tables S1 and S2 in File S1.

Performance evaluation

Using the chosen features, an evaluation test was conducted on the validation dataset. During the validation phase, score threshold (S_{TH}) was calculated for each of the subjects. Each subject's scores (for snore and non-snore events) were shifted using this threshold value, allowing a global alignment of the scores from all the subjects. Hence, the evaluation of the overall performance of the system is feasible. Fig. 8A shows an event's likelihood score distribution (pdf) corresponding to their true labels (snores and non-snores). The corresponding ROC curve is presented in Fig. 8B and C. The overall detection rate (accuracy) was 98.2% with sensitivity of 98.1% (detecting snores as snores), and specificity of 98.2% (detecting noise as noise) with a confusion matrix as shown in Table 3. In addition, we measured performance as a function of the event's SNR, with the assumption that in using only relatively high SNR events (as in most previous studies), the performance of the system will be superior. In our study, the overall performance was calculated using very low SNR events as well in order to detect all snore events, even the very soft ones. The results are shown in Fig. 8C and D. Fig. 9 presents the distribution of snore intensity (5 dB resolution) for the validation dataset (manual and automatic snore detection). In this examination, we investigated the patient's snore intensity distribution throughout the night. The error bars represent the diversity of the participating subjects. By comparing the distribution of manual (open bars) vs. automatic (closed bars) detection of snore intensity, no significant bias was observed in each of the intensity sub-bands.

Fig. 10 shows an example of full-night recording. Data was collected from a 63-year-old woman (BMI = 31, AHI = 14). Snore intensity using the dB scale was measured for each of the detected snores. The snore index was defined as the running number of detected snore events per hour, estimated from 30 sec intervals (for each epoch). Snore intensity and snore index were aligned with the hypnogram, which was calculated using PSG analysis. Note that the snore index dropped considerably during wakefulness and periods of AHI.

Fig. 11 shows three examples of sound intensity histograms from three subjects during the validation phase of the study. The sound intensity of all audio events, i.e., snore and non-snore intensity, prior to snore detection (closed bars) had a similar distribution between subjects. Similar distribution characteristics were found

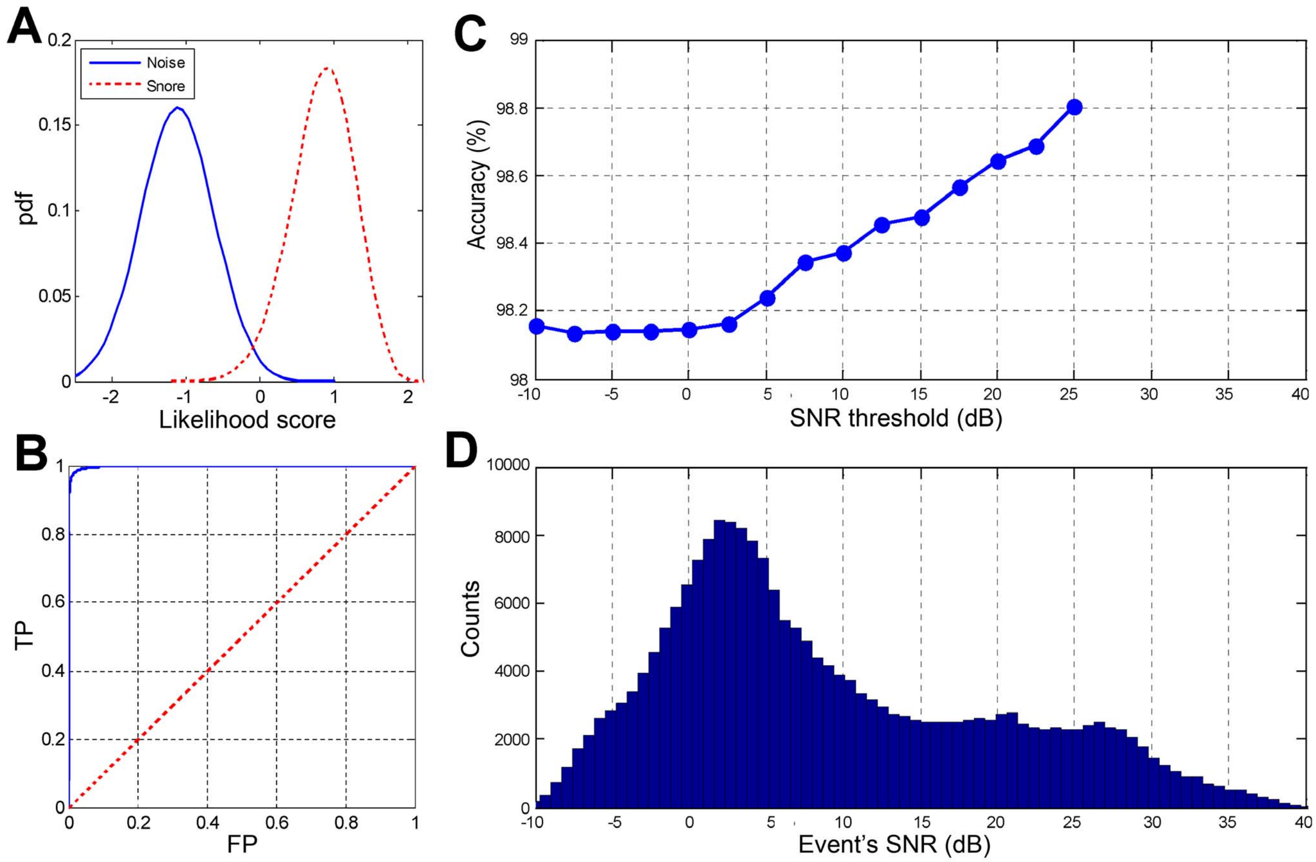

Figure 8. Performance of the snore detection algorithm: A) An event's likelihood score distribution (pdf – of true snores and non-snore events). B) ROC curve – detection rate True positive (TP) vs. false positive (FP) snores; area under the ROC curve = 0.998. The dashed line represents the "random guess" performance. C) The overall detection rate is based on different signal-to-noise ratio (SNR) thresholds of events. D) SNR distribution of overall events.
doi:10.1371/journal.pone.0084139.g008

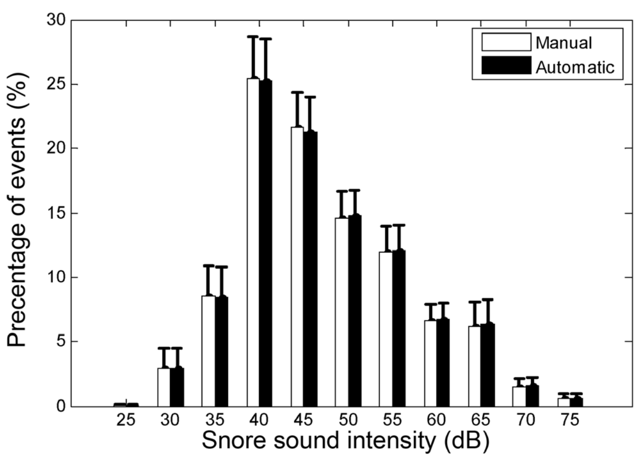

Figure 9. Snore intensity distribution of the validation dataset (n = 45). Open and closed bars display the distribution of snoring intensity on manually segmented events and automatically segmented events, respectively. Note that no consistent bias was found between manually and automatically segmented snore events. Error bars are standard error.
doi:10.1371/journal.pone.0084139.g009

for all 42 subjects included in the validation phase. However, observing the intensity of the automatically detected snoring events (open bars) reveals significant differences of snoring intensity among subjects. Fig. 11A shows a case where 92% of the snoring events of this subject were below 40 dB, suggesting a light snorer. On the other hand, Fig. 11C shows a case where >86% of the snoring events were above 55 dB, suggesting a loud snorer. Spearman correlation revealed no correlation between objective snore intensity and subjective self-reported snore intensity ($R = 0.14$ with $p = 0.46$). Fifteen subjects (35%) reported that they "don't know" if they snore or not. Of these subjects, we found that fourteen (93%) objectively snored (OSI>40 dB).

Table 3. Classification results.

Classified as	Snore	Noise
True label		
Snore	98.1%	1.9%
Noise	1.8%	98.2%

doi:10.1371/journal.pone.0084139.t003

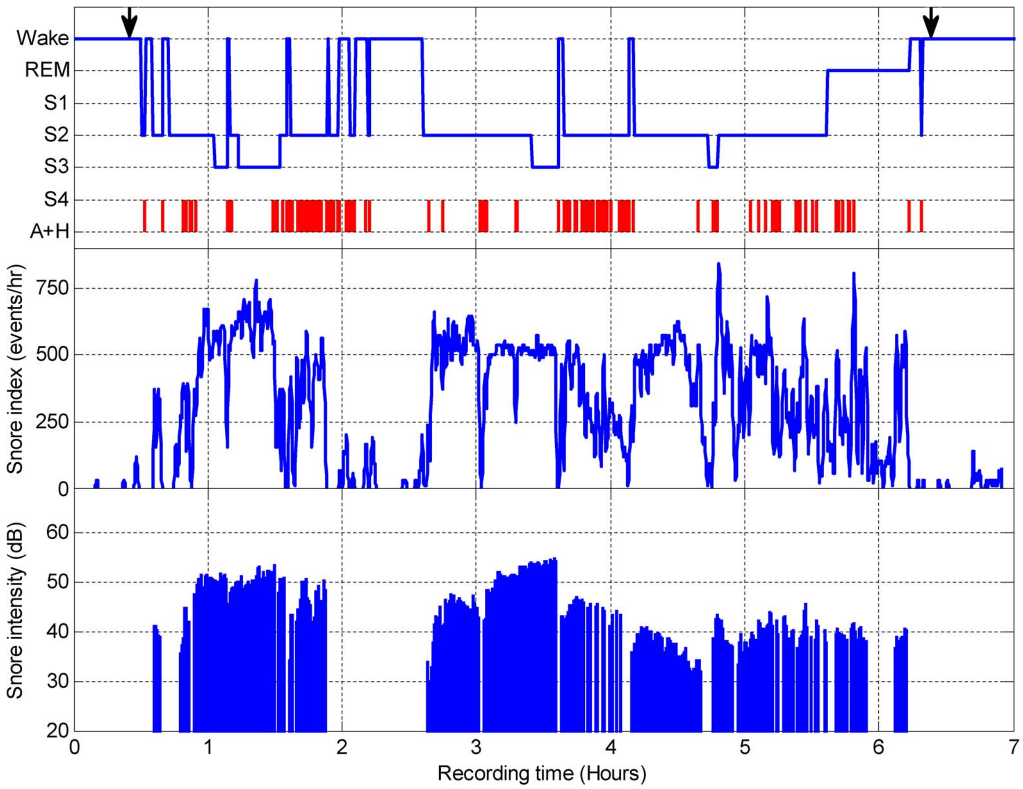

Figure 10. Example of whole-night snore index and snore intensity. Upper panel – sleep stages throughout the night and apnea/hypopnea events (A+H) based on the PSG test. Middle panel – automatically detected and calculated snoring index (events/hr) per 30 second epoch. Lower panel – snore intensity (dB). Arrows indicate lights off and lights on, respectively. Data was collected from a 63-year-old woman (BMI = 31, AHI = 14). For this subject only, a snoring index >240 events/hr is displayed.
doi:10.1371/journal.pone.0084139.g010

Discussion

Our study proposes a robust snore detection system based on audio signals recorded using a non-contact microphone technology with overall accuracy rate of 98.2%. The novelty of our proposed system is its automatic detection of a variety of snore events from a whole-night audio recording. Our approach to snore detection includes comprehensive sets of features that were selected using the feature selection algorithm.

Subjects

Sixty-seven typical subjects referred to PSG evaluation of sleep disorders were included in this study. No significant differences in subjects' demographic characteristics, age, BMI, AHI, and ESS were found between groups (Table 2). We included subjects referred to in-laboratory PSG evaluation including a wide range of age, BMI, and AHI distribution, and both genders. Further studies

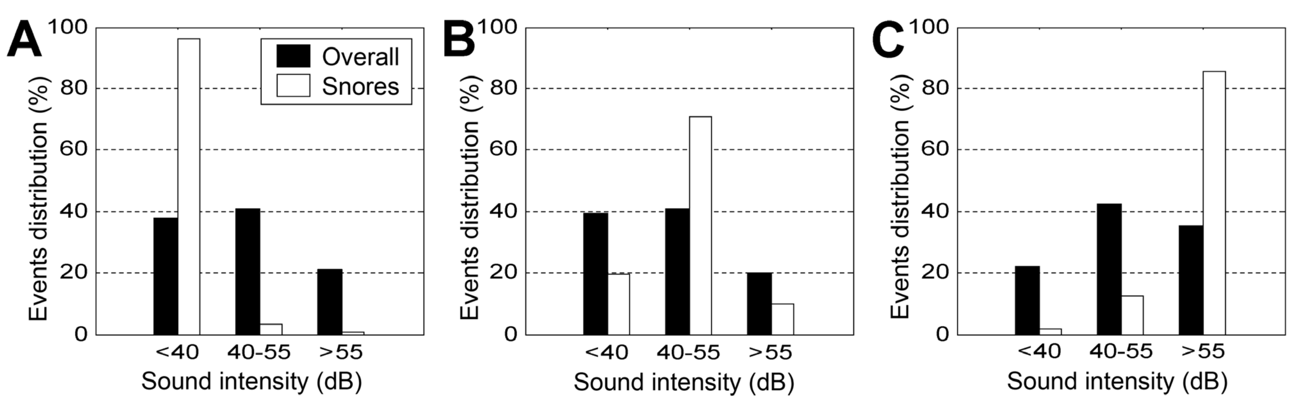

Figure 11. Example of sound intensity distribution for three subjects (arbitrarily selected) during the validation phase of the study. Closed bars are the sound intensity of all the audio events (snore and non-snore events) between "lights off" and "lights on." Open bars are the sound intensity of the detected snoring events. Data are presented as a percentage. In this example, subjects A, B, and C have objective snore intensity (OSI) of 37 dB, 46 dB, and 59 dB, respectively.
doi:10.1371/journal.pone.0084139.g011

are needed to confirm our findings in the general population and in at-home settings.

In this study, we included 107,392 snore events, acoustically ranging from very soft to very loud (20–80 dB). The majority of these snoring events (97.5%) occurred predominantly during inspiration with minimal snoring energy during expiration (Fig. 4), similar to prior studies that concluded that expiratory snoring is relatively rare [31,47]. Most studies [1,4,28,31–33] have defined snores as acoustic events with sound intensity exceeding a certain amplitude value. Other studies have defined them as acoustic events that contain an oscillatory component [30] and even as any sound perceived as such by the observer holding the microphone [29]. Moreover, some studies have explored only selected snores (usually loud events) and did not analyze the whole sleep [48]. Since there is no unified approach to exactly define a snore, and it is more ''in the ear of the beholder'' [4], we included every noisy inhalation sound made during sleep that was >20 dB, i.e., the minimum sensitivity of our recording device.

We noted that the ratio of noise events to snore events was higher in the validation group compared to the design group (Table 2). This finding may be explained by the fact that the validation dataset contains a longer recording time (~30 minutes), predominantly prior to lights off. Since total sleep time (and sleep efficiency) was statistically similar between the design and validation datasets (design: 343±48 minutes, validation: 349±42.0 minutes, $p = 0.594$), this extra recording time contained more noise events, which were mainly generated by patients and technicians prior to lights off. Nevertheless, the vast majority of the additional noise events were successfully detected by our system (>98%). This strengthens our hypothesis that snore events can be successfully detected even in a noisier environment since the training process (in the design phase) included a large variety of noise and snore events.

Snore recording

We used a non-contact microphone to record snoring. This approach was challenging since it was essential to improve SNR in order to expose the acoustic signals that were of interest. To achieve this, we used an adaptive spectral subtraction technique that subtracted the estimated adjacent background noise. The spectral subtraction technique improved signal SNR with a minimal distortion effect on sound intensity. Our findings are supported by Karunajeew et al. [25], who explored the effect of signal enhancement using spectral subtraction prior to a snore detection system on a sample of 12 patients (8 and 4 were included in the design and validation studies, respectively) undergoing PSG. Karunajeew et al. showed that the detection rate could be improved from 90.7% to 96.7%. This technique of signal enhancement is very acceptable in the speech enhancement field, but has not been fully explored in nocturnal sound analysis. Recently, this process was found to be beneficial in cases where the speech signal was contaminated with loud background noise. Lee et al. [48] removed estimated background noise from an entire audio signal using a fixed filter. Their estimation was based on the spectrum from the initial ten minutes of the recording (empty room). This approach was better than most fixed noise reduction techniques (such as linear time invariant filter), but it did not follow the background noise properly through the night. To overcome the SNR challenge, some studies used a contact microphone, e.g., the tracheal microphone [19,26,27,49]; however, data were easily affected by a variety of noises such as cardiac and respiratory sounds and movements. Other studies used a microphone embedded in a face mask [50]. In our case, we developed an adaptive and sensitive event detection algorithm based on energy measurement. This algorithm has proven to be significant when whole-night snoring event detection is necessary. A previous study [48] using an adaptive energy-related threshold supports our findings.

Acoustic features

In this study, we established and explored a large and comprehensive set of features that are the most relevant for snore detection using a feature selection technique. In order to fully explore this variety of features, we have used concepts from speech and audio signal processing areas [22,43] and implemented features from time and spectral domains (Table 1 and Table S1 in File S1). In addition, for the purposes of this study, we developed a novel and unique set of features that are specifically suitable for measuring breathing patterns (snores) during sleep. It is worth noting that the most influential feature set was the novel periodicity set (Table 1, Fig.5), a set of features found to be highly discriminative in classifying snore and non-snore events. The best selected individual feature (E_P) belongs to this periodicity set and yielded an accuracy rate of 83.6% when tested alone on the validation dataset. However, detection of snoring events solely by this feature will not provide the desired performance. Therefore, complementary information from both time and spectral domains contributes considerably to improve our system's performance. Other studies have explored relatively few features based solely on spectra distribution [24,26] or on an event's energy and duration [48]. Karunajeewa et al. [25] did use the two domains' (time and spectra) energy signals with a combination of zero crossing rate, autocorrelation at 1 ms lag, and the first LPC coefficient; their results show the potential of information taken from both domains based on a small database. Some studies have tried to reduce the dimensionality of feature space using principle component analysis (PCA) [24,26] or Fisher's linear discriminant (FLD) [51]. Projecting the features from high dimensionality into a low dimension feature space indeed reduce the complexity of threshold decision making but ignore complicated and tangled patterns (of events). Hence, these kinds of approaches can be problematic since some of the inherent discrimination information between the classes can disappear. One of our study innovations was applying a feature selection algorithm (Table S1 in File S1) in order to evaluate a large set of features. This feature selection approach aimed to retain the discrimination ability between classes while significantly reducing the number of features.

For the design phase, we used the AdaBoost classifier. In preliminary studies [52], we also explored the effect of different classifiers such as a Gaussian mixtures model (GMM). The AdaBoost classifier was chosen because it was found to produce the best results. According to Fig. 7, the difference between the resubstitution and the ten-fold techniques in the optimal feature dimension ($d = 34$) was not greater than 1%, implying that there is no over-fitting even in a hyper-dimensional feature subset.

Body posture during sleep may affect the acoustic characteristics of snores, such as snoring intensity. Since body posture can change several times during sleep, we extracted a variety of features, exploring different normalization processes, and then applied the feature selection approach in order to objectively find the most robust features. Thirty-four features were selected (Table S2 in File S1). Among them, only 3 were energy-related. These features are not affected by the absolute event energy *per se*; i.e., two of the energy features (Tc_4 and Tc_6) are versions of a normalized energy, and the third feature (Tc_8) is related to the event energy shape (skewness). Further study should investigate the effect of sleep position on snore detection.

System performance

Comparing our snore detection performance with other studies, our results (accuracy>98%) are superior, especially when they are statistically proven based on a large dataset containing a variety of sleep disorder breathing (SDB) severity and recorded using an ambient microphone. Azarbarzin et al. [26] achieved an accuracy rate of 93.1% when using an ambient microphone. Karunajeewa et al. [25] published a high accuracy rate of 96.8% when testing four subjects. Cavusoglu et al. [24] produced an accuracy rate of 90.2% when recording using an ambient microphone placed 15 cm from the patient's head. Duckitt et al. [23] achieved 82–87% when trained and tested on a total of 6 snorers. We confirmed the robustness of our detector by using an additional audio recording device (handy *Olympus LS-5*) placed on the dresser beside the patient's head in the laboratory. Similar accuracy rates of 98.4% and 97.8% were found for the *Edirol R-4 Pro* ($n = 30$) and *Olympus LS-5* ($n = 12$, $p = 0.14$), respectively. Further studies are required to explore the usefulness of this snore detection in at-home settings.

Although expiratory sounds are relatively rare (see above), they were not excluded from our study. The snore/non-snore detection results include all the automatically detected sound events, including expiratory sounds. By analyzing the false-detected events (<2%), we noticed that the majority of the misclassified events were between inspiratory and expiratory snores. Further studies are required to explore these types of expiratory sounds.

Objective measure of snoring

This study provides a novel and useful tool to objectively quantify a whole night's snoring events. Early work has concluded that to a large extent snoring is a subjective evaluation [4] when in fact the problem lies with the bed partner being disturbed by essentially normal nocturnal breathing noise [1]. This study shows a poor correlation between self-reported snore intensity and the objective measurement of snoring. This could be related either to the fact that subjects "do not know" or to biased bed partner reporting. Fig. 10 demonstrates a clear whole-night objective visualization tool for a snoring pattern that may aid clinicians in their clinical evaluations of snoring by presenting the subject's snoring index (snoring events per hour of sleep) and intensity (in dB). An innovative parameter for objectively scoring snore intensity was developed in this study. The OSI score was calculated using the detected snores, for the first time allowing very accurate and objective scores regarding the controversial self-reporting questionnaires. This simple tool can provide objective numeric and graphic reports of the automatically detected snoring events (Fig. 11, open bars). Another application for snore detection is to diagnose SDB syndromes [20,27,30,48], the effectiveness of palatal surgeries regarding snores, OSA [18], and even exploration of breathing patterns during sleep time [33].

Summary

One of the main goals of medicine today is to improve early diagnosis and treatment. Clearly, incidence of snoring is very frequent, and it is a common symptom of sleep-disordered breathing and other disorders of the upper airways [4]. The "flood" of subjects presenting with snoring symptoms is a major challenge to decision makers and is governed by prevalence and level of awareness of snoring morbidity [14]. Here, we have proposed a snore detection system that can provide an objective quantitative measure for whole-night snore patterns. Further studies are needed both to reinforce our findings by recruiting subjects from primary care clinics and by validating this snore analysis method as a potential screening tool in an at-home environment.

Supporting Information

File S1 Online Methods Supporting Information.
(PDF)

Acknowledgments

We would like to thank Ms. Bruria Freidman from the Sleep–Wake Disorder Unit of Soroka University Medical Center for her support and collaboration. Soroka University Medical Center Institutional Review Board protocol approval number: 10621.

Author Contributions

Conceived and designed the experiments: YZ ED AT. Performed the experiments: YZ ED. Analyzed the data: ED YZ. Contributed reagents/materials/analysis tools: YZ ED. Wrote the paper: ED AT YZ. Recruitment funds: YZ AT.

References

1. Counter P, Wilson JA (2004) The management of simple snoring. Sleep Med Rev 8: 433–441.
2. Greenberg-Dotan S, Reuveni H, Simon-Tuval T, Oksenberg A, Tarasiuk A (2007) Gender differences in morbidity and health care utilization among adult obstructive sleep apnea patients. Sleep 30: 1173–1180.
3. Tarasiuk A, Greenberg-Dotan S, Simon T, Tal A, Oksenberg A, et al. (2006) Low socioeconomic status is a risk factor for cardiovascular disease among adult obstructive sleep apnea syndrome patients requiring treatment. Chest 130: 766–773.
4. Hoffstein V, Mateika S, Anderson D (1994) Snoring: is it in the ear of the beholder? Sleep 17: 522–526.
5. Hoffstein V (1996) Snoring. Chest 109: 201–222.
6. Skatvedt O (1993) Localization of site of obstruction in snorers and patients with obstructive sleep apnea syndrome: a comparison of fiberoptic nasopharyngoscopy and pressure measurements. Acta Otolaryngol 113: 206–209.
7. Bliwise DL, Nekich JC, Dement WC (1991) Relative validity of self-reported snoring as a symptom of sleep apnea in a sleep clinic population. Chest 99: 600–608.
8. Stoohs R, Guilleminault C (1991) Snoring during NREM sleep: respiratory timing, esophageal pressure and EEG arousal. Respir Physiol 85: 151–167.
9. Marin JM, Gascon JM, Carrizo S, Gispert J (1997) Prevalence of sleep apnoea syndrome in the Spanish adult population. Int J Epidemiol 26: 381–386.
10. Sands M, Loucks EB, Lu B, Carskadon MA, Sharkey K, et al. (2013) Self-Reported Snoring and Risk of Cardiovascular Disease Among Postmenopausal Women (from the Women's Health Initiative). Am J Cardiol 111: 540–546.
11. Stoohs RA, Blum HC, Haselhorst M, Duchna HW, Guilleminault C, et al. (1998) Normative data on snoring: a comparison between younger and older adults. Eur Respir J 11: 451–457.
12. Wiggins CL, Schmidt-Nowara WW, Coultas DB, Samet JM (1990) Comparison of self- and spouse reports of snoring and other symptoms associated with sleep apnea syndrome. Sleep 13: 245–252.
13. Wilson K, Stoohs RA, Mulrooney TF, Johnson LJ, Guilleminault C, et al. (1999) The snoring spectrum: acoustic assessment of snoring sound intensity in 1,139 individuals undergoing polysomnography. Chest 115: 762–770.
14. Reuveni H, Tarasiuk A, Wainstock T, Ziv A, Elhayany A, et al. (2004) Awareness level of obstructive sleep apnea syndrome during routine unstructured interviews of a standardized patient by primary care physicians. Sleep 27: 1518–1525.
15. Hoffstein V, Szalai JP (1993) Predictive value of clinical features in diagnosing obstructive sleep apnea. Sleep 16: 118–122.
16. Iber C, Ancoli-Israel S, L CA, Quan S (2007) The AASM Manual for the Scoring of Sleep and Associated Events: Rules, Terminology, and Tech-nical Specifications; 1, editor. Westchester, IL: The American Academy of Sleep Medicine.
17. Fiz JA, Abad J, Jane R, Riera M, Mananas MA, et al. (1996) Acoustic analysis of snoring sound in patients with simple snoring and obstructive sleep apnoea. Eur Respir J 9: 2365–2370.
18. Jones TM, Swift AC, Calverley PM, Ho MS, Earis JE (2005) Acoustic analysis of snoring before and after palatal surgery. Eur Respir J 25: 1044–1049.

19. Jané R, Fiz JA, Sola-Soler J, Mesquita J, Morera J. Snoring analysis for the screening of sleep apnea hypopnea syndrome with a single-channel device developed using polysomnographic and snoring databases; 2011. IEEE EMBC. pp. 8331–8333.
20. Ben-Israel N, Tarasiuk A, Zigel Y (2012) Obstructive apnea hypopnea index estimation by analysis of nocturnal snoring signals in adults. Sleep 35: 1299–1305C.
21. Fiz JA, Jané R, Solà-Soler J, Abad J, García M, et al. (2010) Continuous analysis and monitoring of snores and their relationship to the apnea-hypopnea index. The Laryngoscope 120: 854–862.
22. Deller JR, Hansen JHL, Proakis JL (2000) Discrete-time processing of speech signals. New York: Institute of Electrical and Electronics Engineers Press.
23. Duckitt WD, Tuomi SK, Niesler TR (2006) Automatic detection, segmentation and assessment of snoring from ambient acoustic data. Physiol Meas 27: 1047–1056.
24. Cavusoglu M, Kamasak M, Erogul O, Ciloglu T, Serinagaoglu Y, et al. (2007) An efficient method for snore/nonsnore classification of sleep sounds. Physiol Meas 28: 841–853.
25. Karunajeewa AS, Abeyratne UR, Hukins C (2008) Silence-breathing-snore classification from snore-related sounds. Physiol Meas 29: 227–243.
26. Azarbarzin A, Moussavi ZM (2011) Automatic and unsupervised snore sound extraction from respiratory sound signals. IEEE Trans Biomed Eng 58: 1156–1162.
27. Azarbarzin A, Moussavi Z (2012) Snoring sounds variability as a signature of obstructive sleep apnea. Med Eng Phys.
28. Issa FG, Morrison D, Hadjuk E, Iyer A, Feroah T, et al. (1993) Digital monitoring of sleep-disordered breathing using snoring sound and arterial oxygen saturation. Am Rev Respir Dis 148: 1023–1029.
29. Leiberman A, Cohen A, Tal A (1986) Digital signal processing of stridor and snoring in children. Int J Pediatr Otorhinolaryngol 12: 173–185.
30. Perez-Padilla JR, Slawinski E, Difrancesco LM, Feige RR, Remmers JE, et al. (1993) Characteristics of the snoring noise in patients with and without occlusive sleep apnea. Am Rev Respir Dis 147: 635–644.
31. Perez-Padilla JR, West P, Kryger M (1987) Snoring in normal young adults: prevalence in sleep stages and associated changes in oxygen saturation, heart rate, and breathing pattern. Sleep 10: 249–253.
32. Rauscher H, Popp W, Zwick H (1991) Quantification of sleep disordered breathing by computerized analysis of oximetry, heart rate and snoring. Eur Respir J 4: 655–659.
33. Series F, Marc I, Atton L (1993) Comparison of snoring measured at home and during polysomnographic studies. Chest 103: 1769–1773.
34. Wilson K, Mulrooney T, Gawtry RR (1985) Snoring: an acoustic monitoring technique. Laryngoscope 95: 1174–1177.
35. Freund YS, R E. (1997) A decision-theoretic generalization of on-line learning and an application to boosting. Journal of Computer and System Sciences 55: 119–139.
36. Kump K, Whalen C, Tishler PV, Browner I, Ferrette V, et al. (1994) Assessment of the validity and utility of a sleep-symptom questionnaire. Am J Respir Crit Care Med 150: 735–741.
37. Simon-Tuval T, Reuveni H, Greenberg-Dotan S, Oksenberg A, Tal A, et al. (2009) Low socioeconomic status is a risk factor for CPAP acceptance among adult OSAS patients requiring treatment. Sleep 32: 545–552.
38. Tarasiuk A, Reznor G, Greenberg-Dotan S, Reuveni H (2012) Financial incentive increases CPAP acceptance in patients from low socioeconomic background. PLoS One 7: e33178.
39. Johns MW (1991) A new method for measuring daytime sleepiness: the Epworth sleepiness scale. Sleep 14: 540–545.
40. Rotem AY, Sperber AD, Krugliak P, Freidman B, Tal A, et al. (2003) Polysomnographic and actigraphic evidence of sleep fragmentation in patients with irritable bowel syndrome. Sleep 26: 747–752.
41. Scalart P (1996) Speech enhancement based on a priori signal to noise estimation. Conf Proc IEEE International Conference on Acoustics, Speech, and Signal Processing 2: 629–632.
42. Cohen J (1960) A coefficient of agreement for nominal scales. Educational and psychological measurement 20: 37–46.
43. Rabiner LR, Schafer WR (1978) Digital processing of speech signals. Englewood Cliffs, New Jersey: Prentice-Hall.
44. Pevernagie D, Aarts RM, De Meyer M (2010) The acoustics of snoring. Sleep medicine reviews 14: 131–144.
45. Jain AK, Duin RPW, Mao J (2000) Statistical pattern recognition: a review. IEEE Transactions on Pattern Analysis and Machine Intelligence 22: 4–37.
46. Hasan MK, Salahuddin S, Khan MR (2004) A modified a priori SNR for speech enhancement using spectral subtraction rules. Signal Processing Letters, IEEE 11: 450–453.
47. Guilleminault C, Stoohs R, Duncan S (1991) Snoring (I). Daytime sleepiness in regular heavy snorers. Chest 99: 40–48.
48. Lee LA, Yu JF, Lo YL, Chen YS, Wang DL, et al. (2012) Energy types of snoring sounds in patients with obstructive sleep apnea syndrome: a preliminary observation. PLoS One 7: e53481.
49. Lee H-K, Lee J, Kim H, Ha J-Y, Lee K-J (2013) Snoring detection using a piezo snoring sensor based on hidden Markov models. Physiological measurement 34: N41.
50. Alshaer H, Levchenko A, Bradley TD, Pong S, Tseng WH, et al. (2013) A system for portable sleep apnea diagnosis using an embedded data capturing module. J Clin Monit Comput.
51. Yadollahi A, Moussavi Z (2010) Automatic breath and snore sounds classification from tracheal and ambient sounds recordings. Med Eng Phys 32: 985–990.
52. Dafna E, Tarasiuk A, Zigel Y (2011) Automatic detection of snoring events using Gaussian mixture models. Proc 7th international workshop of models and analysis of vocal emissions for biomedical applications, MAVEBA: 17–20.

Breathing and Snoring Sound Characteristics during Sleep in Adults

Levartovsky Asaf, Dafna Eliran, Zigel Yaniv, and Tarasiuk Ariel.

Journal of Clinical Sleep Medicine: JCSM: official publication of the American Academy of Sleep Medicine 12.3 (2016): 375-384 pii: jc-00201-15 http://dx.doi.org/10.5664/jcsm.5588

JCSM
Journal of Clinical Sleep Medicine

SCIENTIFIC INVESTIGATIONS

Breathing and Snoring Sound Characteristics during Sleep in Adults

Asaf Levartovsky, BSc[1]; Eliran Dafna, MSc[2]; Yaniv Zigel, PhD[2]; Ariel Tarasiuk, PhD[1]

[1]Sleep-Wake Disorders Unit, Soroka University Medical Center and Department of Physiology and Cell Biology, Faculty of Health Sciences, Ben-Gurion University of the Negev, Israel; [2]Department of Biomedical Engineering, Faculty of Engineering Sciences, Ben-Gurion University of the Negev, Israel

Study Objectives: Sound level meter is the gold standard approach for snoring evaluation. Using this approach, it was established that snoring intensity (in dB) is higher for men and is associated with increased apnea-hypopnea index (AHI). In this study, we performed a systematic analysis of breathing and snoring sound characteristics using an algorithm designed to detect and analyze breathing and snoring sounds. The effect of sex, sleep stages, and AHI on snoring characteristics was explored.

Methods: We consecutively recruited 121 subjects referred for diagnosis of obstructive sleep apnea. A whole night audio signal was recorded using noncontact ambient microphone during polysomnography. A large number (> 290,000) of breathing and snoring (> 50 dB) events were analyzed. Breathing sound events were detected using a signal-processing algorithm that discriminates between breathing and nonbreathing (noise events) sounds.

Results: Snoring index (events/h, SI) was 23% higher for men ($p = 0.04$), and in both sexes SI gradually declined by 50% across sleep time ($p < 0.01$) independent of AHI. SI was higher in slow wave sleep ($p < 0.03$) compared to S2 and rapid eye movement sleep; men have higher SI in all sleep stages than women ($p < 0.05$). Snoring intensity was similar in both genders in all sleep stages and independent of AHI. For both sexes, no correlation was found between AHI and snoring intensity ($r = 0.1$, $p = 0.291$).

Conclusions: This audio analysis approach enables systematic detection and analysis of breathing and snoring sounds from a full night recording. Snoring intensity is similar in both sexes and was not affected by AHI.

Keywords: breathing, obstructive sleep apnea, sex, snoring, sound analysis

Citation: Levartovsky A, Dafna E, Zigel Y, Tarasiuk A. Breathing and snoring sound characteristics during sleep in adults. *J Clin Sleep Med* 2016;12(3):375–384.

INTRODUCTION

Breathing sounds are generated by air turbulence in the upper airway due to increased airway resistance during sleep.[1–7] Inspiratory breathing sounds can vary significantly across sleep and between subjects; in some cases the sounds may be soft (sound intensity < 40 dB), but in others it can be loud.[8–16] Intense breathing sounds are commonly referred to as snoring.[10,13–16] The most accepted estimate for the prevalence of chronic snoring is 40% in adult men and 20% in adult women, although the variability is extremely large.[16] Early work has shown a poor correlation between measured loudness of snoring and subjective appreciation by different observers. It is recognized that to a large extent snoring is "in the ear of the beholder".[14]

Several studies have addressed the issue of detection of snoring sounds from a recorded audio signal during sleep using signal processing and pattern recognition algorithms.[10,17–23] Recently, we showed that audio-based features, extracted from audio recordings, can accurately detect, not only snoring sounds, but also sleep breathing sound events (intensity > 20 dB) even in a very quiet environment, with accuracy > 98%.[10] We also found that more than 97% of the snoring events occurred during inspiration; expiratory sound events are not common, confirming earlier reports.[9,21] This approach of detection of breathing sounds was further validated to reliably estimate apnea-hypopnea index (AHI)[24] and sleep-wake activity[25] in laboratory and at-home environments.[26,27]

BRIEF SUMMARY

Current Knowledge/Study Rationale: It is commonly thought that snoring intensity is greater for men than for women and it is correlated with apnea-hypopnea index (AHI); however, these claims were not critically investigated. In this study, we performed a systematic analysis of breathing and snoring sound characteristics using a novel signal-processing algorithm and analyze breathing and snoring sounds.

Study Impact: Here, we used an objective valid breathing and snoring feature analysis and provided evidence that although snoring index is sex dependent, snoring intensity is similar across sexes and is not correlated with AHI.

It is commonly known that snoring intensity (dB) is higher for men than for women[13,21] and it is correlated with AHI.[9,13,15,21,28] However, some studies reported that there was no difference in the maximal snoring sound intensity between women and men.[29] To our knowledge, these claims were not completely investigated because the sound level meter that has been used in all of these studies captures all the sounds in the room and not just the relevant inspiratory sounds of snoring. Obstructive sleep apnea (OSA) is associated with fragmented sleep that affects the overall sound due to movement noises, expiratory sounds not related to snoring, coughs, etc. It is possible that the reported correlation between AHI and sound intensity[15,28] are not solely related to snoring *per se*. In the current study we extracted inspiratory breathing-sound features

Figure 1—Block diagram of audio data handling and analysis.

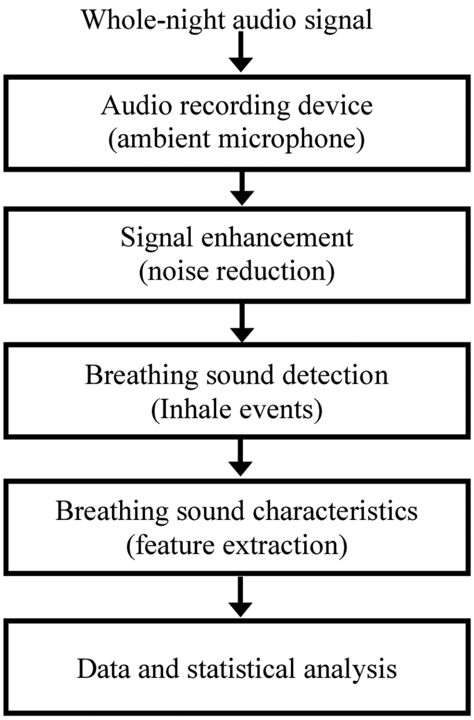

Whole-night audio signal, acoustic signals were recorded using a noncontact directional microphone connected to a digital audio recording device that was synchronized with polysomnography (PSG) recordings. Signal enhancement, following the completion of the PSG study, the audio signal was enhanced by a background noise reduction algorithm. Breathing sound detection, using audio signal processing and pattern recognition techniques, inhale sound events (> 20 dB) were distinguished from irrelevant noises, such as movements, linen noises, and speech. Breathing sound events were automatically located and segmented. Breathing sound characteristics, acoustic features such as sound intensity (dB), breathing sound duration (sec), breathing energy (dB × sec), and frequency centroid (Hz) were calculated for each inhale breathing sound event. Data and statistical analysis, breathing sound features were analyzed separately for women and men in the comparison and obstructive sleep apnea (OSA) groups.

during sleep, from the time and frequency domain, using a validated approach that enables discrimination between inspiratory breathing and snoring sounds (the signal of interest) and other sounds (noise events).[10] Here, we analyzed the effect of sex, OSA severity, and sleep stages on the feature characteristics of inspiratory breathing and snoring sounds during whole-night polysomnography (PSG).

METHODS

Setting

The study was conducted in the university affiliated sleep-wake disorder center and biomedical signal-processing laboratory. The Institutional Review Committee of Soroka University Medical Center approved this study protocol (protocol number 10621).

Subjects

We consecutively recruited a total of 121 adults aged 19 through 86 y (41/80 women/men) referred to the Sleep-Wake Unit for routine PSG study for sleep disorders diagnosis between February 2009 and March 2012. Subjects reported to the laboratory at 20:30 and were discharged at 06:00 the following morning. They were encouraged to maintain their usual daily routine and to avoid any caffeine and/or alcohol intake on the day of the study. The questionnaires were completed prior to the PSG study. Each individual's lifestyle, sleeping habits, and clinical history were recorded using a standardized self-administered questionnaire.[30–32] The Epworth Sleepiness Scale (ESS) was used to evaluate daytime sleepiness.[33]

Polysomnography Study

The laboratory environment was sleep-friendly according to recommendations of the National Sleep Foundation.[34] PSG study (SomniPro 19 PSG, Deymed Diagnostic, Hronov, Czech Republic) included electroencephalography (referential derivations, international 10–20 system, C3/A2, C4/A1, and O2/A1, O1/A2), electrooculography, electromyography, electrocardiography, respiratory activity (abdomen and chest effort belts – respiratory inductance plethysmography), and oxygen saturation. Simultaneous video monitoring was digitally recorded. An apnea was defined as > 90% decrease in the amplitude of airflow. Hypopnea was defined as > 50% decrease in the amplitude of airflow associated with an arousal and/or ≥ 4% oxygen desaturation. A minimum event duration of 10 sec was required. AHI was calculated as the number of respiratory events per hour of sleep. OSA group was defined as AHI ≥ 10 events per hour; AHI < 10 events per hour was defined as the comparison group. Scoring[34] was done by a trained technologist and underwent a second scoring by one of the investigators (AT).

Sound Acquisition

Acoustic signals were recorded using a non-contact directional microphone (RØDE, NTG-1, Silverwater, Australia) placed 1 m above the bed and connected to a digital audio recording device (Edirol R-4 Pro, Bellingham, WA, USA). The acquired audio signals were stored along with the PSG signals for later analysis. Each recorded signal was digitized and synchronized with PSG study onset to enable full night audio signal acquisition. Sound intensity (dBA) calibration of the audio-recorded signals was performed using a sound generator (sinus wave at 1 kHz) and an A-weighted sound level meter (Quest Technology 2700, Orlando, FL, USA). This calibration process was carefully validated across data collection. Audio signal processing was performed using MATLAB (R-2012b, The MathWorks, Inc, Natick, MA, USA).

Sounds Analysis

We developed a system for analyzing breathing and snoring sound properties comprising a non-contact microphone, digital audio recording device, and an algorithm that calculates breathing features from a whole-night audio signal (**Figure 1**). After the conclusion of the PSG study, the audio signal was enhanced by a background noise reduction algorithm.[10,25]

Figure 2—An example of 15-sec interval of audio signal.

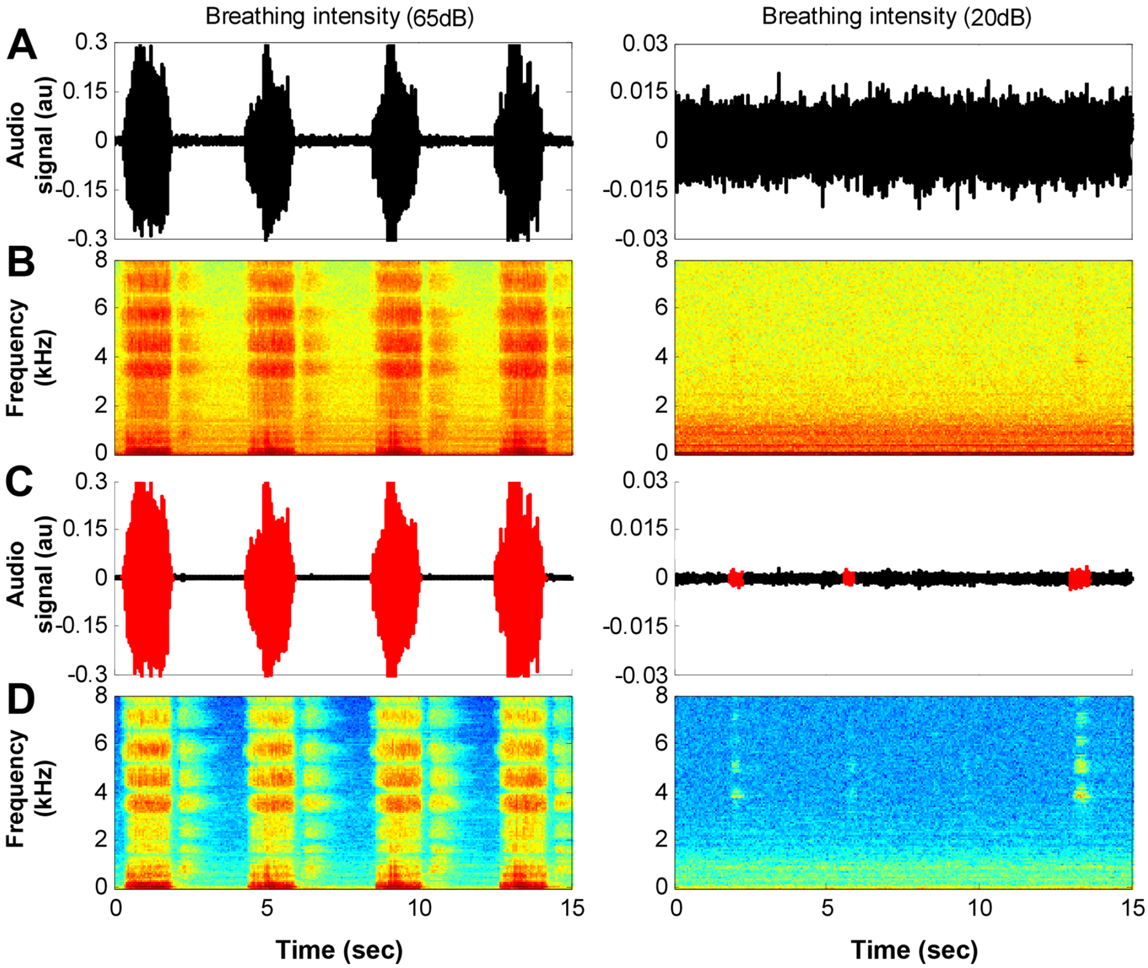

Left column illustrates loud snoring signal; right column illustrates very quiet breathing. **(A)** Raw audio signal; note that the quiet breathing (right panel) is hidden by the background noise (amplitude was magnified for this display). **(B)** The corresponding spectrogram (frequency components) of the raw audio signal in **(A)**. **(C)** Same audio signals following background noise reduction and inhale breathing detection (in red); note that the very quiet breathing sounds were detected (right panel). **(D)** The corresponding spectrogram of the filtered audio signal in **(C)**.

Using audio signal processing and pattern recognition techniques, breathing sound events were automatically located, segmented, and isolated using our breathing detection system[10] that can detect low intensity (> 20 dB) breathing sounds (**Figure 2**). Because there is a considerable amount of breathing sound events below 40 dB (and above 20 dB), for the purpose of this study the analysis was performed for the entire set of detected breathing sounds (range: 20–85 dB). Breathing sounds may occur during inspiration and/or expiration. We analyzed the inspiratory sounds events since 97.5 ± 2.2% of noisy breathing cycles during sleep occurred during inspiration and these events were much louder than the expiratory sound events.[10] This system was validated to distinguish breathing sounds from irrelevant noises, such as movements, linen noises, speech, and other interferences. This system's average detection rate (accuracy) was 98.2% with sensitivity of 98.0% (breathing sound as a breathing sound) and specificity of 98.3% (noise as noise).[10] In the absence of a conclusive definition, the following description of snoring was defined for this study: snoring is relatively loud breathing sounds (> 50 dB) during sleep.[14,15]

Using the detected breathing events, four acoustic features were developed and extracted per subject (**Figure 3**). These four features are calculated from the time and spectral domains for each inhale breathing sound event. The features are: (1) sound intensity (dB), (2) event duration (sec), (3) acoustic energy (dB × sec), and (4) frequency center of mass (frequency centroid, Hz). For further details about feature equations, see the online supplementary file in Dafna et al.[10]

Data and Statistical Analysis

Statistical analyses were performed using SPSS software (IBM, Armonk, New York, USA) for Windows (version 20). Continuous variables are presented as mean with standard deviation; comorbidities are presented as prevalence percentage. From the whole-night audio recordings, inhaled breathing sound features were extracted and sound features were analyzed for women and men in the two groups. The number of

Figure 3—Example of breathing features analyzed.

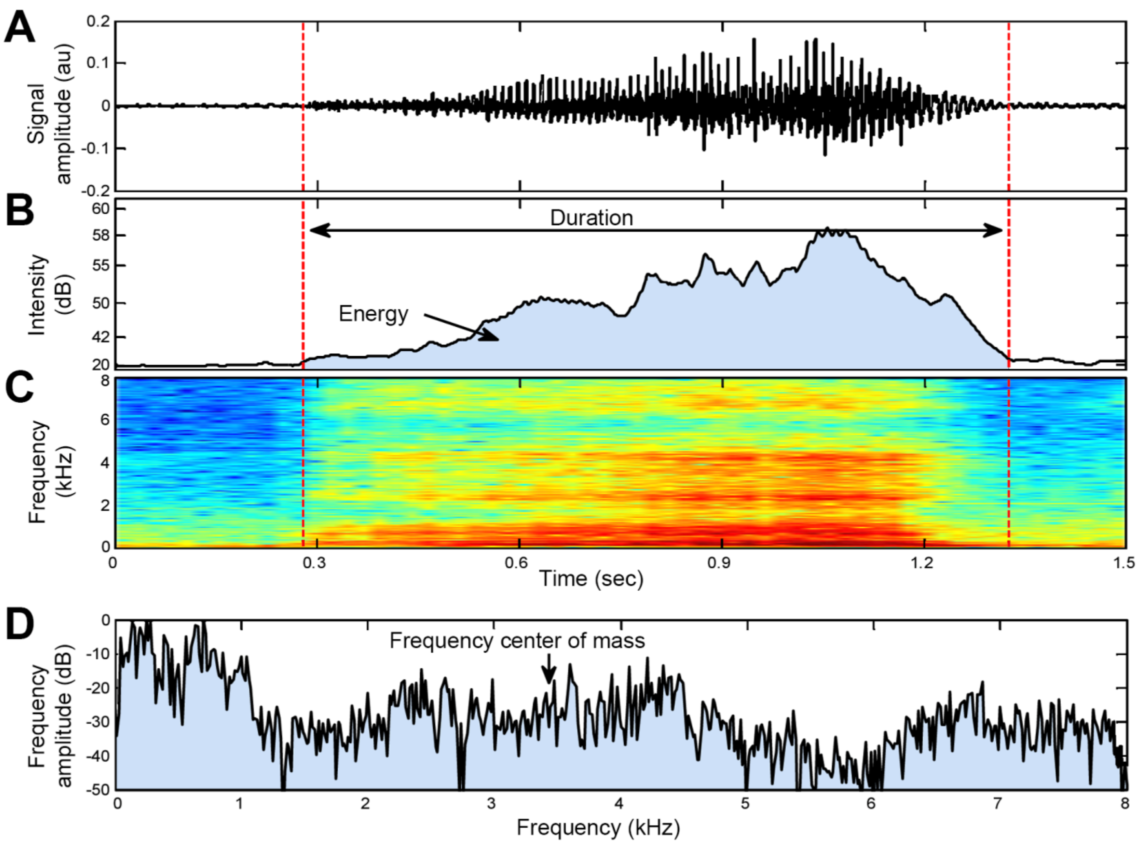

(A) Audio signal of one inhale breathing sound; **(B)** Sound intensity curve of the audio signal associated with breathing loudness as perceived by the human ear; **(C)** Spectrogram of the audio signal (kHz). Data are presented in a color map, hot colors represent high amplitudes; **(D)** Spectrum of the audio signal, calculated from the segmented audio signal (in **A**). The arrow indicates the frequency centroid (center of mass). Dashed vertical lines represent the automatic segmentation of the sound event and the duration feature. The energy (in B) is indicated by the area under the intensity curve.

breathing and snoring sounds index was calculated per hour of sleep and separately for stage 2 (S2), stage 3 + stage 4 (slow wave sleep, SWS), and rapid eye movement sleep (REM). The percent of breaths leading to snoring (% snoring) was calculated for each sleep stage. The Mann-Whitney U test was used to determine the statistical significance of all the continuous variables, including patient characteristics, PSG features, and acoustic parameters of breathing sounds. Two-way analysis of variance (ANOVA-2) for repeated measures was used to examine the effect of sex and sleep time (hours) on breathing or snoring index (events/h) during sleep, using *post hoc* comparisons by Tukey test. Pearson correlation was used to examine the relationships between breathing or snoring sound features and patient characteristics such as age, AHI, and number of arousal (Ar) and awakening (Aw) events per hour of sleep (Ar + Aw index). For the correlation analysis, the values of breathing or snoring sound features were calculated as an average value for each subject, using the entire breathing sound event dataset, and the upper quarter and top 1% of most loud sound events dataset. In order to explore the noises that may be related to sleep fragmentation that are associated with OSA, Pearson correlation was used for the analysis of nonbreathing sounds (average intensity value of top 10% of noise events) and their relation to AHI. In order to avoid technician-induced noises in the study, the noise analysis was conducted between lights off and lights on. Data are presented as mean ± standard error of the mean unless indicated otherwise. The null hypothesis was rejected at the 5% level.

RESULTS

Subjects

The demographics and PSG findings of the subjects included in this study are shown in **Table 1**. Women with OSA are 10 y older than women without OSA ($p < 0.05$) and men with OSA have higher body mass index (BMI) compared to men without OSA ($p < 0.05$). All groups had similar total sleep time and sleep efficiency. However, as expected, both men and women with OSA had 250% more Ar + Aw index events compared to comparison groups ($p < 0.01$).

The whole night mean respiratory rate (calculated from inductance plethysmography) was 16.4 ± 2.5 (breaths/min) and no significant differences were found between sexes or groups. The AHI of women and men of the comparison group were 4.9 ± 2.6 (events/h) and 6.7 ± 2.7 (events/h), respectively, with

Table 1—Subject characteristics.

	Comparison Group			OSA Group		
	Women (n = 25)	Men (n = 18)	Pv	Women (n = 16)	Men (n = 62)	Pv
Age (y)	51.9 ± 13.5	51.2 ± 15.1	0.9	60.9 ± 11.6*	54.9 ± 14.6	0.1
BMI (kg/m²)	32.7 ± 7.7	29.6 ± 4.1	0.2	33.1 ± 4.5	31.8 ± 4.9*	0.6
ESS (score)	9.6 ± 5.4	10.2 ± 6.8	0.9	9.6 ± 5.8	9.3 ± 5.2	0.8
TST (min)	330.8 ± 41.4	316.4 ± 68.4	0.8	341.5 ± 57.5	340.9 ± 58.8	0.9
Sleep efficiency (%)	78 ± 10.5	75.1 ± 14.9	0.4	76.8 ± 11.7	80.4 ± 13.1	0.1
WASO (min)	59 ± 41.6	57.9 ± 39.7	0.9	60.6 ± 46.1	50.5 ± 43.5	0.2
Ar+Aw index (events/h)	13.5 ± 6.5	15.9 ± 6.5	0.1	34.2 ± 16.6	40.1 ± 18.8	0.2
S1 (%)	2.3 ± 2.8	3 ± 4.9	0.8	2 ± 2.6	2 ± 3.7	0.6
S2 (%)	70 ± 13.4	76.4 ± 17.4	0.08	73.56 ± 10.0	75.6 ± 11.5	0.5
SWS (%)	13.2 ± 9.8	11.6 ± 14.6	0.3	9 ± 7.4	8.74 ± 8.4	0.7
REM (%)	14.5 ± 8.9	9.1 ± 8	0.04	15.44 ± 8.43	13.71 ± 9.8	0.4
AHI (events/h)	4.9 ± 2.6	6.7 ± 2.7	0.03	22 ± 15.9	28 ± 17	0.1
T_{90} (%)	4.7 ± 14.2	4.4 ± 9.6	0.5	12.6 ± 18.3	17.5 ± 24.8	0.7
Des. Index (events/h)	6.3 ± 4.5	9.4 ± 5.4	0.04	26.2 ± 22.6	27.7 ± 16.1	0.4
Nadir SaO_2 (%)	87.7 ± 4.4	86.6 ± 5.7	0.6	78.81 ± 8.3	78.5 ± 11.0	0.9
Tobacco smoking (yes)	36%	50%	0.4	44%	53%	0.6
Habitual snoring (yes)	44%	72%	0.07	56%	68%	0.4

*p < 0.05 comparing women or men between groups. Values are mean ± standard deviation or prevalence (%). AHI, apnea hypopnea index; Ar + Aw index, number of arousal and awakening events per hour of sleep; BMI, body mass index; ESS, Epworth Sleepiness Scale; Pv, p value comparing women with men within group. REM, rapid eye movement sleep; SWS, slow wave sleep (S3+4); SaO_2, saturation of oxygen; TST, total sleep time; WASO, wake after sleep onset.

no significant sex differences. Both women and men with OSA had significantly higher AHI relative to the comparison group ($p < 0.01$). Ar + Aw index positively correlated with AHI ($r = 0.91$, $p < 0.001$). Both sexes in the OSA group spent more time with oxygen saturation below 90% ($p < 0.01$), had higher desaturation index ≥ 4% ($p < 0.01$), and lower nadir saturation of oxygen ($p < 0.01$) relative to the comparison group. Both groups reported similar tobacco smoking and habitual snoring with no sex differences.

Acoustic Characteristics of Breathing Sounds

Detection of total breathing sound (intensity > 20 dB) events during sleep was statistically similar in both sexes regardless of OSA. The total number of detected breathing sound events during sleep for women in the comparison group and OSA group was 2,428 ± 340 (events) and 2, 744 ± 296 (events), respectively, and for men 2,278 ± 410 (events) and 2,476 ± 151 (events), respectively. In both sexes breathing sound index was higher in the second hour of the PSG study in comparison to the first hour ($p = 0.04$; **Figure 4A**). Breathing sound index did not change during the duration of the PSG study in both sexes (**Figure 4A**). **Table 2** summarizes acoustic characteristics of the breathing sounds. No significant differences were found between comparison and OSA groups regarding mean breathing sound index and intensity in both sexes. Men with OSA have longer breathing duration ($p < 0.05$) and higher energy ($p < 0.05$) compared to men in the comparison group. The frequency centroid was higher in men with OSA compared to women with OSA ($p < 0.05$) during S2. During REM, men with OSA have longer breathing duration ($p < 0.05$) and higher

Figure 4—Breathing and snoring index for each hour of sleep.

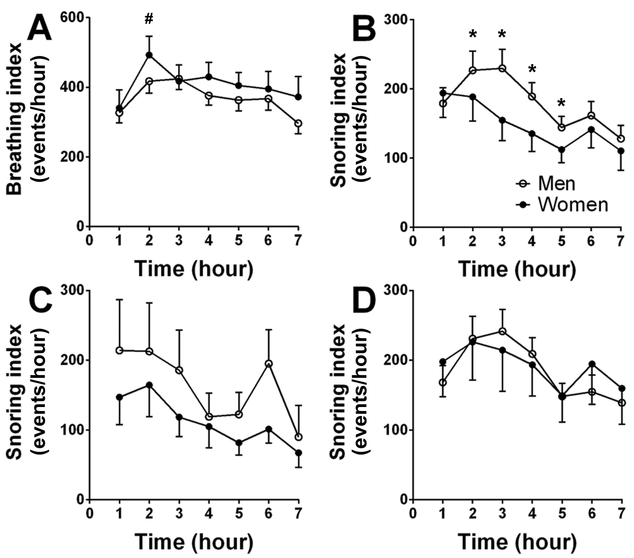

(A) Breathing sound (> 20 dB) index of all subjects. **(B)** Snoring (> 50 dB) index of all subjects. **(C)** Snoring index of the comparison group. **(D)** Snoring index of the OSA group. #significant change of breathing sound index between second and first hour of sleep in both sexes ($p = 0.04$); *significant sex differences ($p = 0.01$). Snoring index **(B)** significantly declined during sleep ($p < 0.01$). Significant differences were determined by two-way analysis of variance. Values are mean ± standard error of the mean

energy ($p < 0.05$) than women with OSA. In the comparison group, no differences were found in breathing intensity (45 ± 1.1

Table 2—Analysis of breathing sounds during sleep.

	Comparison Group			OSA Group		
	Women	Men	Pv	Women	Men	Pv
S2						
Breathing sound index (events/h)	386 ± 50	389 ± 59	0.9	433 ± 54.5	377 ± 22.7	0.2
Intensity (dB)	45.3 ± 1.2	45 ± 1.6	0.5	45.8 ± 1.8	47.9 ± 0.8	0.5
Duration (sec)	1.4 ± 0.04	1.3 ± 0.05	0.5	1.4 ± 0.08	1.5 ± 0.04*	0.3
Energy (dBsec)	62.9 ± 2.7	61.4 ± 3.6	0.5	64.6 ± 3.7	72.1 ± 2.7*	0.2
Frequency centroid (Hz)	3655 ± 61	3651 ± 68	0.9	3568 ± 64.3	3750 ± 32.2	0.02
SWS (S3+4)						
Breathing sound index (events/h)	400 ± 64.4	404 ± 66.5	0.9	573 ± 77.5	489 ± 40.6	0.3
Intensity (dB)	45.8 ± 1.3	45.6 ± 1.9	0.8	44.7 ± 2.2	48.8 ± 0.9	0.1
Duration (sec)	1.4 ± 0.06	1.4 ± 0.07	0.9	1.4 ± 0.08	1.5 ± 0.04	0.2
Energy (dBsec)	62.6 ± 2.9	64.3 ± 4.7	0.8	63.5 ± 4.8	75.3 ± 2.9	0.09
Frequency centroid (Hz)	3582 ± 95.8	3710 ± 70.2	0.5	3682 ± 92.5	3736 ± 40.9	0.6
REM						
Breathing sound index (events/h)	405 ± 61.4	399 ± 57.8	0.8	297 ± 50.8	349 ± 31.6	0.6
Intensity (dB)	44.1 ± 1.6	44.8 ± 1.9	0.8	44.3 ± 2	47 ± 0.9	0.5
Duration (sec)	1.3 ± 0.06	1.4 ± 0.05	0.6	1.2 ± 0.08	1.5 ± 0.05*	0.007
Energy (dBsec)	60 ± 4.2	63 ± 4.6	0.7	53.6 ± 4.6	72.9 ± 2.9*	0.01
Frequency centroid (Hz)	3736 ± 58.6	3569 ± 76.6	0.3	3661 ± 55	3770 ± 39.4*	0.3

*p < 0.05. Values are mean ± standard error of the mean. Breathing sound index, mean number of respiratory sound events that were detected (> 20 dB) and analyzed during each hour (h) of sleep; Pv, p value, comparing women with men within group; REM, rapid eye movement; S2, stage 2; SWS, slow wave sleep, stages 3 and 4.

Figure 5—Snoring index and intensity for each sleep stage.

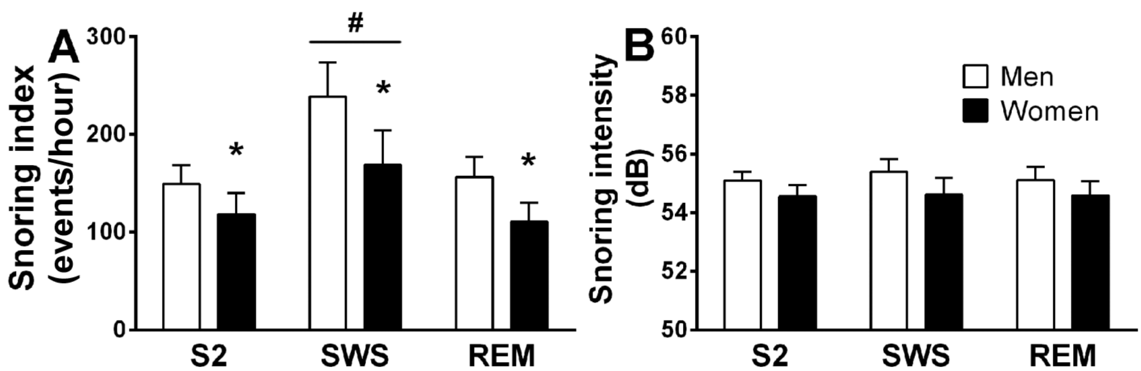

Snoring index **(A)** and intensity **(B)** for each sleep stage. *Significant difference between sexes (p = 0.05); #significant differences between slow wave sleep (SWS) and other sleep stages (p = 0.01). Significant differences were determined by two-way analysis of variance (ANOVA). Values are mean ± standard error of the mean. REM = rapid eye movement.

versus 46.1 ± 2 dB, respectively, p = 0.6) between subjects with BMI < 30 and subjects with BMI ≥ 30.

Acoustic Characteristics of Snoring Sounds

The mean number of snoring events for women in the comparison group and OSA group was 594 ± 127 and 1,042 ± 265 (p = 0.14); for men in the comparison group and OSA group the mean number of snoring events was 902 ± 310 and 1,023 ± 143 (p = 0.4), respectively. Snoring index was higher in SWS (p < 0.03, ANOVA-2; **Figure 5A**) compared to S2 and REM; men have higher snoring index than women in all sleep stages (p < 0.05, ANOVA-2). When combining the groups (OSA and comparison group) and all sleep stages, the % snoring (relative to inductance plethysmography determined respiratory rate) in men and women was 17.4 ± 2.1% and 11.5 ± 2.0% (p < 0.05), respectively. Although the average % snoring was higher in OSA than in control groups (in S2 and SWS, **Table 3**) in both sexes, it did not reach statistical significance.

In both sexes % snoring was higher in SWS compared to stage S2 and REM (p < 0.01, **Table 3**). No significant difference in snoring intensity was found between sexes or sleep stages (**Figure 5B**). **Table 3** summarizes mean snoring sound feature characteristics in sleep stages. No significant differences were found in snoring intensity, duration, and energy between groups in both sexes at all sleep stages.

In all sleep stages frequency centroid was elevated (p < 0.01) in men with OSA compared with men in the comparison group. During REM, men with OSA have longer breathing duration

Table 3—Analysis of snoring sounds (dB > 50) during sleep.

	Comparison Group			OSA Group		
	Women	Men	Pv	Women	Men	Pv
S2						
Snoring index (events/h)	89 ± 18	129 ± 46	0.8	165 ± 45	156 ± 21	0.9
% snoring	9 ± 3	13 ± 4	0.5	17 ± 4	16 ± 3	0.9
Intensity (dB)	54.5 ± 0.5	55 ± 0.7	0.6	54.6 ± 0.6	55.1 ± 0.3	0.4
Duration (sec)	1.4 ± 0.06	1.6 ± 0.07	0.2	1.5 ± 0.08	1.6 ± 0.05	0.3
Energy (dBsec)	75.7 ± 3.7	85.4 ± 4.2	0.1	79.4 ± 4.4	87.4 ± 2.7	0.1
Frequency centroid (Hz)	3249 ± 121	3320 ± 89	0.9	3386 ± 66.5	3539 ± 38*	0.06
SWS (S3+4)						
Snoring index (events/h)	139 ± 38	158 ± 46	0.4	216 ± 59	264 ± 37	0.8
% snoring	14 ± 5	16 ± 6	0.8	23 ± 7	27 ± 4	0.7
Intensity (dB)	54.8 ± 0.8	55.7 ± 0.8	0.4	54.2 ± 0.3	55.3 ± 0.4	0.3
Duration (sec)	1.4 ± 0.08	1.5 ± 0.09	0.5	1.6 ± 0.08	1.6 ± 0.05	0.3
Energy (dBsec)	75.7 ± 4.5	86.9 ± 4.8	0.2	86.6 ± 5.6	89.8 ± 3	0.3
Frequency centroid (Hz)	3322 ± 133	3203 ± 138	0.7	3493 ± 98	3589 ± 44*	0.3
REM						
Snoring index (events/h)	97 ± 28	180 ± 61	0.3	137 ± 28	150 ± 22	0.7
% snoring	10 ± 3	18 ± 7	0.3	14 ± 4	15 ± 3	0.8
Intensity (dB)	54.8 ± 0.6	56.1 ± 1.1	0.6	54.2 ± 0.4	54.9 ± 0.4	0.9
Duration (sec)	1.5 ± 0.08	1.4 ± 0.07	1	1.3 ± 0.1	1.6 ± 0.05	0.03
Energy (dBsec)	79.8 ± 4.7	80.8 ± 4.6	0.7	69.2 ± 5.8	90 ± 3.3	0.02
Frequency centroid (Hz)	3485 ± 93	3094 ± 80	0.02	3375 ± 37	3533 ± 50*	0.1

*p < 0.01 comparing women or men between groups. Values are mean ± standard error of the mean. Snoring index, mean number of snore sound events that were detected and analyzed during each hour (h) of sleep; % snoring, percent of breaths detected as snore (dB > 50); Pv, p value, comparing women with men within group; REM, rapid eye movement; S2, stage 2; SWS, slow wave sleep, stages 3 and 4.

(p = 0.03) and higher energy (p = 0.02) compared to women with OSA. For all sleep stages, snoring index gradually declined across sleep (p < 0.01, ANOVA-2; **Figure 4B**); men had a significantly higher snoring index than women (p = 0.04, ANOVA-2) during the second through fifth hours of PSG study. Snoring in stages S2 and SWS showed a similar trend of declined snoring index over time (data not shown). During REM, men's snoring index tended to gradually increase during the last 4 h of PSG study. For women, no conclusive findings for snoring index pattern during REM were found (due to small sample size).

Figures 4C and **4D** shows the snoring sound index for comparison and OSA groups, respectively. Women in the comparison group had a trend (p = 0.08, ANOVA-2) toward lower snoring index than men in the comparison group (**Figure 4C**); in the OSA group, both sexes had a similar snoring index across the night (**Figure 4D**). Women with OSA have higher snoring index (**Figure 4D**) than women in the comparison group (p = 0.002, ANOVA-2; **Figure 4C**). In the OSA group, no differences were found in breathing intensity (47.2 ± 1.4 versus 47.6 ± 1, dB respectively; p = 0.8) or snoring intensity (55.1 ± 0.9 versus 55 ± 1 dB, respectively; p = 0.6) between subjects with BMI < 30 and subjects with BMI ≥ 30.

Pearson correlations showed no association between AHI and mean breathing or mean snoring intensity (**Figure 6A**). In addition, no association was found between AHI and upper quarter (or top 1%) of snoring intensity (data not shown), duration (**Figure 6B**), or energy (**Figure 6C**). Frequency centroid of breathing and snoring sounds (**Figure 6D**) correlated with AHI; $r = 0.28$ (p < 0.001) and $r = 0.4$ (p < 0.01), respectively. Ar + Aw index positively correlated with noise events sound intensity ($r = 0.26$, p < 0.01). No correlation was found between breathing or snoring index and AHI: $r = -0.009$ (p = 0.923) and $r = 0.04$ (p = 0.7), respectively (**Figure 5**). Analyzing the noise events by calculating the intensity of the top 10% of non-breathing sounds from the whole-night audio signal, a positive correlation ($r = 0.25$, p < 0.0001) between the noise events and AHI was found.

DISCUSSION

This study used a novel and useful tool to objectively quantify a whole night's inhale breathing and snoring events. A large number of breathing events were detected and analyzed. Most studies have defined snores as acoustic events with sound intensity exceeding a certain amplitude value.[8,9,13–17] Some studies have defined snoring as acoustic events that contain an oscillatory component[8] and some have explored only a selected number of snores (usually loud events) and did not analyze the whole sleep.[21] Because snoring appears to be a subjective impression,[14] and there is no valid definition,[35] we used the loud (intensity > 50 dB) breathing sounds for the definition of snoring.[14,15] In the current study more than 97% of breathing sound events occurred during inspiration. This finding confirms early reports showing that snoring occurs mainly during inspiration, and that expiratory sound events are not common.[9,10,21,25] During sleep, upper airway resistance increases,[1–7] leading to

Figure 6—Correlation between breathing or snoring features and apnea-hypopnea index (AHI).

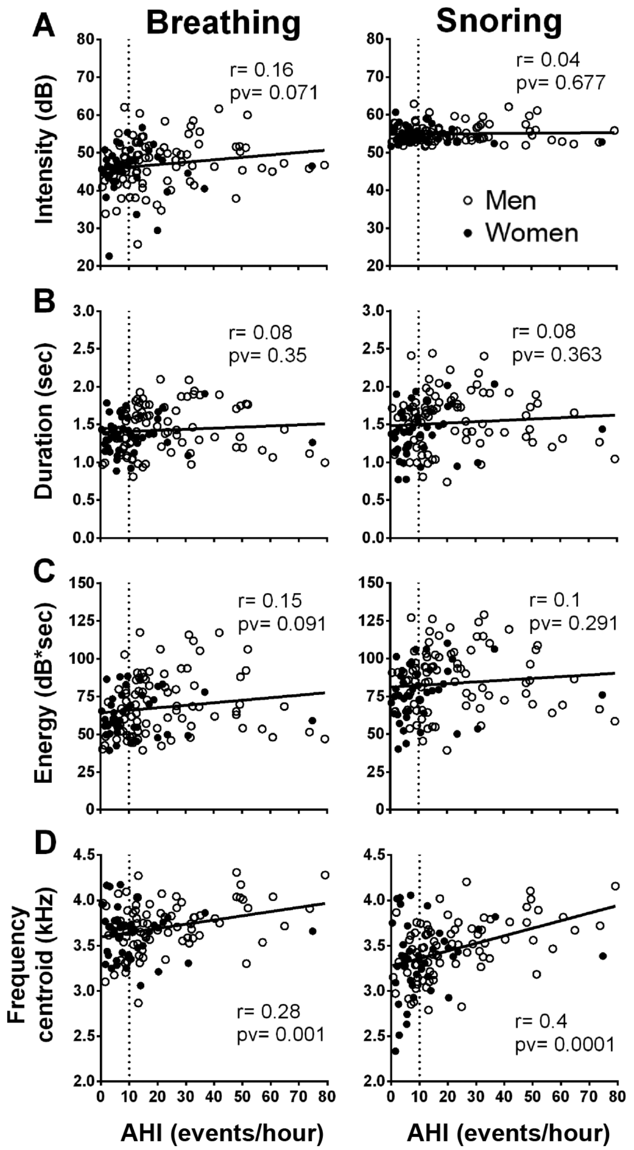

Left column represents breathing sound features and right column represents snoring sound features. **(A)** Intensity. **(B)** Duration. **(C)** Energy. **(D)** Frequency centroid. The feature values are calculated as the mean value for each individual and presented as one data point. Vertical dashed line indicates AHI = 10 (events/h).

amplification of air-pressure oscillations that are perceived as typical breathing sounds.[10,25] These sounds can vary from quiet (< 40 dB) to very loud snoring in the same subject.[10] We found that, on average, 45% of the respiratory events during sleep generated air pressure oscillations that could be detected and analyzed. Breaths "without a sound" (< 20 dB) indicate that no detectable air-pressure oscillation was present and these events were not analyzed. The need for an agreed-upon approach to extract and analyze whole-night snoring sounds is of major importance to the field of sleep disordered breathing. We used a novel robust snore detection algorithm[10] that can capture and analyze breathing sounds > 20 dB.

Our approach includes comprehensive sets of features that were selected using the feature selection algorithm. This algorithm can also detect and analyze nonbreathing sounds (noises), and discriminate these sound events from breathing sounds. This unique approach is in contrast to earlier reports that use a sound level meter without an algorithm that can discriminate between relevant respiratory sounds and other noises.[8,9,12–14,29,36–38] In both sexes, snoring index and % snoring was higher in SWS and men have a significantly higher snoring index and % snoring than women at all sleep stages. This finding is compatible with other reports, which described that snoring index was most prominent in SWS.[8,13,36,37,39] However, our findings (**Figure 5B**) do not support earlier studies claiming that snoring intensity is higher in SWS.[36,39]

In our subjects AHI ranged from 0.3 to 80 (events/h) and mean individual breathing intensity ranged from 20 to 65 (dB); however, no correlation was found between mean (or upper quarter or top 1%) breathing or snoring intensity and AHI. Our finding is in contrast to earlier reports that found that snoring intensity positively correlated with AHI.[15,28] Difference in results can be related to the possibility that in our study the subjects have less severe OSA than that reported by Maimon and Hanly,[28] who included 1,643 patients with AHI range of 10 up to 140 and snoring intensity of 38 to 80 dB; Hunsaker and Riffenburgh[15] included 4,860 patients with AHI range of 0 to 120 and snoring intensity of 50 to ~90 dB. Bland and Altman[40] established that correlation coefficient critically depends on the range of data: if this is wide, the correlation will be greater than if it is narrow. Moreover, most previous studies used the output of a sound level meter that captures all sounds in the testing room. Therefore, our data suggests that the association between snore intensity and OSA severity found in earlier reports[15,28] could be related to noise events that are not related to snoring *per se*. As expected, our OSA patients have fragmented sleep that produces sounds associated with sleep fragmentation, such as bed movements, coughs, etc. Indeed, we found a positive correlation between noise intensity and AHI, and noise intensity and Ar +Aw index.

Because the spectral characteristics of snoring sounds are diverse, we chose to focus on analyzing the frequency (spectral) centroid, since it is a relatively simple generic scalar measure that reflects the center of mass of the spectrum. We found positive correlation between both breathing and snoring frequency centroid and AHI. This observation is reasonable, because higher values of frequency components are associated with narrower tubes[41]; indeed, OSA patients have a narrower upper airway. Our findings are supported by previous studies that explored spectral properties of snoring sounds.[21] Perez Padilla et al.[42] analyzed snoring sounds from a small sample of nonapneic heavy snorers and OSA patients. It was found that the ratio of power above 800 Hz to power below 800 Hz could be used to separate snorers from patients with OSA – the OSA snorers had higher frequencies. McCombe et al.[43] demonstrated that the OSA group displayed a substantially larger high frequency sound component than the non-OSA group. In another study Herzog et al.[44] found that patients with primary snoring revealed peak intensities between 100 and 300 Hz. OSA patients showed peak intensities above 1000 Hz; they confirmed the presence of a high frequency snoring sound pattern in OSA patients compared to simple snores.

We included subjects who represent a diverse population that is typical to our region, across a wide range of ages, BMI, AHI, but are not strictly a generalizable population. In our study, a large number of breathing and snoring events were analyzed from relatively small number of patients (n = 121). Further studies are needed to reinforce our findings on a larger sample of patients. We recognize that this study is based on a single PSG in each patient; further studies are required to determine individual night-to-night variability of breathing and snoring sound properties in laboratory and at-home settings. It is generally accepted that snoring and AHI are very dependent on the body position.[39] Further studies are needed to explore the effect of body position on breathing and snoring sound characteristics. We used a noncontact microphone to record breathing and snoring sounds because this approach enables more natural sleep that is not affected by equipment. Some studies used a contact microphone that was taped to the nasion[14] or to the trachea,[20] or used a microphone embedded in a face mask.[45] Using an audio-based approach, it is important to improve signal-to-noise ratio in order to capture the signals of interest (breathing and snoring sounds). To achieve this, we used an adaptive spectral subtraction technique that subtracted the estimated background noise,[10,25] which has minimal distortion effect on sound intensity.[46,47]

Clinical Implications

The "flood" of subjects presenting with snoring symptoms is a major challenge to decision makers and is governed by prevalence and level of awareness of snoring morbidity.[48] Reliable snoring reporting cannot be made based solely on a patient's (or partner's) history of noisy respiration during sleep,[12,14,16] or sleep laboratory technician reports[14]; a large portion of the subjects respond that they "do not know" if they snore.[49] The need for an agreed-upon approach to extract and analyze whole-night snoring sounds is of major importance to the field of sleep disordered breathing. Here, a novel and valid tool was used to systematically detect and analyze breathing and snoring sounds from a full night recording. This system can capture all the snoring sound events and, interestingly, on average the total number of snoring sounds that were captured by this system was less than 20% of the overall breathing sounds. This finding indicates that most breathing sound events are less than 50 dB. Snoring index and % snoring were higher in men, and in both genders snoring index and % snoring was higher in SWS. Snoring index, % snoring and snoring intensity did not correlate with AHI, however. Frequency centroid of breathing and snoring sounds correlate with AHI. Our data do not support the common belief that snoring intensity (dB) is higher for men than for women[13,21] and is correlated with AHI.[14,15,28] An important problem in dealing with objective respiratory sounds is the comparison of the data of various investigators and correct interpretation.[50] This study shows that a snore detection system can provide an objective quantitative measure for whole-night snore patterns. Further studies are needed both to reinforce our findings by recruiting subjects from primary care clinics and by validating this screening tool in an at-home environment.

Summary

Snoring is measured as part of routine PSG; however, there is no consensus regarding the details of measurement, signal analysis, and data interpretation. Here, we used an objective valid breathing and snoring feature analysis and provided evidence that although snoring index is sex dependent, snoring intensity is similar across sexes and is not correlated with AHI.

ABBREVIATIONS

AHI, apnea-hypopnea index
Ar, arousal
Aw, awakening
BMI, body mass index
dB, decibel
ESS, Epworth Sleepiness Scale
OSA, obstructive sleep apnea
PSG, polysomnography
SI, snoring index

REFERENCES

1. Colrain IM, Trinder J, Fraser G, Wilson GV. Ventilation during sleep onset. J Appl Physiol 1987;63:2067–74.
2. Trinder J, Whitworth F, Kay A, Wilkin P. Respiratory instability during sleep onset. J Appl Physiol 1992;73:2462–69.
3. Phillipson EA. Respiratory adaptations in sleep. Annu Rev Physiol 1978;40:133–56.
4. Orem J, Netick A, Dement WC. Breathing during sleep and wakefulness in the cat. Respir Physiol 1977;30:265–89.
5. White DP, Lombard RM, Cadieux RJ, Zwillich C. Pharyngeal resistance in normal humans: influence of gender, age, and obesity. J Appl Physiol 1985;58:365–71.
6. Pillar G, Malhotra A, Fogel R, et al. Airway mechanics and ventilation in response to resistive loading during sleep: influence of gender. Am J Respir Crit Care Med 2000;162:1627–32.
7. Malhotra A, Huang Y, Fogel RB, et al. The male predisposition to pharyngeal collapse: importance of airway length. Am J Respir Crit Care Med 2002;166:1388–95.
8. Perez-Padilla JR, West P, Kryger M. Snoring in normal young adults: prevalence in sleep stages and associated changes in oxygen saturation, heart rate, and breathing pattern. Sleep 1987;10:249–53.
9. Guilleminault C, Stoohs R, Duncan S. Snoring (I). Daytime sleepiness in regular heavy snorers. Chest 1991;99:40–8.
10. Dafna E, Tarasiuk A, Zigel Y. Automatic detection of whole night snoring events using non-contact microphone. PloS One 2013;8:e84139.
11. Lugaresi E, Crigonotta F, Coccagna G, Piana C. Some epidemiological data on snoring and cardiocirculatory disturbances. Sleep 1980;3:221–4.
12. Stoohs RA, Blum HC, Haselhorst M, et al. Normative data on snoring: a comparison between younger and older adults. Eur Respir J 1998;11:451–7.
13. Wilson K, Stoohs RA, Mulrooney TF, et al. The snoring spectrum acoustic assessment of snoring sound intensity in 1,139 individuals undergoing polysomnography. Chest 1999;115:762–70.
14. Hoffstein V, Mateika S, Anderson D. Snoring: is it in the ear of the beholder? Sleep 1994;17:522–6.
15. Hunsaker DH, Riffenburgh RH. Snoring significance in patients undergoing home sleep studies. Otolaryngol Head Neck Surg 2006;134:756–60.
16. Hoffstein V. Apnea and snoring: state of the art and future directions. Acta Otorhinolaryngol Belg 2002;56:205–36.

17. Duckitt W, Tuomi S, Niesler T. Automatic detection, segmentation and assessment of snoring from ambient acoustic data. Physiol Meas 2006;27:1047.
18. Cavusoglu M, Kamasak M, Erogul O, et al. An efficient method for snore/nonsnore classification of sleep sounds. Physiol Meas 2007;28:841.
19. Karunajeewa AS, Abeyratne UR, Hukins C. Silence–breathing–snore classification from snore-related sounds. Physiol Meas 2008;29:227.
20. Azarbarzin A, Moussavi Z. Snoring sounds variability as a signature of obstructive sleep apnea. Med Eng Phys 2013;35:479–85.
21. Pevernagie D, Aarts RM, De Meyer M. The acoustics of snoring. Sleep Med Rev 2010;14:131–44.
22. Fiz JA, Abad J, Jané R, et al. Acoustic analysis of snoring sound in patients with simple snoring and obstructive sleep apnoea. Eur Respir J 1996;9:2365–70.
23. Solà-Soler J, Fiz JA, Morera J, Jané R. Multiclass classification of subjects with sleep apnoea-hypopnoea syndrome through snoring analysis. Med Eng Phys 2012;34:1213–20.
24. Ben-Israel N, Tarasiuk A, Zigel Y. Obstructive apnea hypopnea index estimation by analysis of nocturnal snoring signals in adults. Sleep 2012;35:1299–305.
25. Dafna E, Tarasiuk A, Zigel Y. Sleep-wake evaluation from whole-night non-contact audio recordings of breathing sounds. PLoS One 2015;10:e0117382.
26. Dafna E, Tarasiuk A, Zigel Y. OSA severity assessment based on sleep breathing analysis using ambient microphone. Conf Proc IEEE Eng Med Biol Soc 2013;2013:2044–7.
27. Rosenwein T, Dafna E, Tarasiuk A, Zigel Y. Detection of breathing sounds during sleep using non-contact audio recordings. Conf Proc IEEE Eng Med Biol Soc 2014:2014:1489–92.
28. Maimon N, Hanly PJ. Does snoring intensity correlate with the severity of obstructive sleep apnea? J Clin Sleep Med 2010;6:475–8.
29. Metes A, Ohki M, Cole P, Haight JS, Hoffstein V. Snoring, apnea and nasal resistance in men and women. J Otolaryngol 1991;20:57–61.
30. Kump K, Whalen C, Tishler PV, et al. Assessment of the validity and utility of a sleep-symptom questionnaire. Am J Respir Crit Care Med 1994;150:735–41.
31. Tarasiuk A, Greenberg-Dotan S, Simon T, Tal A, Oksenberg A, Reuveni H. Low socioeconomic status is a risk factor for cardiovascular disease among adult obstructive sleep apnea syndrome patients requiring treatment. Chest 2006;130:766–73.
32. Simon-Tuval T, Reuveni H, Greenberg-Dotan S, et al. Low socioeconomic status is a risk factor for CPAP acceptance among adult OSAS patients requiring treatment. Sleep 2009;32:545–52.
33. Johns MW. A new method for measuring daytime sleepiness: the Epworth sleepiness scale. Sleep 1991;14:540–54.
34. Iber C, Ancoli-Israel S, Chesson AL, Quan SF. The AASM manual for the scoring of sleep and associated events: rules, terminology, and technical specifications. Westchester, IL: American Academy of Sleep Medicine, 2007.
35. Rohrmeier C, Herzog M, Ettl T, Kuehnel TS. Distinguishing snoring sounds from breath sounds: a straightforward matter? Sleep Breath 2014;18:169–76.
36. Koutsourelakis I, Perraki E, Zakynthinos G, et al. Clinical and polysomnographic determinants of snoring. J Sleep Res 2012;21:693–9.
37. Hoffstein V, Mateika JH, Mateika S. Snoring and sleep architecture. Am Rev Respir Dis 1991;143:92–6.
38. Peng H, Xu H, Gao Z, Huang W, He Y. Acoustic analysis of overnight consecutive snoring sounds by sound pressure levels. Acta Otolaryngol 2015;135:747–53.
39. Nakano H, Ikeda T, Hayashi M, Ohshima E, Onizuka A. Effects of body position on snoring in apneic and nonapneic snorers. Sleep 2003;26:169–72.
40. Bland JM, Altman DG. Statistical methods for assessing agreement between two methods of clinical measurement. Lancet 1986;1:307–10.
41. Kinsler LE, Frey AR, Coppens AB, Sanders JV. Fundamentals of acoustics, 3rd ed. New York, NY: John Wiley & Sons, 1982.
42. Perez Padilla JR, Slawinski E, Difrancesco LM, et al. Characteristics of the snoring noise in patients with and without occlusive sleep apnea. Am Rev Respir Dis 1993;147:635–44.
43. McCombe AW, Kwok V, Hawke WM. An acoustic screening test for obstructive sleep apnoea. Clin Otolaryngol 1995;20:348–51.
44. Herzog M, Schmidt A, Bremert T, Herzog B, Hosemann W, Kaftan H. Analysed snoring sounds correlate to obstructive sleep disordered breathing. Eur Arch Otorhinolaryngol 2008;265:105–13.
45. Alshaer H, Levchenko A, Bradley TD, et al. A system for portable sleep apnea diagnosis using an embedded data capturing module. J Clin Monit Comput 2013;27:303–11.
46. Karunajeewa AS, Abeyratne UR, Hukins C. Silence-breathing-snore classification from snore-related 46 sounds. Physiol Meas 2008;29:227–43.
47. Jané R, Fiz JA, Sola-Soler J, Mesquita J, Morera J. Snoring analysis for the screening of sleep apnea hypopnea syndrome with a single-channel device developed using polysomnographic and snoring databases. IEEE EMBC 2011;8331–3.
48. Reuveni H, Tarasiuk A, Wainstock T, Ziv A, Elhayany A, Tal A. Awareness level of obstructive sleep apnea syndrome during routine unstructured interviews of a standardized patient by primary care physicians. Sleep 2004;27:1518–25.
49. Sands M, Loucks EB, Lu B, et al. Self-reported snoring and risk of cardiovascular disease among postmenopausal women (from the Women's Health Initiative). Am J Cardiol 2013;111:540–6.
50. Dalmasso F, Prota R. Snoring: analysis, measurement, clinical implications and applications. Eur Respir J 1996;9:146–59.

SUBMISSION & CORRESPONDENCE INFORMATION

Submitted for publication May, 2015
Submitted in final revised form September, 2015
Accepted for publication September, 2015

Address correspondence to: Yaniv Zigel, PhD, Department of Biomedical Engineering, Faculty of Engineering Sciences, Ben-Gurion University of the Negev, P.O. Box 105, Beer-Sheva 84105, Israel; Tel: +972-8-6428372; Fax: +972-8-6428371; Email: yaniv@bgu.ac.il

DISCLOSURE STATEMENT

This was not an industry supported study. This research was supported by the Israel Science Foundation, grant No. 1403/15. The authors have indicated no financial conflicts of interest. All authors contributed equally to this work. This study was conducted in partial fulfillment of requirements for an MD degree for Asaf Levartovsky. The work for this study was performed at the Sleep-Wake Disorders Unit, Soroka University Medical Center, Department of Biomedical Engineering, Ben-Gurion University of the Negev. Israel.

Sleep-wake evaluation from whole-night non-contact audio recordings of breathing sounds

Dafna Eliran, Tarasiuk Ariel, and Zigel Yaniv.

PloS one 10.2 (2015): e0117382.

PLOS | ONE

RESEARCH ARTICLE

Sleep-Wake Evaluation from Whole-Night Non-Contact Audio Recordings of Breathing Sounds

Eliran Dafna[1], **Ariel Tarasiuk**[2], **Yaniv Zigel**[1]*

1 Department of Biomedical Engineering, Faculty of Engineering, Ben-Gurion University of the Negev, Beer–Sheva, Israel, **2** Sleep-Wake Disorders Unit, Soroka University Medical Center, and Department of Physiology, Faculty of Health Sciences, Ben-Gurion University of the Negev, Israel

* yaniv@bgu.ac.il

Citation: Dafna E, Tarasiuk A, Zigel Y (2015) Sleep-Wake Evaluation from Whole-Night Non-Contact Audio Recordings of Breathing Sounds. PLoS ONE 10(2): e0117382. doi:10.1371/journal.pone.0117382

Academic Editor: Ian McLoughlin, The University of Science and Technology of China, CHINA

Received: August 13, 2014

Accepted: December 22, 2014

Published: February 24, 2015

Data Availability Statement: All relevant data are within the paper and its Supporting Information files.

Funding: This work was supported by the Israel Ministry of Economics - the Kamin Program, award no. 46168 to YZ and AT. The funder had no role in study design, data collection and analysis, decision to publish, or preparation of the manuscript.

Competing Interests: The authors have declared that no competing interests exist.

Abstract

Study Objectives

To develop and validate a novel non-contact system for whole-night sleep evaluation using breathing sounds analysis (BSA).

Design

Whole-night breathing sounds (using ambient microphone) and polysomnography (PSG) were simultaneously collected at a sleep laboratory (mean recording time 7.1 hours). A set of acoustic features quantifying breathing pattern were developed to distinguish between sleep and wake epochs (30 sec segments). Epochs (n = 59,108 design study and n = 68,560 validation study) were classified using AdaBoost classifier and validated epoch-by-epoch for sensitivity, specificity, positive and negative predictive values, accuracy, and Cohen's kappa. Sleep quality parameters were calculated based on the sleep/wake classifications and compared with PSG for validity.

Setting

University affiliated sleep-wake disorder center and biomedical signal processing laboratory.

Patients

One hundred and fifty patients (age 54.0±14.8 years, BMI 31.6±5.5 kg/m2, m/f 97/53) referred for PSG were prospectively and consecutively recruited. The system was trained (design study) on 80 subjects; validation study was blindly performed on the additional 70 subjects.

Measurements and Results

Epoch-by-epoch accuracy rate for the validation study was 83.3% with sensitivity of 92.2% (sleep as sleep), specificity of 56.6% (awake as awake), and Cohen's kappa of 0.508.

Comparing sleep quality parameters of BSA and PSG demonstrate average error of sleep latency, total sleep time, wake after sleep onset, and sleep efficiency of 16.6 min, 35.8 min, and 29.6 min, and 8%, respectively.

Conclusions

This study provides evidence that sleep-wake activity and sleep quality parameters can be reliably estimated solely using breathing sound analysis. This study highlights the potential of this innovative approach to measure sleep in research and clinical circumstances.

Introduction

Polysomnography (PSG) is currently considered the gold standard for sleep evaluation [1]. This method requires a full night laboratory stay and subjects are connected to numerous electrodes and sensors, which are attached on the patient's body. Time series data are aggregated, processed, and visually examined or mathematically transformed in order to reveal insights about sleep-wake states and many aspects of physiology. Moreover, in routine sleep diagnostic procedures, sleep scoring is done manually by applying complex and visual scoring rules simultaneously on multiple signals acquired by applying contact sensors, e.g., electroencephalography (EEG), electrooculography (EOG), electromyography (EMG), electrocardiography (ECG), and respiratory activity [1,2]. PSG is time-consuming, tedious, and costly due to complexity and the need for technical expertise.

Currently, the biomedical engineering field of sleep disorders evaluation is on a "fast track" towards ambulatory sleep medicine [3–5]. In recent years, extensive effort has been devoted to seeking alternative simple cost-effective technologies for objective sleep-wake evaluation to increase accessibility in sleep disorders diagnosis. These new technologies are based on reduced-channels and sensors, and sophisticated computer-based algorithms [3,4,6–9]. Under the assumption that movement is associated with wake phase and lack of movement implies a sleep phase, clinicians and researchers have attempted to measure the binary presence of sleep or wake phases by measuring wrist movements using actigraphy [5,10,11]. Field-based activity monitoring devices are increasingly used as simple and cheap accelerometer-based devices [12–14]. Montgomery-Downs et al. [13] recently reported that this new technology has specificity limitations similar to those of a traditional actigraphy device. These devices consistently misidentify wake as sleep and thus overestimate both sleep time and quality.

It was long established that central control of ventilation and upper airway patency are strongly affected by transitions from sleep to wake and vice versa [4,15,16]. During sleep, there is a considerable increase of upper airway resistance [4,17,18] due to decreased activity of the pharyngeal dilator muscles [19,20]. This elevated resistance is reflected by amplification of air-pressure oscillations in the upper airways during breathing. These air-pressure oscillations are perceived as breathing sounds during sleep [21]. In contrast, during wakefulness, there is an increase in activity of the upper airway dilating muscles, hence decreased upper airway resistance and airway oscillations. Recently, we have shown that it is possible to accurately detect and distinguish a whole night's breathing sounds and snoring events from environmental noises [22]. We also demonstrated that the audio signal can be acquired using a non-contact sensor (ambient microphone), which minimizes the interruption of sleep [22,23]. However, little is known about whether acoustic-breathing parameters can distinguish between sleep-wake patterns.

Table 1. Subject anthropometric parameters.

Anthropometric parameters	System Design (n = 80)	System Validation (n = 70)	*p*
Gender (M/F)	54/26	43/27	.437
Age (yr)	52.8±13.1 (19–82)	55.4±16.8 (19–86)	.289
BMI (kg/m^2)	31.8±5.0 (20.2–52.1)	31.4±6.0 (16.8–47.2)	.400
ESS (score)	9.7±6.0 (0–23)	10.3±5.9 (0–24)	.539
AHI (events/hr)	19.0±18.3 (0.4–76.7)	17.9±16.8 (0.0–84.1)	.703

BMI—body mass index, ESS—Epworth sleepiness scale, AHI—apnea hypopnea index. All values are mean ± SD (range). *p* value was calculated using unpaired t-test for age, BMI, ESS, and AHI; and chi square for gender.

doi:10.1371/journal.pone.0117382.t001

We hypothesize that sleep-wake activity can be estimated using audio signal analysis of breathing sounds, which are altered by changes in ventilation and upper airway patency. The objectives of our work are: 1) to develop a breathing sound analysis (BSA) algorithm for distinguishing between sleep and wake phases using non-contact technology; 2) to reliably estimate sleep quality parameters such as total sleep time, sleep latency, sleep efficiency, wake after sleep onset time, and arousal index; and 3) to validate the proposed algorithms in comparison to PSG.

Methods

This article has online Supporting Information, S1 Dataset.

Setting

University affiliated sleep-wake disorder center and biomedical signal processing laboratory. This study analyzed routinely collected data and the data were analyzed anonymously; therefore informed consent was not required. The Institutional Review Committee of Soroka University Medical Center approved this study protocol (protocol number 10141). The institutional review board waived the need for written informed consent from the participants.

Subjects

We prospectively recruited 150 consecutive adults (aged 19 to 86 years, 53/97 female/male) referred to the Sleep-Wake Unit for routine PSG study for sleep disorders diagnosis, starting February 2008. We selected the first 80 subjects (patients) for the system design (training) study; the remaining 70 subjects (starting July 2010) were included in the blind validation study. See Table 1 and Table 2 for patient characteristics and sleep quality assessments.

PSG study

Subjects reported to the laboratory at 20:30 and were discharged at 06:00 the following morning. They were encouraged to maintain their usual daily routine and to avoid any caffeine and/or alcohol intake on the day of the study. The laboratory environment was sleep-friendly according to recommendations of the National Sleep Foundation [24].

PSG study (SomniPro 19 PSG, Deymed Diagnostic, Hronov, Czech Republic) included EEG (referential derivations, international 10–20 system, C3/A2, C4/A1, and O2/A1, O1/A2), EOG, EMG, ECG, respiratory activity (abdomen and chest effort belts—respiratory inductance plethysmography), oxygen saturation, and snore level intensity (Quest Technology 2700, Orlando, FL, USA). Simultaneous video monitoring was digitally recorded. PSG scoring includes sleep-wake pattern determined by a trained technician and underwent a second scoring by one

Table 2. Sleep Quality Parameters.

Sleep quality parameter	PSG System Design (n = 80)	PSG System Validation (n = 70)	BSA System Validation (n = 70)	Difference (BSA-PSG)	Absolute Error
TIB	422.2±54.5	428.5±51.0	428.5±51.0	–	–
(min)	(285.0–503.0)	(339.0–496.0)	(339.0–496.0)		
TST	333.0±52.4	339.1±60.3	343.0±54.1	7.6±48.1	35.8±32.8
(min)	(187.0–411.0)	(148.5–432.0)	(151–499)	(-105.0–119.5)	(1–119.5)
SL	30.1±29.8	36.0±23.6	34.4±18.6	-3.3±23.6	16.6±16.9
(min)	(0.5–100.0)	(0.5–125.0)	(1–125)	(-59.0–67.0)	(0–67)
SE	79.8±12.9	76.1±13.5	76.8±11.3	1.5±10.7	8.0±7.3
(%)	(39.4–97.5)	(30.9–97.7)	(31–95)	(-26.7–27.1)	(0.2–27.1)
WASO	46.1±39.2	56.9±46.0	60.7±39.3	7.8±41.3	29.6±29.7
(min)	(3.0–179.0)	(7.0–253.0)	(12–244)	(-117–116)	(0–117)
AwI	1.4±1.1	1.2±0.9	1.3±0.7	0.2±1.0	0.8±0.8
(events/hr)	(0.0–6.2)	(0.0–2.8)	(0.1–2.8)	(-1.3–3.9)	(0–3.9)

TIB—Time in bed; PSG—Polysomnography; BSA—breathing sound analysis; TST—Total sleep time; SL—Sleep latency; SE—Sleep efficiency; WASO—Wake time after sleep onset; AwI—Awakening index. The differences between the sleep quality parameters as measured by PSG and BSA are presented to show the direction of any bias. Absolute error (difference) was presented to quantify the overall magnitude of differences among measurements. Values are mean ± SD (range) between subjects.

doi:10.1371/journal.pone.0117382.t002

of the investigators (AT); scoring followed the American Academy of Sleep Medicine criteria [1]. The scoring included labeling of each (30 sec) epoch as sleep or wake using the PSG signals—this was used as the gold-standard labeling for the training and validation of the proposed breathing sound analysis system. For labeled data visualization see Figure A in S1 Dataset.

Study protocol

We developed a system for sleep-wake pattern estimation and sleep quality evaluation. The system is composed of a non-contact microphone, digital audio recording device, and an algorithm that estimates sleep and wake states from a full night audio recording (Fig. 1). Using concepts from audio signal processing and pattern recognition techniques, acoustic properties of breathing were classified into two states: sleep and wake. Breathing sounds events were automatically located, segmented, and isolated using our breathing detection system [22] that is capable of detecting even low intensity (>20 dB) breathing sounds. This system was validated to distinguish breathing sounds from irrelevant noises, such as movements, linen noises, speech, and other interferences. Using the detected breathing events and the calculated energy signal from the audio recordings, eight acoustic features were developed and extracted per subject; these features express the acoustic properties of breathing events and emphasize the differences between sleep and wake phases. These eight features were used for training an AdaBoost [25] classifier configured as a time-series model that aimed to classify each 30-sec epoch as sleep or awake. Finally, sleep quality parameters were estimated (i.e., total sleep time, sleep latency, sleep efficiency, wake time after sleep onset, and awakening index). Validation study was performed prospectively on a separate group of consecutive subjects for whom the breathing analysis was performed using a blind design.

The experimental system

A digital audio recorder device (Edirol R-4 pro, Bellingham, WA, USA) with a directional microphone (RØDE, NTG-1, Silverwater, NSW, Australia) placed at a distance of 1 meter above the

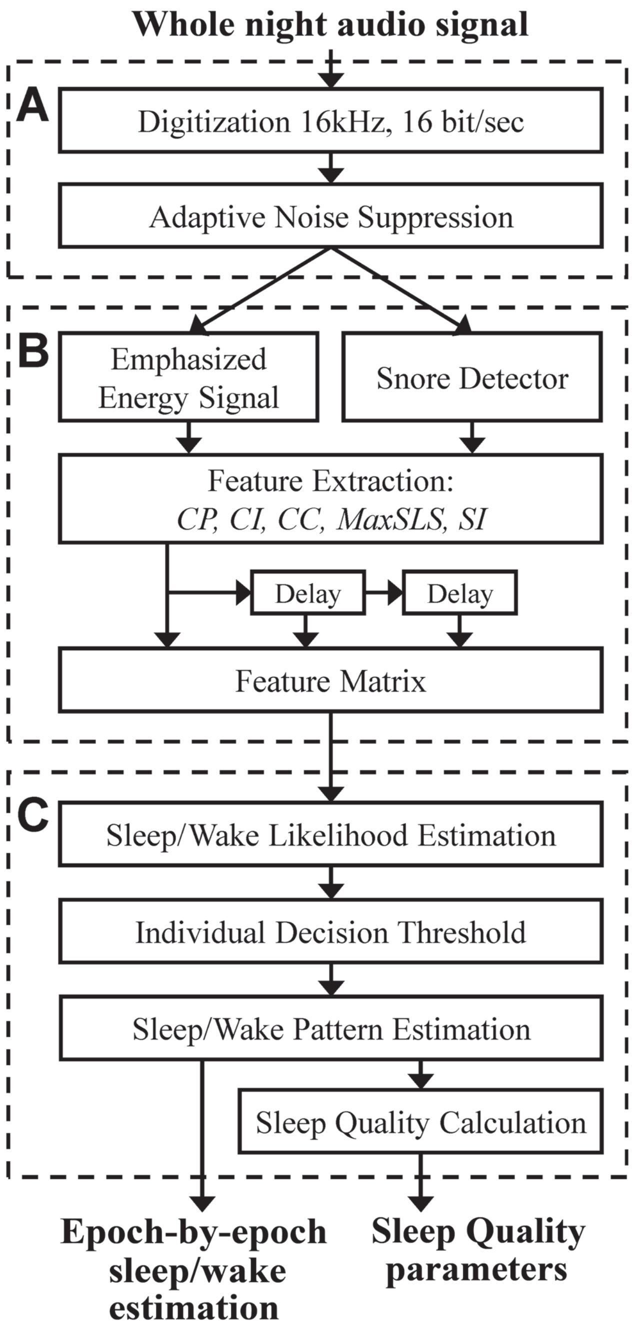

Fig 1. Block diagram of the proposed system. The system consists of three main stages: A) Preprocessing and signal enhancement. B) Feature extraction. C) Sleep/wake Estimation.

doi:10.1371/journal.pone.0117382.g001

subject's head, was used for acquiring the audio signals. Fig. 2A and E illustrates examples of audio signal (12-sec interval). Data was acquired from a 65-year-old female, body mass index (BMI) of 36 kg/m^2, apnea-hypopnea index (AHI) of 12 events/hr. The audio signals were stored along with the PSG signals for later analysis. Each audio signal was synchronized with the PSG study at 15 ms resolution according to cross-correlation technique between the PSG (snore intensity level channel) and the digital audio signal (after matching energy sampling rate).

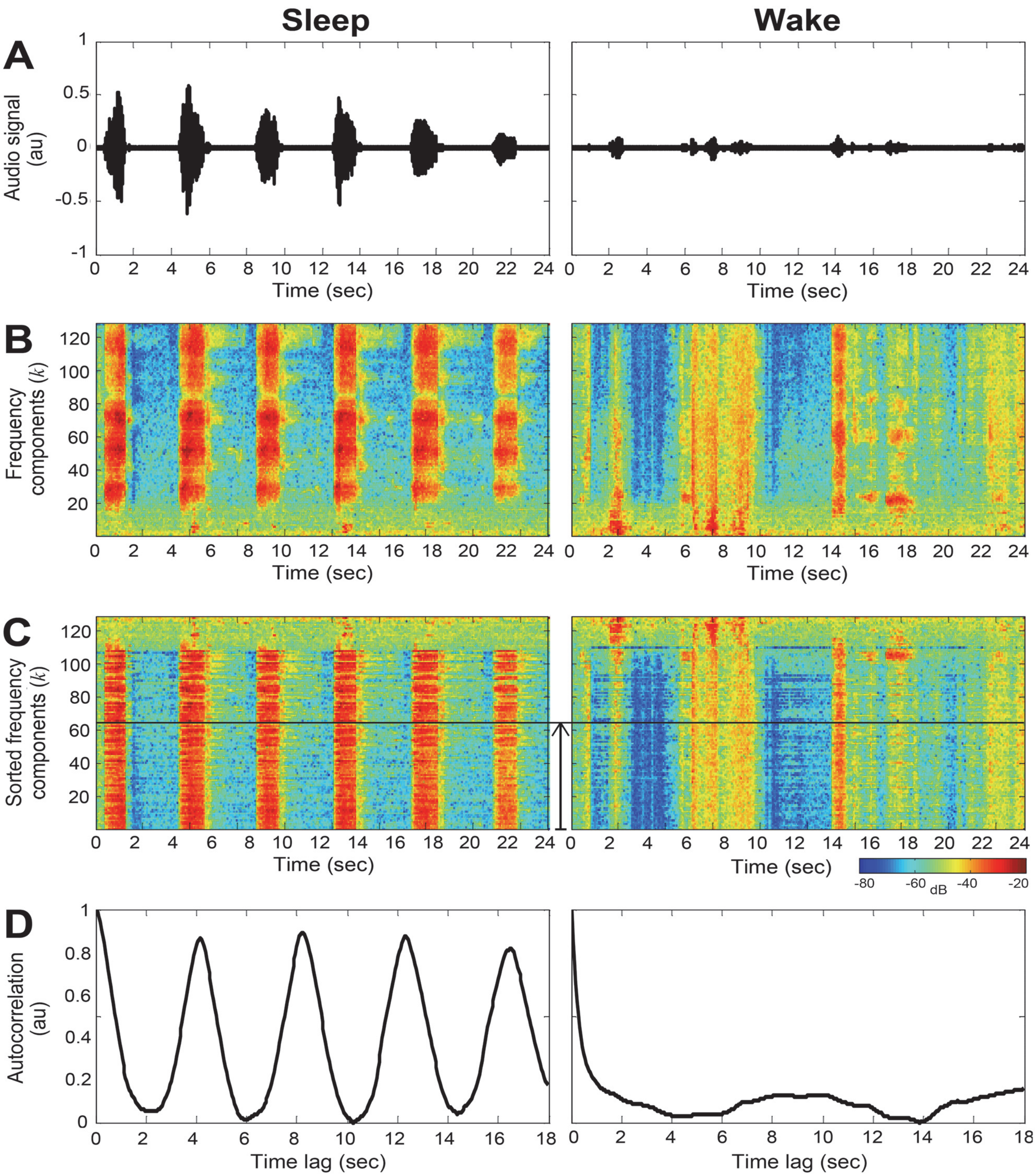

Fig 2. An example of 24-sec interval of audio signal collected from 65-year-old female, BMI 36, AHI 12. Left column illustrates data collected during sleep; right column illustrates data collected during wake. (A) Audio signal following noise suppression. (B) The corresponding spectrogram (frequency components) of the audio signal in (A). (C) The sorted frequency components according to periodicity measure. (D) The enhanced autocorrelation of the interval calculated from the lower half of the sorted frequency components (C), visualized by the vertical solid line.

doi:10.1371/journal.pone.0117382.g002

$$\text{(A)}\quad \mathbf{t_p} = \text{peaks}\left\{R_i(t)\right\};\ \mathbf{t_p} = [t_1, t_2, \ldots, t_p]$$

$$\text{(B)}\quad CP_i = t_1 \times Fr$$

$$\text{(C)}\quad CI_i = R_i(t_1)$$

$$\text{(D)}\quad CC_i = \text{std}\left\{R_i(t_1), R_i(t_2), \ldots, R_i(t_P)\right\}$$

$$\text{(E)}\quad MaxSLS_l = \max\left\{SLS_j^l\right\}$$

$$\text{(F)}\quad SI_l = \underset{j}{\text{sum}}\left\{SLS_j^l > SLS_{TH}\right\} \times 120$$

Fig 3. Summary of the equations used for feature extraction process. (A) The function: peaks{·} stands for an operator that finds positive peaks and returns their time-frame index. std{·} stands for standard-deviation function. Index *i* represents the interval of interest (12 or 24 sec), index *j* represents the j^{th} snore index within the l^{th} epoch index. (B) Cycle period feature. (C) Cycle intensity. (D) Cycle consistency. (E) Maximum snore likelihood score in epoch. (F) Snore index.

doi:10.1371/journal.pone.0117382.g003

The sleep-wake pattern estimation algorithm

To estimate sleep/wake activity from audio signal, several steps must be applied. Fig. 1 is the block diagram of the proposed sleep-wake pattern estimation algorithm for the design and validation phases of the study. The algorithm is composed of three basic steps: A) pre-processing, B) feature extraction, and C) sleep-wake pattern estimation. This last step (C) is designed to classify each 30-sec epoch as sleep or awake. It includes classification parameters that were estimated (trained) in the design phase; the training was performed using labeled epochs (sleep and wake) that were derived from the PSG study. The outputs of this algorithm are the whole-night sleep-wake pattern and sleep quality parameters.

Preprocessing & noise reduction

For design and validation phases, the acquired audio signals were digitized and stored at 16 kHz, 16 bits per sample. Each audio signal underwent adaptive noise suppression (spectral subtraction) process based on the Wiener-filter. The use of the noise suppression in this system is crucial, since it is designed to emphasize low intensity breathing sounds while suppressing any stationary background noise, such as air-conditioner or fan noises. This process relies on automatically and adaptively tracking background noise segments in order to estimate their spectra and subtracting them from the audio signal [26]. For more information see preprocessing section in the supplements part of Dafna et al [22].

Feature extraction

Eight features were extracted from the full-night audio signal; these features can be divided into 2 categories: A) *breathing pattern*—which is based on periodicity of the energy signal, and B) *Snore properties*—which are based on snore likelihood scores (SLS) [22]. Fig. 3 contains the equations used for the feature extraction process.

A) Breathing pattern—these features are designed to capture and quantify breathing pattern such as breathing cycle period, period intensity, and consistency. Since the breathing pattern changes over time, the audio signal is divided into (fixed-length) time intervals. In order to calculate breathing pattern features such as breathing rate, each audio interval should consist of at least two breathing cycles. Therefore we chose an interval length of 12 seconds. In each time interval the autocorrelation of the audio signal is calculated. The autocorrelation function is a mathematical tool for finding repeating patterns; informally, it measures the similarity between signal samples as a function of time lag between them [27]. Since the audio signal may contain noises in different frequencies, the autocorrelation was calculated selectively from part of the spectrum in order to emphasize the periodicity of the interval. For this, a spectrogram, $X(k,n)$, was calculated for each interval (Fig. 2B). The spectrogram of the i^{th} interval, $X_i(k,n)$, presents the running frequency (spectral) components that are calculated from 60-msec signal frames (k is the frequency component index and n is the time frame index). In order to find repeating breathing patterns, we keep the most periodic information in the spectrogram using the autocorrelation function. Therefore, the autocorrelation is calculated separately for each frequency component:

$$R_i(k,t) = \frac{1}{N-t}\sum_{n=1}^{N-t} X_i(k,n) \times X_i(k,n+t), \tag{1}$$

where t is the time-frame-lag index and N represents the total number of frames in the interval.

For each time interval, we calculate an emphasized version of autocorrelation function. The emphasized autocorrelation function, $R_i(t)$, was calculated as an average function from only the most periodic frequency components according to the $R_i(k,t)$. For that, we sorted the frequency components according to the first peak amplitude value as criterion (see Fig. 3A), and summed the top 50% components (see Fig. 2C). In this stage, the i^{th} interval is represented with a single function of emphasized autocorrelation, $R_i(t)$ (see Fig. 2D). From every 12 sec time interval, three features are extracted using the emphasized autocorrelation (see equations in Fig. 3): **Cycle period (*CP*)**—which is the location of the first peak, t_1, excluding the zero-lagged peak; **Cycle intensity (*CI*)**—which is the corresponding peak amplitude, $R_i(t_1)$; and **Cycle consistency (*CC*)**—which measures how much the breathing pattern is homogenously periodic and consistent within an interval. The more harmonic and repetitive the interval, the lower this feature's value, and vice versa. The same "breathing pattern" feature extraction process is repeated for 24 sec intervals of the audio signal. Fig. 4 presents an example of the running autocorrelation (used for breathing pattern features extraction) and the running snore properties calculated from a whole-night audio recording. When observing the acoustic energy during sleep (Fig. 4B), breathing becomes more energetic and noisy (sometimes referred to as snores) compared to wake phase. The probability of snores (SLS distribution, Fig. 4C) is also increased during sleep (SLS>0). The running autocorrelation of the breathing pattern, $R_i(t)$, is shown in Fig. 4D; the running autocorrelation is composed of autocorrelation functions (Fig. 2D) calculated for each epoch (30 sec). Note that sleep episodes exhibit more "zebra-like" stripes patterns compared to the more chaotic one in wake phases, meaning that during sleep, respiration is more periodic, as expected. Fig. 5 illustrates the association between the different vigilance states and the main acoustic features, extracted from specific locations (epochs from Fig. 4C, D). It is clearly notable that there is a similar autocorrelation function during sleep epochs (Fig. 5E, F) in contrast to wakefulness (Fig. 5D). In order to match the *breathing pattern*'s features' time-resolution (24 sec and 12 sec) to the epoch resolution (i.e., 30 sec, the same as the PSG's hypnogram), the *breathing pattern* features were linear-interpolated to be sampled at 30 sec resolution.

B) Snore properties—these features are based on our previously designed snore detector [22]. Each energetic acoustic event from the audio signal is assigned an SLS that represents its probability of being a snore event; the more positive this score is, the greater its probability to be a snore event. Fig. 4C shows the running SLS distribution (calculated for each 30 sec epoch). Note that in Fig. 4C during sleep phases there are more SLS values that are above zero (above the horizontal dashed line), indicating the presence of snoring events and, consequently,

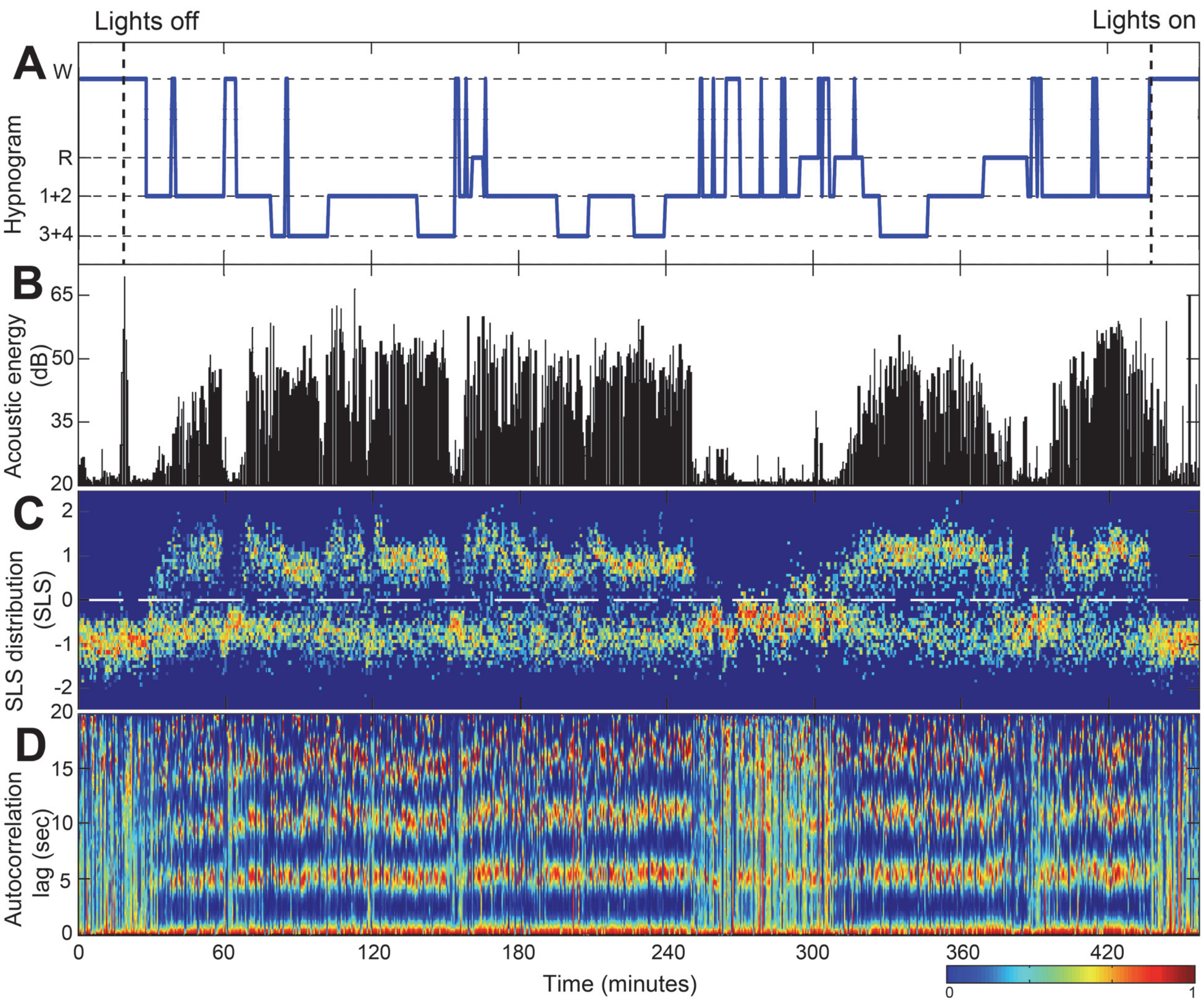

Fig 4. Example of whole night recording and main features. (A) Hypnogram determined by PSG. (B) Audio energy signal after noise reduction. (C) SLS distribution. (D) Autocorrelation of the audio signal over time. Warmer colors represent higher values of SLS distribution (C), and higher values of autocorrelation (D). Note that in (C) during sleep phases there are more SLS values that are above zero (above the horizontal dashed line). In these sleep phases, the autocorrelation (in D) exhibits a more homogeneous stripes pattern compared to the more chaotic behavior in wake phases. For more detailed illustration of the SLS and autocorrelation values during difference vigilance states, see Fig. 5. Data was collected from 52-year-old male, BMI 31. W—wake; R—rapid eye movement (REM); 1+2, 3+4—light and deep non-REM sleep stages, respectively. SLS—snore-likelihood score.

doi:10.1371/journal.pone.0117382.g004

evidence of sleep phase. Fig. 5 left illustrates the association between the different vigilance states and the SLS distribution. It is clearly noticeable that there is a similar SLS histogram during sleep phases (Fig. 5B, C) in contrast to wakefulness (Fig. 5A). Two features were extracted using this SLS parameter: ***Maximum SLS*** in epoch ($MaxSLS_l$) and ***Snore Index*** (SI_i). $MaxSLS_l$ feature is calculated as the maximum of SLS within 30-sec epoch l (see Fig. 3E). The rationale behind this feature is to determine the epoch's maximum likelihood to contain a snore event. The higher this score is, the more probable this epoch is to contain a sleep episode. The second feature is *snoring index* (SI_i) [22], which is the estimation of the number of snores per hour; this estimation is based on counting the snore events within the l^{th} epoch and multiplying by the number of epochs per hour; see Fig. 3F for equation details. It is worth noting that each feature was developed to capture breathing sound while minimizing the effect of sound intensity

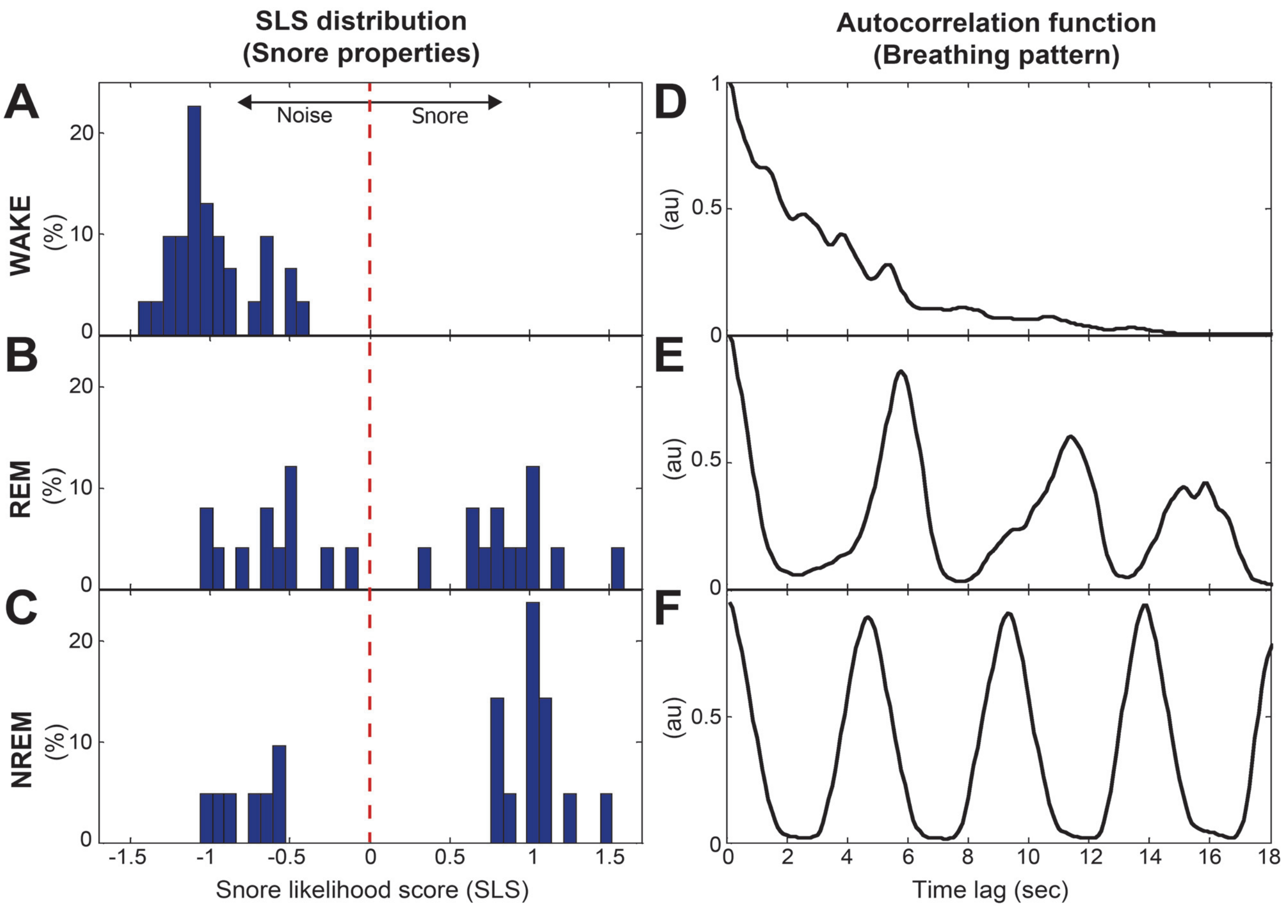

Fig 5. Detailed presentation of the SLS and autocorrelation values during different 30 sec epochs of wake (A, D), REM (B, E), and NREM (C, F). Left panel (A-C): SLS distribution (snore properties), right panel (D-F): autocorrelation function (breathing pattern periodicity). Data is presented from three epochs (wake, REM, NREM) derived from Fig. 4C and D. The dashed line in the left panel represents the decision threshold for snore detection (SLS = 0); higher SLS values indicate greater likelihood of snore event. REM—rapid eye movement, NREM—non-REM.

doi:10.1371/journal.pone.0117382.g005

including body posture and distance to microphone [22]. Table 3 summarizes the extracted features.

Sleep/wake likelihood estimation

Using the eight sleep/wake features, sleep-wake likelihood (SWL) curve is estimated for each patient at 30 second epoch resolution. In this study we chose AdaBoost classifier [25] as a time-series model in which each feature was fed along with two previous epochs (at l-1 and l-2). In this way, the sleep/wake estimation of the current epoch is supported with the previous epochs' estimations; this approach is suitable for a quasi-stationary process such as sleep and wake phases. Fig. 1B presents a visualization of the time series feature matrix configuration. Generally, a k-order AdaBoost classifier involves k binary discriminations in a d-dimensional feature space (in our case d = 24, 8×3), based on the true labeling of the epochs. In the design phase, the classifier parameters were estimated to discriminate two classes: sleep and awake. Sleep was assigned the value '-1' and wake with '+1' (arbitrarily to match the hypnogram), hence producing a linear estimation within that range, i.e., a sleep epoch is more likely to have a negative score than a wake phase. The optimal order was found to be k = 100 empirically. Fig. 6 shows a typical example of SWL curve estimated from whole-night audio recording of a subject from

Table 3. Extracted features.

Category	Feature name
Breathing pattern (12 sec)	Cycle period$_{12}$ (CP^{12})
	Cycle intensity^{12} (CI^{12})
	Cycle consistency^{12} (CC^{12})
Breathing pattern (24 sec)	Cycle period^{24} (CP^{24})
	Cycle intensity^{24} (CI^{24})
	Cycle consistency^{24} (CC^{24})
Snore properties (30 sec)	Maximum SLS (*MaxSLS*)
	Snore index (*SI*)

doi:10.1371/journal.pone.0117382.t003

the validation design set. Higher values of SWL indicate increased likelihood towards wake state. Note the impressive similarity between the Hypnogram (Fig. 6B) and the proposed acoustic-based SWL curve (Fig. 6C). It should be emphasized that there is a considerable increase in SWL values as soon as wake initiates and it declines immediately during sleep onset.

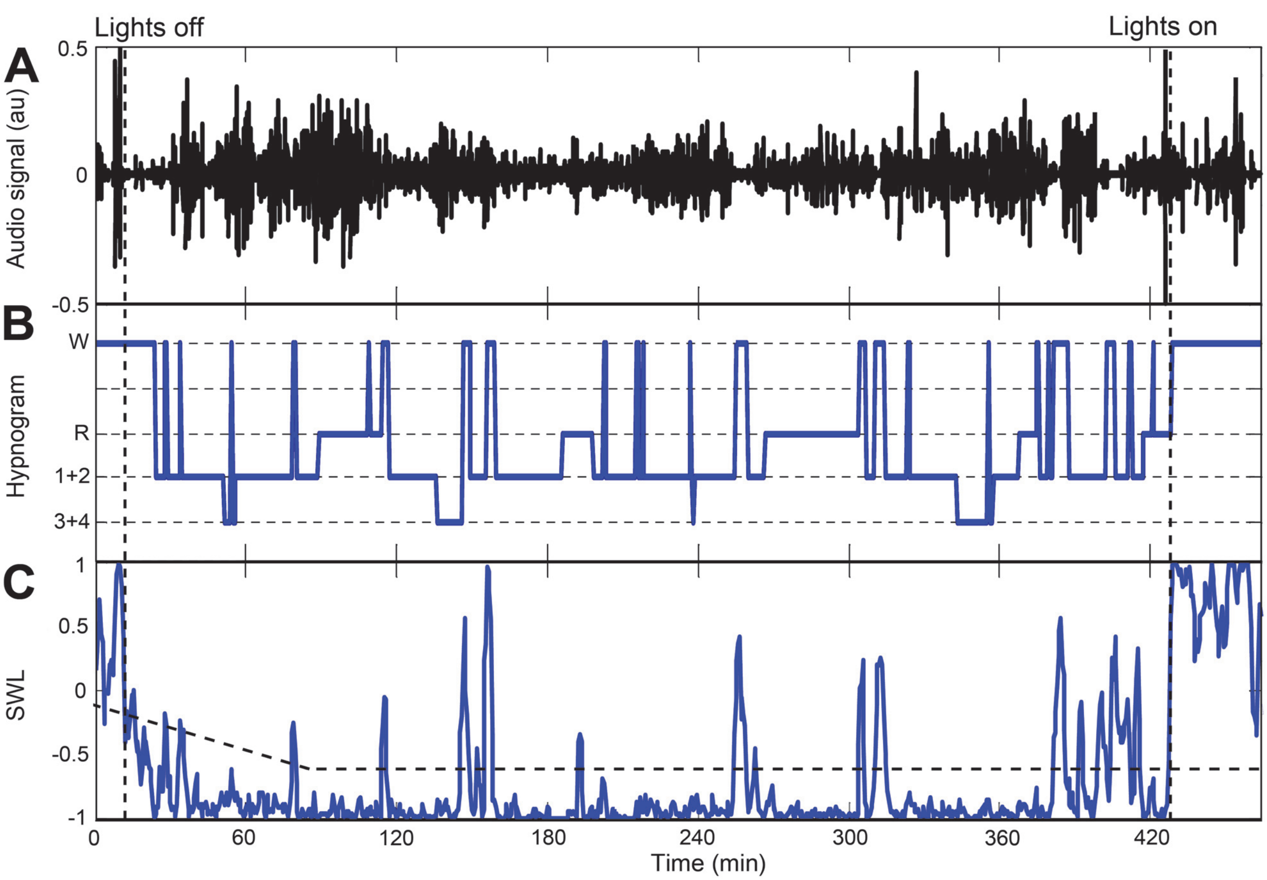

Fig 6. Example of sleep-wake likelihood (SWL) score curve. (A) Audio signal of whole-night recording. (B) Hypnogram. (C) The estimated whole-night SWL score curve. SWL was calculated using the eight acoustic features fed into AdaBoost classifier. Higher values of SWL indicate increased likelihood towards wake state. When focusing on sleep and wake phases, note the similarity between the hypnogram (B) and the SWL (C). The horizontal dashed line represents the corresponding individual decision threshold over time; for more details see main body. Data was collected from 52-year-old male, BMI 31.

doi:10.1371/journal.pone.0117382.g006

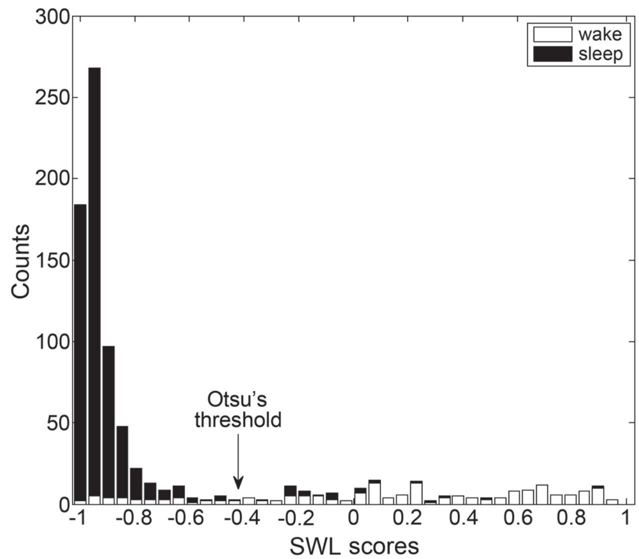

Fig 7. Example of individual decision threshold determination. Stacked-bar-histogram of SWL scores of one subject. Black bars represent sleep epoch scores and white bars represent wake epoch scores. The individual threshold (arrow) was calculated using Otsu's method [28].

doi:10.1371/journal.pone.0117382.g007

Individual decision threshold

Since breathing properties can vary between subjects, we found that applying an individual decision threshold improved system performance. Firstly, for each subject, a likelihood threshold (L_{TH}) was calculated using his SWL epoch scores (example presented in Fig. 6C). These SWL values' distribution (histogram) is considered to behave as a bi-modal distribution, since it is assumed to be composed of sleep and wake phases. The threshold was determined using Otsu's method [28], which searches for the threshold that minimizes the intra-class variance (see Fig. 7). Secondly, according to our preliminary results, we modified the fixed L_{TH} to better cope with pinpointing the beginning of sleep, as it may considerably affect estimation of sleep parameters. Therefore, for the first 90 minutes of the recording, the threshold gradually decreases, starting from a higher value towards L_{TH}, in order to reduce false detection of sleep epochs:

$$L_{TH}(t) = L_{TH} + \max\{0.5 - t/360, 0\}, \tag{2}$$

where t represents the time index of the epoch, and 360 is a parameter empirically obtained using the design SWL distribution. Note that higher L_{TH} scores will reduce false detection of sleep episodes. See Fig. 6C for demonstration.

Sleep quality parameterization

Using the detected sleep-wake states, we calculated five sleep quality parameters: **1) *Total sleep time*** (*TST*)—actual sleep time in a sleep period; equal to total sleep period less movement and awake time. Total sleep time is the total of all REMS and NREMS in a sleep period. **2) *Sleep latency*** (*SL*)—time period measured from "lights out", or bedtime, to the beginning of sleep. We measured from start of the recording. **3) *Sleep efficiency*** (*SE*)—The ratio of total sleep time to time in bed. **4) *Wake time after sleep onset*** (*WASO*)—the time spent awake after sleep has been initiated and before final awakening. **5) *Awakening index*** (*AwI*)—the average awakening per hour of time in bed.

(A) $$Sensitivity = \frac{TP}{TP + FN}$$

(B) $$Specificity = \frac{TN}{TN + FP}$$

(C) $$PPV = \frac{TP}{TP + FP}$$

(D) $$NPV = \frac{TN}{TN + FN}$$

(E) $$Accuracy = \frac{TP + TN}{TP + TN + FP + FN}$$

(F) $$\kappa = \frac{Accuracy - Pe}{1 - Pe}$$

where:

(G) $$Pe = \frac{(TP+FP)\times(TP+FN)+(TN+FP)\times(TN+FN)}{(TP+TN+FP+FN)^2}$$

Fig 8. Epoch-by-epoch sleep-wake performance evaluation equations. All of these equations rely on four basic classification parameters: True positive (TP), true negative (TN), false positive (FP), and false negative (FN). We denote 'sleep' as positive and 'wake' as negative. PPV and NPV stand for positive and negative predictive values, respectively. κ—the Cohen's kappa coefficient. *Pe*—probability of agreement by chance.

doi:10.1371/journal.pone.0117382.g008

Data and statistical analyses

Audio signal processing and statistical analyses were performed using MATLAB (R-2012b, The MathWorks, Inc., Natick, MA, USA). Both the system design study ($n = 80$) and the validation study ($n = 70$) had similar data handling protocols. A sample size of 64 subjects was calculated to provide a statistical power of 0.80 ($\alpha = 0.05$) in order to achieve >0.45 Cohen's kappa agreement (sleep/wake estimation) for each subject. Therefore, 70 subjects were recruited for the validation study. PSG, demographic, and audio data were compared between design and validation study groups using unpaired two-tailed student t-test or χ^2 test. Epoch-by-epoch sleep-wake estimation performances were calculated using sensitivity (Fig. 8A), specificity (Fig. 8B), positive and negative predictive values (Fig. 8C and D), accuracy (Fig. 8E), and Cohen's kappa (Fig. 8F). We denote "sleep" as positive of interest and "wake" as negative. Hence *TP* (true positive) and *TN* (true negative) represent the counts of true detection of sleep as sleep and wake as wake, respectively. In addition, performances for different working points were obtained from a receiver-operating curve (ROC) and the area under its curve (AUC). Cohen's kappa values are usually associated with five agreement categories [27] (0–0.2 is slight, 0.2–0.4 is fair, 0.4–0.6 is moderate, 0.6–0.8 is substantial, and 0.8–1 is almost perfect). To assess how parameters such as age, gender, BMI, AHI, and signal-to-noise-ratio (SNR) affected the kappa agreement of our BSA system, we tested the person correlation coefficient for each of these parameters.

In the analyses, first, for each subject in the validation dataset, we performed epoch detection performances as described above. A global average and standard deviation were calculated among all validation subjects. Second, based on the estimated epochs, for each subject, we calculated the five sleep quality parameters and compared to PSG. Then a global average and standard deviation were calculated among subjects. For better visualization of system performance, we presented each subject's sleep quality parameter using Bland-Altman plot method [29].

Results

Subjects and PSG characteristics

One hundred and fifty subjects referred to PSG evaluation of sleep disorders were included in our study (Table 1). An average of 7.1±0.9 hours of audio signals were recorded from each subject with no significant differences between design and validation studies; a total of 562.9 hours and 499.9 hours were analyzed in the design and validation studies, respectively (Table 2). No significant differences in subject anthropometric parameters (Table 1) and sleep quality parameters (Table 2) were found between system design and validation study groups. As a group, both design and validation patients have moderate obstructive sleep apnea and fragmented sleep. In this study we included 127,668 manually examined epochs: 59,108 design study and 68,560 validation study. Figure A in S1 Dataset illustrates individual big-data visualization for the design study (n = 80) and validation study (n = 70).

Feature extraction

Eight acoustic features were developed in this study (Table 3). These features were calculated at different interval durations in order to capture breathing sounds and to extract sleep-wake pattern information. These features are based on short- and long-term analyses, and later were adjusted to construct a time-series feature matrix at a 30 sec epoch resolution. Fig. 6D shows an example of sleep-wake prediction according to each of the developed features from a 52-year-old male, AHI 22 events/hr, BMI 31 kg/m^2. Note that each feature exhibits the actual sleep-wake pattern determined by PSG.

Fig. 9 presents evaluation (kappa values) of each individual feature to distinguish between sleep and wake epochs using the study validation dataset. Each feature is presented as a box-plot, measuring the quartile distribution of kappa agreements of sleep-wake epochs among various patients. Note the relatively wide range of kappa values, indicating the large variability between subjects. The median kappa agreement of each feature is between 0.2 and 0.4. However, when combining all features, the overall kappa agreement is improved to a narrower distribution, i.e., median kappa of 0.5 and quartiles of 0.4 to 0.7.

Sleep/wake pattern estimation

During the design phase, an AdaBoost model was trained on the entire design dataset in order to classify sleep and wake epochs. Based on the SWL score for each subject, an individual threshold was picked to better fit the global sleep-wake model to the individual. Each subject's scores (for sleep and awake epochs) were shifted using this threshold value, allowing adaptation for the global sleep-wake model to better fit the individual subject. Moreover, global alignment of the scores from all the subjects will allow standardization and overall evaluation of system performance. On average, the individual L_{TH} improved system accuracy by 3%. Fig. 6C shows a typical example of the SWL curve of an individual; the horizontal dashed line represents the calculated L_{TH} score.

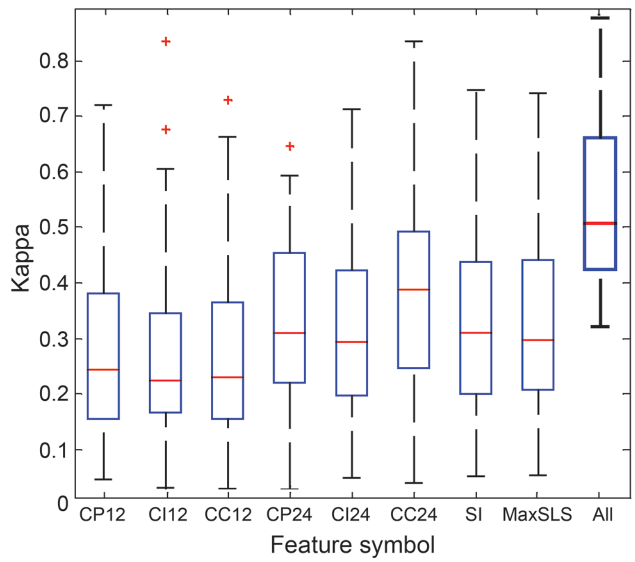

Fig 9. Feature performances. Boxplot representing the distribution of kappa agreement values for all subjects within the validation dataset using Otsu's threshold [28]. The rightmost box represents the agreement derived using all features as a group (using the AdaBoost classifier).

doi:10.1371/journal.pone.0117382.g009

Epoch-by-epoch system performances (sleep/wake estimation) were analyzed for each subject (individual performances). Based on the individual performances, we calculated a global mean and standard deviation between subjects. Table 4 shows the comparison between the proposed BSA and PSG for the entire group of subjects using the validation dataset. The overall (global) accuracy between subjects of the BSA system was 0.833. The sensitivity (detecting sleep epochs as sleep epochs) was 0.922 and the specificity was 0.566. Cohen's kappa agreement was 0.508. The ROC curve (Fig. 10, solid line) has an area under the curve of 0.829. Accuracy, sensitivity, specificity, positive and negative predictive values, area under the curve, and Cohen's kappa were also calculated for the entire pool of validation epochs (regardless of subjects' epoch origin), and no discernable differences were observed between the two cases (data not shown). To assess how parameters such as age, gender, BMI, AHI, and SNR affected the kappa agreement of our breathing sound analysis (BSA) system, we tested the Pearson correlation coefficient for each of these parameters. Our calculations reveal negligible correlations (<0.1) for age, gender, BMI, and AHI. Correlation between system performances and breathing SNR reveals positive correlation of 0.37 ($p<.001$) (Figure B in S1 Dataset).

Table 4. Performance of BSA vs. PSG classification (epoch-by-epoch).

Performance	SEN	SPC	PPV	NPV	ACU	AUC	kappa
Subject's Mean	.922	.566	.859	.723	.833	.829	.508
Subject's standard deviation	.078	.179	.102	.184	.076	.065	.156

SEN = sensitivity; SPC = Specificity; PPV = Positive predictive value; NPV = negative predictive value; ACU = accuracy; AUC = Area under ROC curve; kappa = Cohen's kappa coefficient. The mean and standard deviation values represent the distributions of subject's performances (validation dataset).

doi:10.1371/journal.pone.0117382.t004

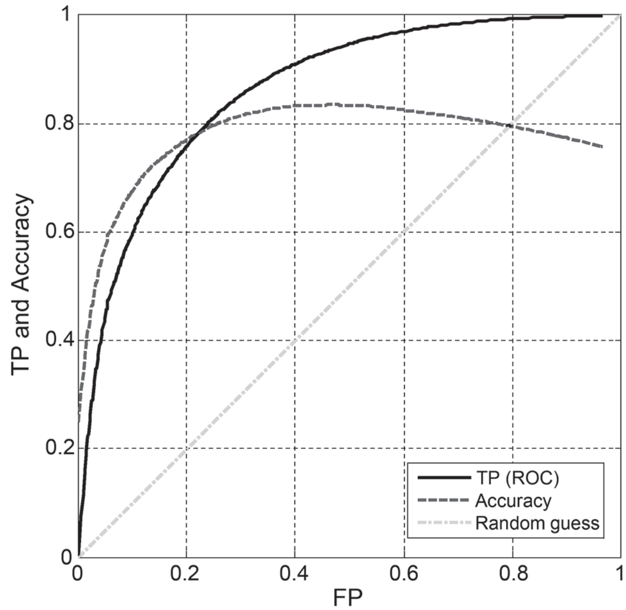

Fig 10. Receiver operating characteristics (ROC) plot of epoch-by-epoch sleep/wake estimation system performances. Solid line represents the TP of the system as a function of FP, the dashed line represents the accuracy as a function of FP. Dot-dashed line represents the random-guess performance. TP—True positive of detecting sleep epochs. FP—false positive.

doi:10.1371/journal.pone.0117382.g010

Sleep quality parameterization

No significant differences in sleep quality parameters as measured by PSG and BSA were found (Table 2). The differences between the sleep quality parameters as measured by PSG and BSA are presented to show the direction of any bias. The average difference between SPG and BSA were: TST (7.6±48.1 min), SL (-3.3±23.5 min), SE (1.5±10.7%), WASO (7.8±41.3 min), and AwI (0.2±1.0 per hr). Moreover, the absolute error (differences) was presented to quantify the overall magnitude of differences among measurements. The absolute error between SPG and BSA were: TST (35.8±32.8 min), SL (16.6±16.9 min), SE (8.0±7.3%), WASO (29.6±29.7 min), and AwI (0.8±0.8 per hr). Fig. 11A-E shows evaluation of five sleep quality parameters: TST, SL, SE, WASO, and AwI, according to the Bland-Altman plot. Examining the Bland-Altman plots and comparing the proposed breathing sound analysis (BSA) approach versus PSG, we found good agreement. All sleep quality parameters show no major consistent bias (Fig. 11 and Table 2). The plots also show (for SL, WASO, and AI) that the BSA values are closely matched to PSG in the left part of the plot, and therefore present less difference when the parameter values are relatively small; this implies reliability of the estimated parameters.

Discussion

In this paper a novel method for evaluation of sleep-wake patterns using non-contact microphone is proposed. This method utilizes analysis of breathing sounds and machine-learning techniques in order to reliably estimate sleep-wake activity and to reliably estimate sleep quality parameters. The main idea beyond this approach is that central control of ventilation and upper airway patency are strongly affected by sleep and wake activity [4,15]. The human upper airway is a complicated structure comprising a number of muscles whose functional integration is essential for several complex tasks including speech [30] and breathing [20]. From the respiratory perspective, the primary goal of these pharyngeal muscles is to keep the airway

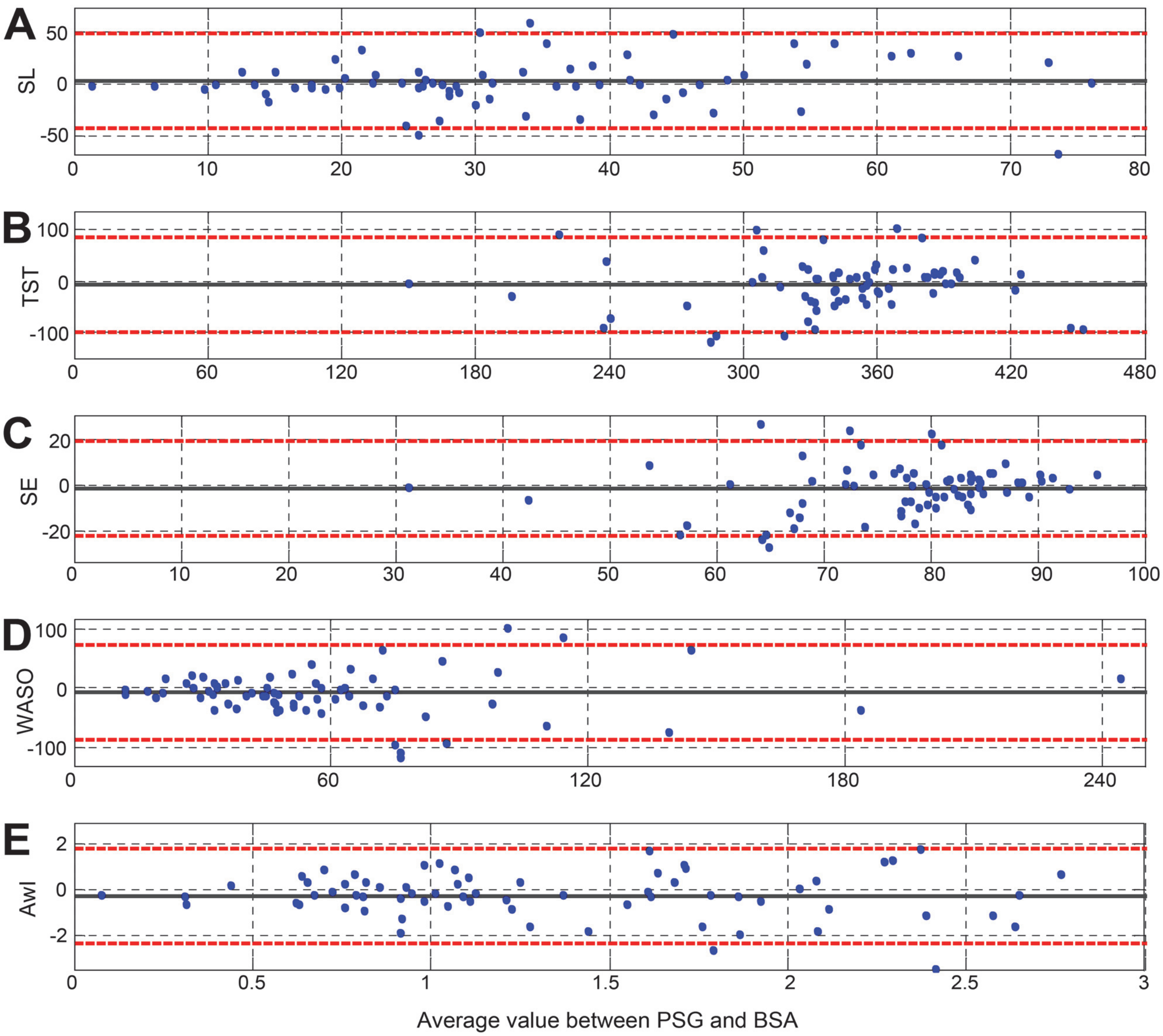

Fig 11. Bland-Altman plot of the PSG & BSA. X-axis represents the mean sleep parameter value between the PSG & BSA (in the relevant parameter units). The Y-axis is the difference between the PSG and BSA sleep quality parameter. The dashed lines represent the 95% CI. (A) SL—Sleep latency, (B) TST—Total sleep time, (C) SE—Sleep efficiency, (D) WASO—Wake time after sleep onset, (E) AwI—the average awakening per hour of time in bed.

doi:10.1371/journal.pone.0117382.g011

open. While the pharyngeal muscles manage this task with relative ease during wakefulness, their activity is often diminished at sleep onset [19,31,32]. During sleep, there is a considerable increase of upper airway resistance [4,17,18,33] due to decreased activity of the pharyngeal dilator muscles [19,20]. This elevated resistance is reflected by amplification of air-pressure oscillations in the upper airways during breathing. These air-pressure oscillations are perceived as typical breathing sounds during sleep. In contrast, during wakefulness, there is an increase in activity of the upper airway dilating muscles, hence decreased upper airway resistance [19] and airway oscillations.

This study provides evidence that by audio analysis of breathing sounds, the breathing pattern and hence the sleep-wake activity can be estimated. We developed and validated a system that incorporates eight features (extracted mainly from the audio energy signal; see Methods) that were designed to measure and quantify breathing pattern and breathing properties. These features were used for training an AdaBoost [25] classification model to estimate sleep and wake activity at 30 sec epoch resolution. Using the estimated epoch labels (sleep/wake), we calculated five acceptable sleep quality parameters. System performances were analyzed epoch-by-epoch. The accuracy was 0.833, the sensitivity was 0.922, and the specificity was 0.566. Cohen's kappa agreement was 0.508. When analyzing sleep quality parameters (BSA vs. PSG), the average error (in minutes) of sleep-latency, total sleep time, and wake after sleep onset was 16.6, 35.8, and 29.6, respectively.

Breathing signals and analysis

Extracting sleep-wake activity pattern from breathing sounds using a non-contact microphone is challenging. Since breathing sounds may be "contaminated" by background noise, it is essential to improve SNR prior to analysis in order to enhance the breathing events. To achieve this, we used an adaptive spectral subtraction technique [26] that subtracts the estimated background noise. This technique is acceptable in the speech and audio signal enhancement field [34]; however, it was not fully explored on whole-night breathing sounds. By applying this technique, background noise was considerably reduced, similar to earlier studies [22,34].

We developed a unique set of features that are specifically designed to distinguish between sleep and wake phases (Table 3, Fig. 4). These features can be categorized into two categories: *breathing pattern* and *snore-characteristics*. The *breathing pattern* features are designed to capture and to quantify variations in breathing periodicity as they may contribute to distinguishing between sleep and wake epochs. The basic idea here is that the new developed features: CP, CC, and CI (collectively named "periodicity features"; see Methods) are strongly influenced by breathing properties, such as rate and consistency. It was well established that changes in vigilance states strongly affect breathing rate and regularity in humans and animals [4,16,19,33,35–39]. The *snore-characteristics* features are designed to find the probability of a given epoch to contain snores. The basic idea is that the probability of detecting snoring events is increased during sleep. Snoring is caused by the vibration of soft tissue in the upper airways due to elevated upper airway resistance during sleep [21]. Recently, it was shown that snore analysis may carry valuable information about sleep conditions [23,40]. In order to calculate these *snore-characteristics* features, we used our high performance (>98% detection accuracy rate) snore detector [22] module. By using all these (eight) features as a multi-dimensional input to our sleep-wake classifier, the performances were superior to using each feature separately (Fig. 9).

We used the AdaBoost [25] algorithm to classify epochs as sleep or wake. The main advantage of this algorithm is its ability to discriminate multi-dimensional complex-patterns using a non-parametric, non-linear boundary threshold [25]. The use of this kind of classifier was supported by an earlier study [41], which claimed that sleep and wake activity (using wrist-actigraph) should be discriminated using non-linear classifiers. In addition, other studies have shown that there is a strong correlation between the labels (sleep/wake) of adjacent (30 sec) epochs [28,42]. Therefore, we configured our AdaBoost classifier as a time-series model, in which the prediction of each epoch state is influenced by the adjacent epochs, i.e., it is unlikely (though it's possible) to find a fragmented sequence of [wake-sleep-wake] and vice versa. In our earlier study [43] we also explored the effect of different classifiers such as two states hidden Markov models [44]. The time-series AdaBoost classifier was found to produce the best results and therefore was chosen.

Comparison to existing approaches

Little information is available about sleep evaluation using a non-contact audio-based approach. In recent years, several other simple cost-effective technologies for sleep evaluation have been presented. These technologies are based on reduced-channels and sensors, in which the preferred methods to detect sleep and wake phases are based on detecting patient movement. The most validated approach is actigraph [5,45]. Hedner et al. [3], Marino et al. [11], Lotjonen et al. [46], and Tilmanne et al. [41] have validated the performance of actigraphy versus PSG using in-laboratory data collection. They showed an agreement (accuracy) ranging between 80% and 86%. Innovations in mobile and electronic healthcare are revolutionizing the involvement of both doctors and patients in the modern healthcare system by extending the capabilities of physiological monitoring devices. Incorporating smart wearable sensors into the routine care of patients could augment physician-patient relationships, and increase the autonomy and involvement of patients in their healthcare [12]. However, such systems are rarely tested scientifically [13]. Our BSA system yields matched and even superior performances relative to an actigraph technology. Furthermore, in our system, according to Bland-Altman plot (Fig. 11), all sleep quality parameters showed no consistent bias, where actigraphy-based technology showed some bias in the sleep quality parameters [11,47,48]. When calculating the average error (mean absolute difference) of the sleep quality parameters between PSG and actigraph, Lotjonen at el. [46] and Blackwell et al. [49] showed a TST estimation error of 54 min and 44 min, respectively. Blackwell et al. [49] also calculated the estimation error of SE and WASO; they showed an average error of 9.8% for sleep efficiency and 39 min for WASO. By comparing the errors of these sleep quality parameters, our BSA system yields superior performances (TST 35.8 min, SE 8%, and WASO 29.6 min).

In addition to actigraphy-based methods, some researchers took movement detection even further in order to estimate sleep and wake activity in non-contact technologies [50–52]. Collectively, these studies showed performances that are inferior to or close to actigraphy-based approaches. It is generally recognized that body-movement-based technologies (contact and non-contact) are biased [9,11,47,48], since any lack of movement is interpreted as sleep, while movement is interpreted as awake. In contrast, our approach of estimating sleep-wake from breathing sounds is based on the notion that during sleep onset there are considerable changes in upper airway mechanics, affecting airflow and pressure oscillations. In contrast to these movement-based technologies, we found that our system performance is not influenced by any physiological variables, such as age, BMI, AHI, and gender.

Strengths and limitations

We provide evidence that sleep-wake activity can be reliably estimated by audio analysis of breathing sounds. In this study 127,668 epochs were analyzed from 150 subjects who were referred to sleep evaluation; these subjects represent a diverse population, across a wide range of ages, BMI, AHI, and from both genders, but are not strictly a generalizable population. Our proposed non-contact technology may enable more natural sleep that is not affected by the equipment. It is expected that the wear and tear and costs will be relatively low; however, further studies should determine whether this technology is valid in at-home conditions and its cost-effectiveness. Clearly, the transition of this technology to at-home sleep evaluation mainly depends on third party reimbursements for the use of home study equipment [11,53]. It should be recognized that the main limitation of this technology is its sensitivity to low SNR, which results from quiet breathing relative to high environmental background noise. In addition, at the current state of operation, our system is limited to operate in a single-subject environment (one person in the room); since other person's breathing sounds can interrupt. Further studies should investigate methods to cope with several subjects in the room and to further improve SNR mechanically and algorithmically.

Summary

One of the main goals of sleep medicine today is to improve early diagnosis and treatment of the "flood" of subjects presenting with sleep disorders. New simple technologies are needed in order to improve patient accessibility to sleep diagnosis; this in turn will reduce the cost of management and treatment [53], and improve quality of life and health.

This study presents a pioneering approach for determining sleep-wake pattern using non-contact audio-based signals. We found that by analyzing breathing sounds a reliable estimation of sleep quality parameters can be achieved. This study highlights the potential of breathing sound analysis to measure sleep in research and clinical situations.

Supporting Information

S1 Dataset. This file contains Figure A and Figure B. Figure A, Individual big-data visualization for the study design (training, n = 80) and validation (testing, n = 70): design dataset—upper panels; validation dataset—lower panels. Each horizontal line represents one individual's data. Sleep/wake activity pattern was manually annotated epoch-by-epoch using polysomnography (PSG) scoring criteria. Note the large individual differences in sleep-wake pattern, especially the sleep latency (from time zero to the first black mark of sleep) and the large individual variability of awakening during sleep (mustard colors between black regions). The onset of the gray area indicates study termination for each individual. Cohen's kappa (epoch-by-epoch sleep/wake) agreement score for each subject was calculated comparing our proposed breathing sound analysis (BSA) system and the PSG scoring. For study protocol, see main body of the manuscript. Figure B, The correlation between sleep-wake estimation performances (using kappa score) and subject's breathing sound recording quality (signal to noise ratio, SNR). Each dot represents the mean SNR of one individual from the validation (testing) dataset (n = 70).
(PDF)

Acknowledgments

We would like to thank Ms. Bruria Freidman from the Sleep Wake Disorder Unit of Soroka University Medical Center, for her support and collaboration.

Soroka University Medical Center Institutional Review Board protocol approval number: 10141.

Author Contributions

Conceived and designed the experiments: ED AT YZ. Performed the experiments: ED YZ. Analyzed the data: ED YZ. Contributed reagents/materials/analysis tools: ED AT YZ. Wrote the paper: ED AT YZ. Designed the software used in analysis: ED YZ.

References

1. Iber C, Ancoli-Israel S, Chesson A, Quan SF (2007) The AASM Manual for the Scoring of Sleep and Associated Events: Rules, Terminology, and Tech-nical Specifications; 1, editor. Westchester, IL: The American Academy of Sleep Medicine.
2. Collop N, Anderson WM, Boehlecke B, Claman D, Goldberg R, et al. (2007) Clinical guidelines for the use of unattended portable monitors in the diagnosis of obstructive sleep apnea in adult patients. J Clin Sleep Med 3: 737–747. PMID: 18198809
3. Hedner J, Pillar G, Pittman SD, Zou D, Grote L, et al. (2004) A novel adaptive wrist actigraphy algorithm for sleep-wake assessment in sleep apnea patients. Sleep 27: 1560–1566. PMID: 15683148
4. Colrain IM, Trinder J, Fraser G, Wilson G (1989) Ventilation during sleep onset: University of Tasmania.
5. Sadeh A, Acebo C (2002) The role of actigraphy in sleep medicine. Sleep medicine reviews 6: 113–124. PMID: 12531147

6. Sommermeyer D, Schwaibold M, Schöller B, Grote L, Hedner J, et al. (2010) Detection of sleep disorders by a modified Matching Pursuit algorithm. Springer. pp. 1271–1274.
7. Berthomier C, Drouot X, Herman-Stoïca M, Berthomier P, Prado J, et al. (2007) Automatic analysis of single-channel sleep EEG: validation in healthy individuals. Sleep 30: 1587. PMID: 18041491
8. Choi JH, Kim EJ, Kim YS, Choi J, Kim TH, et al. (2010) Validation study of portable device for the diagnosis of obstructive sleep apnea according to the new AASM scoring criteria: Watch-PAT 100. Acta oto-laryngologica 130: 838–843. doi: 10.3109/00016480903431139 PMID: 20082567
9. Hwang S, Chung G, Lee J, Shin J, Lee S- J, et al. (2012) Sleep/wake estimation using only anterior tibialis electromyography data. Biomed Eng Online 11: 1–15. doi: 10.1186/1475-925X-11-1 PMID: 22208504
10. Johnson NL, Kirchner HL, Rosen CL, Storfer-Isser A, Cartar LN, et al. (2007) Sleep estimation using wrist actigraphy in adolescents with and without sleep disordered breathing: a comparison of three data modes. Sleep 30: 899. PMID: 17682661
11. Marino M, Li Y, Rueschman MN, Winkelman J, Ellenbogen J, et al. (2012) Measuring sleep: accuracy, sensitivity, and specificity of wrist actigraphy compared to polysomnography. Sleep 36: 1747–1755.
12. Appelboom G, Camacho E, Abraham ME, Bruce SS, Dumont EL, et al. (2014) Smart wearable body sensors for patient self-assessment and monitoring. Archives of Public Health 72: 28. doi: 10.1186/2049-3258-72-28 PMID: 25232478
13. Montgomery-Downs HE, Insana SP, Bond JA (2012) Movement toward a novel activity monitoring device. Sleep and Breathing 16: 913–917. doi: 10.1007/s11325-011-0585-y PMID: 21971963
14. Vashist SK, Schneider EM, Luong JH (2014) Commercial Smartphone-Based Devices and Smart Applications for Personalized Healthcare Monitoring and Management. Diagnostics 4: 104–128.
15. Malik V, Smith D (2012) Respiratory Physiology During Sleep. Sleep Medicine Clinics 7: 497–505.
16. Phillipson EA (1978) Respiratory adaptations in sleep. Annual review of Physiology 40: 133–156. PMID: 345949
17. Trinder J, Whitworth F, Kay A, Wilkin P (1992) Respiratory instability during sleep onset. Journal of Applied Physiology 73: 2462–2462. PMID: 1490959
18. Trinder J, Kay A, Kleiman J, Dunai J (1997) Gender differences in airway resistance during sleep. Journal of applied physiology 83: 1986–1997. PMID: 9390972
19. Worsnop C, Kay A, Kim Y, Trinder J, Pierce R (2000) Effect of age on sleep onset-related changes in respiratory pump and upper airway muscle function. Journal of Applied Physiology 88: 1831–1839. PMID: 10797148
20. Edwards BA, White DP (2011) Control of the pharyngeal musculature during wakefulness and sleep: implications in normal controls and sleep apnea. Head & neck 33: S37–S45.
21. Hoffstein V, Mateika S, Anderson D (1994) Snoring: is it in the ear of the beholder? Sleep 17: 522–526. PMID: 7809565
22. Dafna E, Tarasiuk A, Zigel Y (2013) Automatic Detection of Whole Night Snoring Events Using Non-Contact Microphone. PLoS One 8: e84139. doi: 10.1371/journal.pone.0084139 PMID: 24391903
23. Ben-Israel N, Tarasiuk A, Zigel Y (2012) Obstructive apnea hypopnea index estimation by analysis of nocturnal snoring signals in adults. Sleep 35: 1299–1305C. doi: 10.5665/sleep.2092 PMID: 22942509
24. National Sleep Foundation. Avalible: http://sleepfoundation.org/bedroom/. Accessed 2014 Dec 30.
25. Freund YS, Schapire RE (1997) A decision-theoretic generalization of on-line learning and an application to boosting. Journal of Computer and System Sciences 55: 119–139.
26. Scalart P (1996) Speech enhancement based on a priori signal to noise estimation. Conf Proc IEEE International Conference on Acoustics, Speech, and Signal Processing 2: 629–632.
27. Landis JR, Koch GG (1977) The measurement of observer agreement for categorical data. biometrics 33: 159–174. PMID: 843571
28. Kim J, Lee J-S, Robinson P, Jeong D-U (2009) Markov analysis of sleep dynamics. Physical review letters 102: 178104. PMID: 19518839
29. Martin Bland J, Altman D (1986) Statistical methods for assessing agreement between two methods of clinical measurement. The lancet 327: 307–310.
30. Goldshtein E, Tarasiuk A, Zigel Y (2011) Automatic detection of obstructive sleep apnea using speech signals. Biomedical Engineering, IEEE Transactions on 58: 1373–1382. doi: 10.1109/TBME.2010.2100096 PMID: 21172747
31. Wilkinson V, Malhotra A, Nicholas CL, Worsnop C, Jordan AS, et al. (2008) Discharge patterns of human genioglossus motor units during sleep onset. Sleep 31: 525. PMID: 18457240

32. Fogel RB, Trinder J, White DP, Malhotra A, Raneri J, et al. (2005) The effect of sleep onset on upper airway muscle activity in patients with sleep apnoea versus controls. The Journal of physiology 564: 549–562. PMID: 15695240

33. Smith L, Schwartz AR (2012) Effect of end-expiratory lung volume on upper airway. J Appl Physiol 113: 691–699. doi: 10.1152/japplphysiol.00091.2012 PMID: 22628372

34. Hasan MK, Salahuddin S, Khan MR (2004) A modified a priori SNR for speech enhancement using spectral subtraction rules. IEEE Signal Processing Letters 11: 450–453.

35. Coote J (1982) Respiratory and circulatory control during sleep. Journal of Experimental Biology 100: 223–244. PMID: 6757369

36. Coote J, Tsang G, Baker A, Stone B (1993) Respiratory changes and structure of sleep in young high-altitude dwellers in the Andes of Peru. European journal of applied physiology and occupational physiology 66: 249–253. PMID: 8477682

37. Douglas N, White D, Pickett C, Weil J, Zwillich C (1982) Respiration during sleep in normal man. Thorax 37: 840–844. PMID: 7164002

38. Kantelhardt JW, Penzel T, Rostig S, Becker HF, Havlin S, et al. (2003) Breathing during REM and non-REM sleep: correlated versus uncorrelated behaviour. Physica A: Statistical Mechanics and its Applications 319: 447–457.

39. Rostig S, Kantelhardt JW, Penzel T, Cassel W, Peter JH, et al. (2005) Nonrandom variability of respiration during sleep in healthy humans. Sleep 28: 411. PMID: 16171285

40. Akhter S, Abeyratne UR, Swarnkar V (2013) Variations of snoring properties with macro sleep stages in a population of Obstructive Sleep Apnea patients. Conf Proc IEEE Eng Med Biol Soc 2013: 1318–1321. doi: 10.1109/EMBC.2013.6609751 PMID: 24109938

41. Tilmanne J, Urbain J, Kothare MV, Wouwer AV, Kothare SV (2009) Algorithms for sleep–wake identification using actigraphy: a comparative study and new results. Journal of sleep research 18: 85–98. doi: 10.1111/j.1365-2869.2008.00706.x PMID: 19250177

42. Robinson P, Phillips A, Fulcher B, Puckeridge M, Roberts J (2011) Quantitative modelling of sleep dynamics. Philosophical Transactions of the Royal Society A: Mathematical, Physical and Engineering Sciences 369: 3840–3854.

43. Dafna E, Tarasiuk A, Zigel Y (2012) Sleep-quality assessment from full night audio recordings of sleep apnea patients. 34th Annual International IEEE EMBS Conference, IEEE EMBS. San diego.

44. Elliott RJ, Aggoun L, Moore JB (1995) Hidden Markov Models: Springer.

45. Acebo C, Sadeh A, Seifer R, Tzischinsky O, Wolfson A, et al. (1999) Estimating sleep patterns with activity monitoring in children and adolescents: how many nights are necessary for reliable measures? Sleep 22: 95–103. PMID: 9989370

46. Lotjonen J, Korhonen I, Hirvonen K, Eskelinen S, Myllymaki M, et al. (2003) Automatic sleep-wake and nap analysis with a new wrist worn online activity monitoring device vivago WristCare. Sleep 26: 86–90. PMID: 12627738

47. Lichstein KL, Stone KC, Donaldson J, Nau SD, Soeffing JP, et al. (2006) Actigraphy validation with insomnia. Sleep 29: 232. PMID: 16494091

48. Ancoli-Israel S, Cole R, Alessi C, Chambers M, Moorcroft W, et al. (2003) The role of actigraphy in the study of sleep and circadian rhythms. American Academy of Sleep Medicine Review Paper. Sleep 26: 342–392. PMID: 12749557

49. Blackwell T, Redline S, Ancoli-Israel S, Schneider JL, Surovec S, et al. (2008) Comparison of sleep parameters from actigraphy and polysomnography in older women: the SOF study. Sleep 31: 283. PMID: 18274276

50. Liao WH, Yang CM (2008) Video-based Activity and Movement Pattern Analysis in Overnight Sleep Studies. 19th International Conference on Pattern Recognition, Vols 1–6: 1774–1777.

51. De Chazal P, Fox N, O'hare E, Heneghan C, Zaffaroni A, et al. (2011) Sleep/wake measurement using a non-contact biomotion sensor. Journal of sleep research 20: 356–366. doi: 10.1111/j.1365-2869.2010.00876.x PMID: 20704645

52. Scatena M, Dittoni S, Maviglia R, Frusciante R, Testani E, et al. (2012) An integrated video-analysis software system designed for movement detection and sleep analysis. Validation of a tool for the behavioural study of sleep. Clinical Neurophysiology 123: 318–323. doi: 10.1016/j.clinph.2011.07.026 PMID: 21873109

53. Reuveni H, Tarasiuk A, Wainstock T, Ziv A, Elhayany A, et al. (2004) Awareness level of obstructive sleep apnea syndrome during routine unstructured interviews of a standardized patient by primary care physicians. Sleep 27: 1518–1525. PMID: 15683143

Discussion

One of the main goals of sleep medicine today is to improve early diagnosis and treatment of the "flood" of subjects presenting with sleep disorders. New simple technologies are needed in order to improve patient accessibility to sleep diagnosis; this in turn will reduce the cost of management and treatment, and improve quality of life and health.

Paper 1 – breathing detector

In this paper [29] we present a robust snore detection system based on audio signals recorded using a non-contact microphone technology with overall accuracy rate of 98.2%. The detector was trained and validated on 67 patients. The novelty of our proposed system is its automatic detection of a variety of snore events from a whole-night audio recording. Our approach to snore detection includes comprehensive sets of features that were selected using the feature selection algorithm.

Here we developed and explored a large and comprehensive set of features that are the most relevant for snore detection using a feature selection technique. In order to fully explore this variety of features, we have used concepts from speech and audio signal processing areas [34, 35] and implemented features from time and spectral domains. It is worth noting that the most influential feature set was the novel periodicity set, which was found to be highly discriminative in classifying snore and non-snore events.

Comparing our snore detection performance with other studies, our results (accuracy > 98%) were superior, especially as they are statistically proven based on a large dataset containing a variety of sleep disorder breathing (SDB) severity and recorded using an ambient microphone. Azarbarzin et al. [36] achieved an accuracy rate of 93.1% when using an ambient microphone. Karunajeewa et al. [37] published a high accuracy rate of 96.8% when testing four subjects. Cavusoglu et al. [38] produced an accuracy rate of 90.2% when recording using an ambient microphone placed 15 cm from the patient's head. Duckitt et al. [39] achieved 82–87% when trained and tested on a total of 6 snorers. We confirmed the robustness of our detector by using an additional audio recording device (handy Olympus LS-5) placed on the dresser beside the patient's head in the laboratory. Similar accuracy rates of 98.4% and 97.8% were found for the Edirol R-4 Pro (n=30) and Olympus LS-5 (n=12, $p = 0.14$), respectively. Further studies are required to explore the usefulness of this snore detection in at-home settings.

An innovative parameter for objectively scoring, snore intensity was developed in this study. For the first time, this score allows very accurate and objective scores regarding the controversial self-reporting questionnaires. This simple tool can provide objective numeric and graphic reports of the automatically detected snoring events (Fig. 11, in paper 1). Another application for snore detection is to diagnose sleep-disordered breathing syndromes [40-43], the effectiveness of palatal surgeries regarding snores, obstructive sleep apnea [44], and even exploration of breathing patterns during sleep time [45].

Clearly, incidence of snoring is very high, and it is a common symptom of sleep-disordered breathing and other disorders of the upper airways [21]. The “flood” of subjects presenting with snoring symptoms is a major challenge to decision makers and is governed by prevalence and level of awareness of snoring morbidity [46]. Here, we have proposed a snore detection system that can provide an objective quantitative measure for whole-night snore patterns.

Paper 2 – Breathing and Snoring Sound Characteristics during Sleep

In this study [30], a whole night audio signal was recorded using a non-contact ambient microphone during polysomnography. We included 121 subjects who represent a diverse population that is typical to our region, across a wide range of ages, BMI, and AHI, but are not strictly a generalizable population. A large number (>290,000) of breathing and snoring (>50 dB) events were analyzed. Breathing sound events were detected using a signal-processing algorithm that discriminates between breathing and non-breathing (noise events) sounds. Snoring index (SI; events/hr) was 23% higher for men ($p = 0.04$), and in both genders SI gradually declined by 50% across sleep time ($p < 0.01$) independent of apnea-hypopnea index (AHI). SI was higher in slow wave sleep ($p < 0.03$) compared to S2 and REM sleep; men have higher SI in all sleep stages than women ($p < 0.05$). Snoring intensity was similar in both genders in all sleep stages and independent of AHI. For both genders, no correlation was found between AHI and snoring intensity (r=0.1, p=0.291).

The “flood” of subjects presenting with snoring symptoms is a major challenge to decision makers and is governed by prevalence and level of awareness of snoring morbidity. Reliable snoring reporting cannot be made based solely on a patient's (or partner's) history of noisy respiration during sleep, or sleep laboratory technician reports; a large portion of the subjects respond that they “do not know” if they snore. The need for an agreed-upon approach to extract and analyze whole-night snoring sounds is of major importance to the field of sleep disordered breathing. Here, a novel and valid tool was used to systematically detect and analyze breathing and snoring sounds from a full night recording. This system can capture all the snoring sound events and, interestingly, on average the total number of snoring sounds that were captured by this system was less than 20% of the overall breathing sounds. This finding indicates that most breathing sound events are less than 50 dB. Snoring index and % snoring were higher in men, and in both genders snoring index and % snoring was higher in slow waves sleep (SWS). Snoring index, % snoring, and snoring intensity did not correlate with AHI, however. frequency centroid of breathing and snoring sounds correlate with AHI. Our data do not support the common belief that snoring intensity (dB) is higher for men than for women and is correlated with AHI. An important problem in dealing with objective respiratory sounds is the comparison of the data of various investigators and correct interpretation. This study shows that a snore detection system can provide an objective quantitative measure for whole-night snore patterns.

Paper 3 – Sleep-wake evaluation

This study [31] presents a pioneering approach for determining sleep-wake pattern using non-contact audio-based signals. We found that by analyzing breathing sounds a reliable estimation of sleep quality parameters can be achieved. This study highlights the potential of breathing sound analysis to measure sleep in research and clinical situations. In order to achieve that, we developed a high detection rate breathing detector, and explored the association between breathing and sleeping states along with the effect of anthropomorphic parameters.

The system was trained and validated on 150 patients who were referred to routine polysomnography test. Epoch-by-epoch accuracy rate for the validation study was 83.3% with sensitivity of 92.2% (sleep as sleep), specificity of 56.6% (awake as awake), and Cohen's kappa of 0.508. Comparing sleep quality parameters of our audio-based approach and PSG demonstrate average error of sleep latency, total sleep time, wake after sleep onset, and sleep efficiency of 16.6 min, 35.8 min, 29.6 min, and 8%, respectively.

Our proposed non-contact technology may enable more natural sleep that is not affected by the equipment. It is expected that the wear and tear and costs will be relatively low; however, further studies should determine whether this technology is valid in at-home conditions and its cost effectiveness. Clearly, the transition of this technology to at-home sleep evaluation mainly depends on third party reimbursement for the use of home study equipment [11, 46]. It should be recognized that the main limitation of this technology is its sensitivity to low SNR, which results from quiet breathing relative to high environmental background noise. In addition, at the current state of operation, our system is limited to operating in a single-subject environment (one person in the room), since another person's breathing sounds can interrupt. Further studies should investigate methods to cope with several subjects in the room and to further improve SNR mechanically and algorithmically.

Macro sleep stages evaluation

In a recent conference paper[1] [22] (see Appendix I) at the IEEE EMBC 2016, we showed preliminary results that using audio analysis, the sleep and wake estimation can be extended into three macro sleep stages including wake, REM, and non-REM phases. To the best of our knowledge, this study is the first to show that non-contact technology can reliably estimate MSS. Some of the current sleep trackers [3, 5, 31, 32] are able to estimate binary sleep or wake phases; however, they cannot monitor REM sleep. Watch-PAT [33] is a wearable device that measures MSS via actigraphy and peripheral arterial tone signals. It has a detection rate of 76%, 81%, and 73% compared to our 69%, 54%, and 79% for detecting wake, REM, and NREM, respectively.

Our system was validated on clinical cases in which patients are referred to a sleep study. Patients slept alone in a relatively quiet room, making a favorable SNR. In future work we are planning to expand our database and to record subjects in at-home conditions, where SNR is more challenging. The demand for accessible sleep diagnosis and simple/easy to use PSG alternative is high. The performances of the system are very encouraging and could serve as a screening tool for MSS estimation using a simple single-channel, non-contact audio technology.

[1] Selected as a finalist for a prestigious "student paper competition" of IEEE EMBC 2016.

References

[1] C. Iber, S. Ancoli-Israel, C. A. L., and S. Quan, *The AASM Manual for the Scoring of Sleep and Associated Events: Rules, Terminology, and Tech-nical Specifications*, 1 ed. Westchester, IL: The American Academy of Sleep Medicine, 2007.

[2] N. Collop, W. M. Anderson, B. Boehlecke, D. Claman, R. Goldberg, D. Gottlieb, *et al.*, "Clinical guidelines for the use of unattended portable monitors in the diagnosis of obstructive sleep apnea in adult patients," *J Clin Sleep Med,* vol. 3, pp. 737-747, 2007.

[3] J. Hedner, G. Pillar, S. D. Pittman, D. Zou, L. Grote, and D. P. White, "A novel adaptive wrist actigraphy algorithm for sleep-wake assessment in sleep apnea patients," *Sleep,* vol. 27, pp. 1560-1566, 2004.

[4] I. M. Colrain, J. Trinder, G. Fraser, and G. Wilson, *Ventilation during sleep onset*: University of Tasmania, 1989.

[5] A. Sadeh and C. Acebo, "The role of actigraphy in sleep medicine," *Sleep medicine reviews,* vol. 6, pp. 113-124, 2002.

[6] D. Sommermeyer, M. Schwaibold, B. Schöller, L. Grote, J. Hedner, and A. Bolz, "Detection of sleep disorders by a modified Matching Pursuit algorithm," in *World Congress on Medical Physics and Biomedical Engineering, September 7-12, 2009, Munich, Germany*, 2010, pp. 1271-1274.

[7] C. Berthomier, X. Drouot, M. Herman-Stoïca, P. Berthomier, J. Prado, D. Bokar-Thire, *et al.*, "Automatic analysis of single-channel sleep EEG: validation in healthy individuals," *Sleep,* vol. 30, p. 1587, 2007.

[8] J. H. Choi, E. J. Kim, Y. S. Kim, J. Choi, T. H. Kim, S. Y. Kwon, *et al.*, "Validation study of portable device for the diagnosis of obstructive sleep apnea according to the new AASM scoring criteria: Watch-PAT 100," *Acta oto-laryngologica,* vol. 130, pp. 838-843, 2010.

[9] S. Hwang, G. Chung, J. Lee, J. Shin, S.-J. Lee, D.-U. Jeong, *et al.*, "Sleep/wake estimation using only anterior tibialis electromyography data," *Biomed Eng Online*, vol. 11, pp. 1-15, 2012.

[10] N. L. Johnson, H. L. Kirchner, C. L. Rosen, A. Storfer-lsser, L. N. Cartar, S. Ancoli-Israel, *et al.*, "Sleep estimation using wrist actigraphy in adolescents with and without sleep disordered breathing: a comparison of three data modes," *Sleep,* vol. 30, p. 899, 2007.

[11] M. Marino, Y. Li, M. N. Rueschman, J. Winkelman, J. Ellenbogen, J. Solet, *et al.*, "Measuring sleep: accuracy, sensitivity, and specificity of wrist actigraphy compared to polysomnography," *Sleep,* vol. 36, pp. 1747-1755, 2012.

[12] G. Appelboom, E. Camacho, M. E. Abraham, S. S. Bruce, E. L. Dumont, B. E. Zacharia*, et al.*, "Smart wearable body sensors for patient self-assessment and monitoring," *Archives of Public Health,* vol. 72, p. 28, 2014.

[13] H. E. Montgomery-Downs, S. P. Insana, and J. A. Bond, "Movement toward a novel activity monitoring device," *Sleep and Breathing,* vol. 16, pp. 913-917, 2012.

[14] S. K. Vashist, E. M. Schneider, and J. H. Luong, "Commercial Smartphone-Based Devices and Smart Applications for Personalized Healthcare Monitoring and Management," *Diagnostics,* vol. 4, pp. 104-128, 2014.

[15] V. Malik and D. Smith, "Respiratory Physiology During Sleep," *Sleep Medicine Clinics,* vol. 7, pp. 497-505, 2012.

[16] E. A. Phillipson, "Respiratory adaptations in sleep," *Annual review of Physiology,* vol. 40, pp. 133-156, 1978.

[17] J. Trinder, F. Whitworth, A. Kay, and P. Wilkin, "Respiratory instability during sleep onset," *Journal of Applied Physiology,* vol. 73, pp. 2462-2462, 1992.

[18] J. Trinder, A. Kay, J. Kleiman, and J. Dunai, "Gender differences in airway resistance during sleep," *Journal of applied physiology,* vol. 83, pp. 1986-1997, 1997.

[19] C. Worsnop, A. Kay, Y. Kim, J. Trinder, and R. Pierce, "Effect of age on sleep onset-related changes in respiratory pump and upper airway muscle function," *Journal of Applied Physiology,* vol. 88, pp. 1831-1839, 2000.

[20] B. A. Edwards and D. P. White, "Control of the pharyngeal musculature during wakefulness and sleep: implications in normal controls and sleep apnea," *Head & neck,* vol. 33, pp. S37-S45, 2011.

[21] V. Hoffstein, S. Mateika, and D. Anderson, "Snoring: is it in the ear of the beholder?," *Sleep,* vol. 17, pp. 522-6, Sep 1994.

[22] E. Dafna, M. Halevi, D. B. Or, A. Tarasiuk, and Y. Zigel, "Estimation of macro sleep stages from whole night audio analysis," in *Engineering in Medicine and Biology Society (EMBC), 2016 IEEE 38th Annual International Conference of the*, 2016, pp. 2847-2850.

[23] E. Dafna, A. Tarasiuk, and Y. Zigel, "OSA severity assessment based on sleep breathing analysis using ambient microphone," in *2013 35th Annual International Conference of the IEEE Engineering in Medicine and Biology Society (EMBC)*, 2013, pp. 2044-2047.

[24] T. Rosenwein, E. Dafna, A. Tarasiuk, and Y. Zigel, "Detection of breathing sounds during sleep using non-contact audio recordings," *Conf Proc IEEE Eng Med Biol Soc.,* 2014.

[25] T. Rosenwein, E. Dafna, A. Tarasiuk, and Y. Zigel, "Breath-by-breath detection of apneic events for OSA severity estimation using non-contact audio recordings," in *2015 37th Annual International Conference of the IEEE Engineering in Medicine and Biology Society (EMBC)*, 2015, pp. 7688-7691.

[26] E. Dafna, T. Rosenwein, A. Tarasiuk, and Y. Zigel, "Breathing rate estimation during sleep using audio signal analysis," in *2015 37th Annual International Conference of the IEEE Engineering in Medicine and Biology Society (EMBC)*, 2015, pp. 5981-5984.

[27] M. Halevi, E. Dafna, A. Tarasiuk, and Y. Zigel, "Can we discriminate between apnea and hypopnea using audio signals?," in *Engineering in Medicine and Biology Society (EMBC), 2016 IEEE 38th Annual International Conference of the*, 2016, pp. 3211-3214.

[28] D. Ben Or, E. Dafna, A. Tarasiuk, and Y. Zigel, "Obstructive sleep apnea severity estimation: Fusion of speech-based systems," in *Engineering in Medicine and Biology Society (EMBC), 2016 IEEE 38th Annual International Conference of the*, 2016, pp. 3207-3210.

[29] E. Dafna, A. Tarasiuk, and Y. Zigel, "Automatic Detection of Whole Night Snoring Events Using Non-Contact Microphone," *PLoS One,* vol. 8, p. e84139, 2013.

[30] A. Levartovsky, E. Dafna, Y. Zigel, and A. Tarasiuk, "Breathing and Snoring Sound Characteristics During Sleep in Adults," *Journal of clinical sleep medicine: JCSM: official publication of the American Academy of Sleep Medicine,* 2016.

[31] E. Dafna, A. Tarasiuk, and Y. Zigel, "Sleep-Wake Evaluation from Whole-Night Non-Contact Audio Recordings of Breathing Sounds," *PloS one,* vol. 10, p. e0117382, 2015.

[32] T. Blackwell, S. Redline, S. Ancoli-Israel, J. L. Schneider, S. Surovec, N. L. Johnson, *et al.*, "Comparison of sleep

parameters from actigraphy and polysomnography in older women: the SOF study," *SLEEP-NEW YORK THEN WESTCHESTER-*, vol. 31, p. 283, 2008.

[33] S. Herscovici, A. Pe'er, S. Papyan, and P. Lavie, "Detecting REM sleep from the finger: an automatic REM sleep algorithm based on peripheral arterial tone (PAT) and actigraphy," *Physiological measurement,* vol. 28, p. 129, 2006.

[34] J. R. Deller, J. H. L. Hansen, and J. L. Proakis, *Discrete-time processing of speech signals*, 2 ed. New York: Institute of Electrical and Electronics Engineers Press, 2000.

[35] L. R. Rabiner and W. R. Schafer, *Digital processing of speech signals*, 1 ed. Englewood Cliffs, New Jersey: Prentice-Hall, 1978.

[36] A. Azarbarzin and Z. M. Moussavi, "Automatic and unsupervised snore sound extraction from respiratory sound signals," *IEEE Trans Biomed Eng,* vol. 58, pp. 1156-62, May 2011.

[37] A. S. Karunajeewa, U. R. Abeyratne, and C. Hukins, "Silence-breathing-snore classification from snore-related sounds," *Physiol Meas,* vol. 29, pp. 227-43, Feb 2008.

[38] M. Cavusoglu, M. Kamasak, O. Erogul, T. Ciloglu, Y. Serinagaoglu, and T. Akcam, "An efficient method for snore/nonsnore classification of sleep sounds," *Physiol Meas,* vol. 28, pp. 841-53, Aug 2007.

[39] W. D. Duckitt, S. K. Tuomi, and T. R. Niesler, "Automatic detection, segmentation and assessment of snoring from ambient acoustic data," *Physiol Meas,* vol. 27, pp. 1047-56, Oct 2006.

[40] N. Ben-Israel, A. Tarasiuk, and Y. Zigel, "Obstructive apnea hypopnea index estimation by analysis of nocturnal snoring signals in adults," *Sleep,* vol. 35, pp. 1299-305C, Sep 2012.

[41] A. Azarbarzin and Z. Moussavi, "Snoring sounds variability as a signature of obstructive sleep apnea," *Med Eng Phys,* Jul 21 2012.

[42] L. A. Lee, J. F. Yu, Y. L. Lo, Y. S. Chen, D. L. Wang, C. M. Cho, *et al.*, "Energy types of snoring sounds in patients with obstructive sleep apnea syndrome: a preliminary observation," *PLoS One,* vol. 7, p. e53481, 2012.

[43] J. R. Perez-Padilla, E. Slawinski, L. M. Difrancesco, R. R. Feige, J. E. Remmers, and W. A. Whitelaw, "Characteristics of the snoring noise in patients with and without occlusive sleep apnea," *Am Rev Respir Dis,* vol. 147, pp. 635-44, Mar 1993.

[44] T. M. Jones, A. C. Swift, P. M. Calverley, M. S. Ho, and J. E. Earis, "Acoustic analysis of snoring before and after palatal surgery," *Eur Respir J,* vol. 25, pp. 1044-9, Jun 2005.

[45] F. Series, I. Marc, and L. Atton, "Comparison of snoring measured at home and during polysomnographic studies," *Chest,* vol. 103, pp. 1769-73, Jun 1993.

[46] H. Reuveni, A. Tarasiuk, T. Wainstock, A. Ziv, A. Elhayany, and A. Tal, "Awareness level of obstructive sleep apnea syndrome during routine unstructured interviews of a standardized patient by primary care physicians," *Sleep,* vol. 27, pp. 1518-25, Dec 15 2004.

Appendix

This section includes three chapters:

1) Conference paper "Estimation of macro sleep stages from whole night audio analysis"
2) Supplementary information for paper 1:
   Study protocol, *preprocessing*, *event detection and segmentation*, *agreement between scorers*, *feature extraction*, and *feature selection*.
3) Supplementary information for paper 3 – *Dataset*.

Estimation of macro sleep stages from whole night audio analysis

Dafna Eliran, Matan Halevi, Dvir Ben Or, Tarasiuk Ariel, and Zigel Yaniv.

The 38th Annual International Conference of the Engineering in Medicine and Biology Society (EMBC), 2016 IEEE, 2016, pp. 2847-2850.

Estimation of Macro Sleep Stages from Whole Night Audio Analysis

E. Dafna, M. Halevi, D. Ben Or, A. Tarasiuk, Y. Zigel, *member, IEEE*

Abstract: **During routine sleep diagnostic procedure, sleep is broadly divided into three states: rapid eye movement (REM), non-REM (NREM) states, and wake, frequently named macro-sleep stages (MSS). In this study, we present a pioneering attempt for MSS detection using full night audio analysis. Our working hypothesis is that there might be differences in sound properties within each MSS due to breathing efforts (or snores) and body movements in bed. In this study, audio signals of 35 patients referred to a sleep laboratory were recorded and analyzed. An additional 178 subjects were used to train a probabilistic time-series model for MSS staging across the night. The audio-based system was validated on 20 out of the 35 subjects. System accuracy for estimating (detecting) epoch-by-epoch wake/REM/NREM states for a given subject is 74% (69% for wake, 54% for REM, and 79% NREM). Mean error (absolute difference) was 36±34 min for detecting total sleep time, 17±21 min for sleep latency, 5±5% for sleep efficiency, and 7±5% for REM percentage. These encouraging results indicate that audio-based analysis can provide a simple and comfortable alternative method for ambulatory evaluation of sleep and its disorders.**

Keywords: **Macro Sleep Stages Estimation, Audio Signal Processing, Sound Analysis, Sleep Evaluation.**

I. Introduction

Polysomnography (PSG) is the gold standard for sleep evaluation [1]. However, this method requires a full night laboratory stay while subjects are connected to numerous electrodes and sensors. Sleep is scored by a certified technologist who examines dozens of full-night physiological signals. This procedure is time-consuming and costly.

In recent years, extensive efforts have been devoted to seeking alternatives for PSG evaluation. These technologies [2, 3] typically rely on the assumption that movement is associated with wakefulness phase and vice versa. Some approaches evaluate sleep using heart rate variability [4] and even using peripheral arterial tone signals [5]. The most popular method for at home sleep evaluation is wristwatch actigraphy [6, 7]. However, this method estimates a binary decision about sleep and wake patterns and cannot monitor REM. In a previous study [8] we showed that binary decision of sleep and wake phases can be reliably determined using only breathing sound analysis. Nevertheless, we showed matched and even superior performances compared to actigraphy-based technologies.

Our working hypothesis is that there are differences in sound properties within each MSS enabling separation between them. Some properties differences are respiratory-related sounds due to alternation of upper airways patency during each MSS, and some involve sounds of body movements in bed.

In order to evaluate sleep and its disorders, it is necessary to determine sleep quality parameters [9] such as: 1) *total sleep time* (TST) – the overall duration of sleep stages, 2) *sleep latency* (SL) – the time span between lying in bed and the start of sleeping, 3) *sleep efficiency* (SE) – the ratio between TST and total time in bed, 4) *wake-time after sleep onset* (WASO) – the summation of all awakening episodes during sleep, 5) *awakening index* (AwI) – the average number of awakenings per hour of sleep, 6) REM latency (RL) – the time span between sleep onset and the first REM cycle, and 7) *REM percentage* (RP) – the ratio between REM duration and TST.

To the best of our knowledge, there is no technology available to estimate MSS pattern using a non-contact inexpensive sensor. This study describes a pioneering attempt to estimate MSS using only audio signal analysis recorded by a non-contact microphone and a digital audio recorder.

II. Methods

We prospectively acquired sleep data from 213 patients (>18 years) who were scheduled for routine PSG study at the sleep-wake disorder unit at Soroka University Medical Center. Thirty-five of them were simultaneously recorded with a digital audio recorder device (EDIROL R-4) and an ambient microphone (RØDE NTG-1). The microphone was attached to the ceiling and hung about one meter above the subject's head. Subjects' characteristics are summarized in Table I. Audio signals were recorded at a sampling frequency of 16 kHz, 16 bits per sample, PCM and stored with the PSG sleep manual scoring by a certified technologist [1]. The raw audio signal was then processed off-line using the proposed system, which is shown in Figure I.

TABLE I. Patient Characteristics.

Parameter	Design (HMM)	Design (ANN)	Validation (ANN+HMM)
# of Patients	178	15	20
Male/Female	108/70	10/5	13/7
Age (years)	55±15 19–87	49±13 25–66	53±14 23–70
BMI (kg/m2)	32±6 20-58	29±6 23-45	35±5 25–45
AHI (events/hr)	21±18 0–88	17±10 2–34	20±13 5–52
# of Epochs	866±55 560–987	920±62 782–1007	870±75 720–1025

BMI – Body mass index, AHI – Apnea and hypopnea index. Values are mean ± SD, and range min–max.

*This work was supported in part by the Israel Science Foundation, number 1403/15.

E. Dafna, M. Halevi, and D. Ben Or are with the Department of Biomedical Engineering, Ben-Gurion University of the Negev, Beer–Sheva, Israel (corresponding author, e-mail: elirand@post.bgu.ac.il).

A. Tarasiuk is with the Sleep-Wake Disorders Unit, Soroka University Medical Center, and Department of Physiology, Faculty of Health Sciences, Ben-Gurion University of the Negev, Israel (tarasiuk@bgu.ac.il).

Y. Zigel is with the Department of Biomedical Engineering, Ben-Gurion University of the Negev, Beer–Sheva, Israel (yaniv@bgu.ac.il).

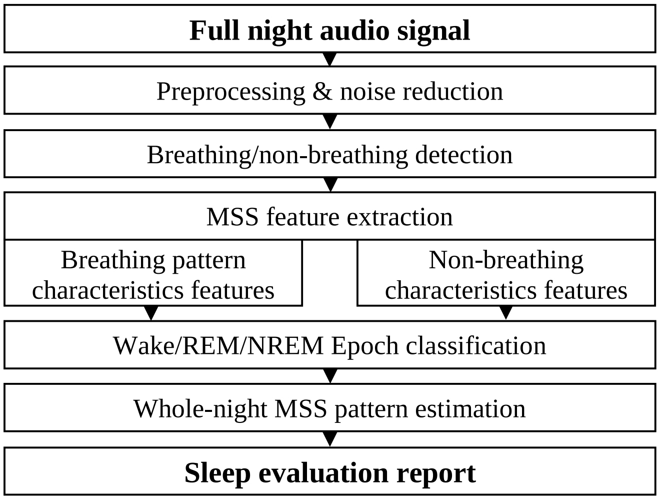

Figure I: Block diagram of the system.

A. *Preprocessing & noise reduction*

The raw whole-night audio signal is enhanced (signal-to-noise manner) by an adaptive noise reduction algorithm based on a spectral subtraction approach [10]. This step is crucial since it reduces the background noise, which is subject-independent, and emphasizes the transient events that were recorded during sleep such as quiet breaths and body movements.

B. *Breathing/non-breathing detection*

Recently, we have developed a breathing detection system [10, 11] that is capable of detecting very low energy audio events and distinguishing between breathing and non-breathing episodes. Non-breathing events may be categorized into three categories: 1) vocally self-generated sounds such as talking, coughing, moaning, and mumbling; 2) body movement sounds such as linen, pillow, and clothes rubbing and twitching; and 3) third party sounds such as door slams, cars, dogs, TV, etc. The output of the detector is the exact time location of each audio event captured. An overall accuracy of 95% was reported for breathing detection and 98% for non-breathing detection; sensitivity of capturing quiet audio events as low as 20dB was reported.

C. *Macro-sleep stages feature extraction*

Once the whole night audio signal is enhanced, the signal is divided into 30s intervals (epochs) across the night. From each epoch, nine features are extracted designed to discriminate between the three classes of MSS: Wake, REM, and NREM. These features can be categorized into two types: breathing characteristics and noise characteristics. We applied the breathing detector described in section II.B to effectively detect the events of interests.

Breathing characteristics features – Six breathing-related features were empirically designed in order to test our hypotheses regarding the differences in MSS.

1) Respiratory cycle duty – this feature measures the time proportion of breathing effort relative to the respiratory cycle duration. *2) Respiratory cycle period* [8] – this feature measures the average respiratory cycle duration based on autocorrelation approach. *3) Respiratory cycle intensity* [8] feature is determined by the value of the autocorrelation first peak. *4) Respiratory cycle consistency* [8] – measures the homogeneity of the respiratory cycles. *5) Respiratory mean SNR* feature – measures the average signal-to-noise ratio (dB scale) of all respiratory events detection. 6) *Respiratory Frequency centroid* – is the average frequency centroid of all breathing detected.

Non-breathing characteristics features – The hypothesis is that body movement is associated with wakefulness, i.e., the same assumption used in actigraphy devices. Moreover, REM is characterized by a paralyzed-limbs phenomenon, which prevents the patient from harming himself during dreaming; therefore, we hypothesize that REM epochs will contain fewer body movements. Three non-breathing-related features were empirically developed:

1) Non-breathing percentage feature is calculated as the ratio between all non-breathing detected durations combined relative to the 30s epoch duration. *2) Non-breathing 90% SNR* feature represents the SNR value of the 10% upper percentile of all non-breathing detected. *3) Non-breathing frequency centroid* feature is calculated in the same way as for the breathing frequency centroid.

D. *Epoch's Wake/REM/NREM classification*

In this study, we used an artificial neural network (ANN) classifier [12] with 9D inputs that projects the decision into a 3D score (3 states). Each dimension in the output represents a likelihood score for a specific class (Wake/REM/NREM). We configured a 'feed-forward' neural network architecture with two hidden layers composed of 50 and 20 hyperbolic tangent sigmoid neurons, respectively, followed by a 'softmax' transfer function for the output layer. The output of the classifier, $\mathbf{p}(\mathbf{x})$, can be written as:

$$\mathbf{p}(\mathbf{x}) = \mathbf{f}^3\left(\mathbf{W}^3\mathbf{f}^2\left(\mathbf{W}^2\mathbf{f}^1\left(\mathbf{W}^1\mathbf{x}+\mathbf{b}^1\right)+\mathbf{b}^2\right)+\mathbf{b}^3\right), \quad (1)$$

where $\mathbf{p}$ is a 3-class score; $\mathbf{x}$ is the input vector, i.e., feature set; $\mathbf{f}^{\mathbf{i}}$ is the i^{th} transfer function, with its corresponding weights $\mathbf{W}^{\mathbf{i}}$**;** and bias values $\mathbf{b}^{\mathbf{i}}$. For classifier illustration see Figure II.A; more details about ANN can be found in [12].

E. *Whole-night macro-sleep stages pattern estimation*

Once each epoch is represented by three scores (wake, REM, and NREM), a time series model is applied. The purpose of this model is to insert additional knowledge that estimates a more realistic sleep pattern sequence. We used three-state time-dependent hidden Markov model (HMM) [12] as shown in Figure II.B. In our configuration, the transition probability between each state varies along time, i.e., across the night. For example, one would expect that at the beginning, transitions will pull toward wakefulness, while in the middle of the night toward REM and NREM. The probability for a given epoch n to be classified into each of the three states can be calculated using the following equation:

$$\mathbf{s}^{n+1} = \mathbf{T}^n \times \mathbf{p}^{n+1}, \quad (2)$$

where $\mathbf{s}^{n+1}$ is the 3×1 estimated state vector probabilities of a given epoch n+1. $\mathbf{T}^n$ is a 3×3 transition matrix at a given epoch n, and $\mathbf{p}^{n+1}$ is the 3×1 state probabilities vector of an epoch n+1 estimated by the ANN classifier, i.e., determined by the acoustic features. For a given states sequence (s_1,s_2,…,s_N) ∈ {Wake,REM,NREM}, the probability value can be calculated using (3).

$$\Pr\left(\mathbf{s}^1 = s_1, \mathbf{s}^2 = s_2, \ldots, \mathbf{s}^N = s_N\right) = \prod_{n=1}^{N}\left(\mathbf{s}^n = s_n\right), \quad (3)$$

Please note that three classes across N epochs will yield 3^N possible state sequences. The most probable state sequence will be represented by the maximum Pr score. We applied the Viterbi algorithm [12] to find the maximum Pr score efficiently. Figure II.C shows the probability of each MSS state during the night calculated at the training phase, Section II.G. Please note that these curves were generated solely by state transition probabilities and regardless of the epoch's score, hence presenting the global states probability.

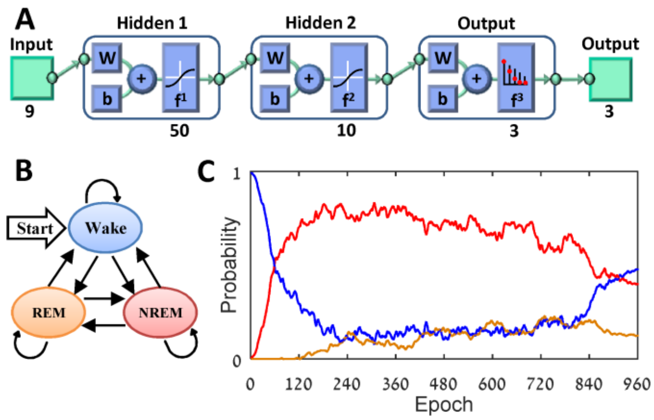

Figure II: Macro-sleep stages classifiers. Panel A shows the feed-forward neural network configuration. Panel B shows the three-state HMM. Panel C shows the probability of each state across the night (blue is wake, orange is REM, and red is NREM).

F. *Sleep evaluation report*

Once a whole-night MSS hypnogram is estimated, it is possible to generate a clinical sleep evaluation report. We chose to assess seven sleep parameters as described in the introduction section: TST, SL, SE, WASO, AwI, RL, RP.

G. *System training and validation*

System development is composed of two phases: a training phase and validation phase.

Training phase – Our proposed system is developed using a supervised learning approach, meaning we trained the classifiers using manually annotated sleeping scores. The sleeping annotations involve three MSS (Wake, REM, and NREM) across the night determined by a sleep expert following the standard scoring rules [1].

The ANN classifier training process was conducted on the annotated sleep-scoring of 15 subjects as shown Table I. The input for this classifier is the same 9D audio-based feature vector described in Section II.C.

For the time-series HMM, we estimated the state transition matrix (probabilities) for the MSS patterns based on the annotated sleep scores of 178 subjects, listed in Table I. These transitions are time dependent and were estimated for each state and for each time index (epoch) across the night.

Validation phase – For the validation phase, we estimated the MSS patterns of 20 subjects, and respectively compared to the manually annotated MSS (Shown in Table I). The most probable MSS sequence for a subject was estimated using the Viterbi algorithm [12].

H. *System performance evaluation*

For each subject from the validation dataset (Table I), we compared epoch-by-epoch between the manually annotated PSG sleep scoring against the automated audio-based analysis (ABA) sleep scoring. Two agreement measurements were calculated, simple accuracy and Cohen's kappa [13]. Moreover, we compared these parameters calculated from PSG and from the audio-based-analysis (ABA) approach using mean difference (subtraction), mean error (absolute difference), and two-tail paired t-test.

III. Results

This study was performed on the database summarized in Table I. For each subject, we compared epoch-by-epoch MSS between ABA and the PSG annotated sleep stages. The comparison was measured using simple agreement and using Cohen's kappa (Figure III). We also tested the contribution of the time-series model (HMM), presented as filled bars (Figure III). For the ANN model, the accuracy was 0.63±0.10 and kappa of 0.32±0.12. After applying the HMM, the performance was increased to 0.75±0.09 and 0.42±0.17. A confusion matrix is shown in Table II.

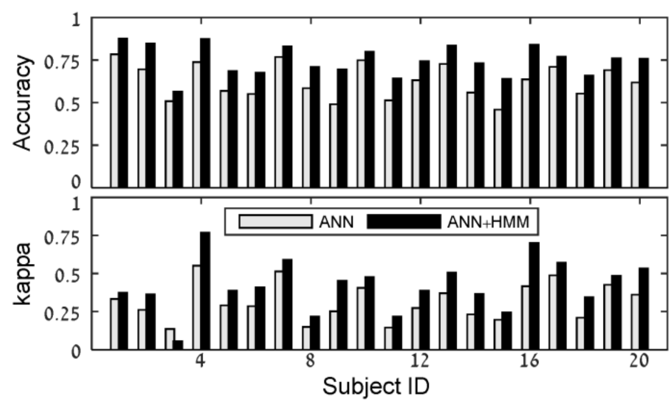

Figure III: Epoch detection performance. Upper panel – Subject epochs accuracy. Lower panel – Subject's epochs Cohen's kappa agreement. White bars represent epochs agreements based on ANN classification alone, and black bars represent the agreements after HMM procedure.

TABLE II. Classifiers confusion matrix.

		ANN Estimation			HMM Estimation		
		W	R	N	W	R	N
PSG annotation	W	66%	15%	19%	69%	5%	26%
	R	8%	64%	28%	5%	54%	41%
	N	12%	26%	62%	10%	11%	79%

W – Wake, R – REM sleep, and N – NREM sleep. States a priori probability is 14%, 12%, and 74% for Wake, REM, and NREM, respectively.

Figure IV presents a typical example of MSS estimation for a subject (ID #7 from Figure III).

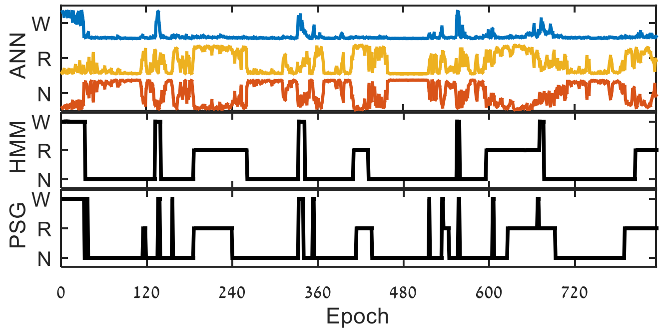

Figure IV: Typical example of MSS estimation. Upper panel presents the three classes MSS scores (probabilities) estimated by the ANN classifier (scores are summed to one). Center panel presents the HMM's most probable MSS sequence. Lower panel presents the PSG annotation. W–Wake, R–REM, N–NREM. Subject ID is #7 from Figure 3: Male, age=44, BMI=28, AHI=11. This example exhibits an accuracy rate of 83% and kappa of 0.58.

Once MSS is estimated across the night, sleep quality parameters can be calculated. Table III shows the mean and SD values of the estimated sleep quality parameters for the validation study.

TABLE III. SLEEP PARAMETERS FOR THE VALIDATION DATASET.

Param.	PSG	ABA	ABA-PSG	Error	*p*
TST (min)	374±38 274–426	358±48 295–435	-16±47 -115–78	36±34 3–115	.26
SL (min)	29±28 1–108	33±29 1–92	4±27 -33–80	17±21 0–80	.70
SE (%)	92±5 81–98	91±7 73–100	-1±7 -20–14	5±5 0–20	.62
WASO (min)	30±17 9–66	33±29 0–114	3±28 -46–86	20±19 1–86	.69
AwI (#/hr)	2.6±1.1 0.6–5.7	0.6±0.3 0.0–1.2	-2.0±1.2 -5.3–-0.2	2.0±1.2 0.2–5.3	.00
RL (min)	185±85 42–336	133±63 32–253	-45±96 -271–83	77±71 2–271	.04
RP (%)	13±6 4–25	17±8 0–27	4±8 -9–20	7±5 0–20	.09

TST – total sleep time, SL – sleep latency, SE – sleep efficiency, WASO – wake-time after sleep onset, AwI – awakening index, RL – REM latency, RP – REM percentage. Values are mean ± SD and range min–max. ABA – audio-based analysis, PSG – the gold standard polysomnography. Error defined as the absolute difference, and *p* represents the p-value of two-tail, paired t-test comparison. These analyses were based on 20 subjects from the validation dataset.

When analyzing sleep parameters agreements, only AwI and RL (two out of seven) sleep parameters were ruled out due to a significant difference ($\alpha<0.05$).

IV. DISCUSSION AND CONCLUSION

We proposed a pioneering attempt to estimate MSS and sleep quality parameters using audio signal analysis acquired by an ambient microphone. To the best of our knowledge, this study is the first to show that non-contact technology can reliably estimate MSS. Some of the current sleep trackers [6-9] are able to estimate binary sleep or wake phases; however, they cannot monitor REM sleep. Watch-PAT [5] is a wearable device that measures MSS via actigraphy and peripheral arterial tone signals. It has a detection rate of 76%, 81%, and 73% compared to our 69%, 54%, and 79% for detecting wake, REM, and NREM, respectively.

Table III shows that TST, SL, SE, WASO, and RP can reliably be estimated using ABA. However, AwI and RL estimations exhibit considerable deviations from PSG findings. We hypothesized that the estimated AwI was lower in the ABA system due to the HMM states' "prolonging" properties. This might be addressed with a proper post-algorithm that searches awakening episodes among the sleep stages. The system was validated on clinical cases in which patients are referred to a sleep study. Patients slept alone in a relatively quiet room, making a favorable SNR. In future work we are planning to expand our database and to record subjects in at-home conditions, where SNR is more challenging.

The demand for accessible sleep diagnosis and simple/easy to use PSG alternative is high. The performances of the system are very encouraging and could serve as a screening tool for MSS estimation using a simple single-channel, non-contact audio technology.

ACKNOWLEDGMENT

We would like to thank Mrs. Bruria Freidman from the Sleep-Wake Disorder Unit of Soroka University Medical Center, for her support and collaboration.

REFERENCES

[1] C. Iber, S. Ancoli-Israel, C. A. L., and S. Quan, *The AASM Manual for the Scoring of Sleep and Associated Events: Rules, Terminology, and Tech-nical Specifications*, 1 ed. Westchester, IL: The American Academy of Sleep Medicine, 2007.

[2] C. Berthomier, X. Drouot, M. Herman-Stoïca, P. Berthomier, J. Prado, D. Bokar-Thire, *et al.*, "Automatic analysis of single-channel sleep EEG: validation in healthy individuals," *Sleep,* vol. 30, p. 1587, 2007.

[3] D. Sommermeyer, M. Schwaibold, B. Schöller, L. Grote, J. Hedner, and A. Bolz, "Detection of sleep disorders by a modified Matching Pursuit algorithm," in *World Congress on Medical Physics and Biomedical Engineering, September 7-12, 2009, Munich, Germany*, 2010, pp. 1271-1274.

[4] T. Fukuda, Y. Wakuda, Y. Hasegawa, F. Arai, M. Kawaguchi, and A. Noda, "Sleep Quality Estimation based on Chaos Analysis for Heart Rate Variability," *IEEJ Transactions on Electronics, Information and Systems,* vol. 125, pp. 43-49, 2005.

[5] S. Herscovici, A. Pe'er, S. Papyan, and P. Lavie, "Detecting REM sleep from the finger: an automatic REM sleep algorithm based on peripheral arterial tone (PAT) and actigraphy," *Physiological measurement,* vol. 28, p. 129, 2006.

[6] J. Hedner, G. Pillar, S. D. Pittman, D. Zou, L. Grote, and D. P. White, "A novel adaptive wrist actigraphy algorithm for sleep-wake assessment in sleep apnea patients," *Sleep,* vol. 27, pp. 1560-1566, 2004.

[7] A. Sadeh and C. Acebo, "The role of actigraphy in sleep medicine," *Sleep medicine reviews,* vol. 6, pp. 113-124, 2002.

[8] E. Dafna, A. Tarasiuk, and Y. Zigel, "Sleep-Wake Evaluation from Whole-Night Non-Contact Audio Recordings of Breathing Sounds," *PloS one,* vol. 10, p. e0117382, 2015.

[9] T. Blackwell, S. Redline, S. Ancoli-Israel, J. L. Schneider, S. Surovec, N. L. Johnson, *et al.*, "Comparison of sleep parameters from actigraphy and polysomnography in older women: the SOF study," *SLEEP-NEW YORK THEN WESTCHESTER-,* vol. 31, p. 283, 2008.

[10] E. Dafna, A. Tarasiuk, and Y. Zigel, "Automatic Detection of Whole Night Snoring Events Using Non-Contact Microphone," *PLoS One,* vol. 8, p. e84139, 2013.

[11] T. Rosenwein, E. Dafna, A. Tarasiuk, and Y. Zigel, "Detection of breathing sounds during sleep using non-contact audio recordings," *Conf Proc IEEE Eng Med Biol Soc.,* 2014.

[12] Y. Anzai, *Pattern Recognition & Machine Learning*: Elsevier, 2012.

[13] J. Cohen, "Weighted kappa: Nominal scale agreement provision for scaled disagreement or partial credit," *Psychological bulletin,* vol. 70, p. 213, 1968.

Supplementary information for paper 1

Automatic detection of whole night snoring events using non-contact microphone.

Dafna Eliran, Tarasiuk Ariel, and Zigel Yaniv.

PloS one 8.12 (2013): e84139.

On line METHODS supplement

Automatic Detection of Whole Night Snoring Events Using Non-Contact Microphone

Eliran Dafna, Ariel Tarasiuk, Yaniv Zigel

ONLINE METHODS SUPPLEMENT

Study Protocol

A system-design study was performed in which a system for automatic detection of whole night snoring events was developed (Fig. 1 in the main text). The preprocessing step included noise reduction based on spectral subtraction in order to enhance the audio signal and improve the robustness of the system. Distinguishing snore and non-snore events was performed using ad hoc acoustic features that were developed and collected for this purpose. Thirty-four features were chosen using a feature selection technique that was designed to extract the most discriminative features, while removing those that were irrelevant. The chosen features were fed into an AdaBoost Classifier to produce a single snore-likelihood score using an individual score threshold, and the accuracy rate of performance was improved.

Presented here is supplemental technical information regarding the snore detection process.

Preprocessing (Adaptive noise suppression)

Each audio signal underwent an adaptive noise suppression (spectral subtraction) process based on the Wiener-filter. This process relies on automatically tracking background noise segments in order to estimate their spectra and subtracts them from the audio signal [E1].

First, the audio signal was divided into 40 ms frames (50% overlapping). For each frame, frequency components were calculated using a discrete Fourier transform (DFT) technique. The suppression was done by suppressing each frequency's magnitude, while leaving its phase unchanged according to the noise spectral template.

This template was initially estimated from the lowest energy frame of the first 10 sec of the audio signal and was updated during the adaptive noise suppression process.

Updating the template occurs when one of two conditions is met: 1) the current processed frame is assumed to be a background noise candidate, or 2) no background noise candidates were found in the previous 10 sec.

Adaptation was calculated using weighted averaging of 10% from the new noise candidate and 90% from the old noise spectral template. When no noise candidate is found, it is forced to find a noise candidate (the minimal frame energy) in the last 10 seconds.

The frequency suppression factor $G(k)$ was determined using an estimation of *a priori* SNR of the processed frame at time index t and limited to the range [0, -25dB] in order to prevent a major distortion when low SNR was present. See Eq. (S1)

$$G^t(k) = \max\left(\frac{SNR^t_{prio}(k)}{SNR^t_{prio}(k)+1}, -25dB \right) \tag{S1}$$

where $G(k)$ is the suppression factor corresponding to the k^{th} frequency component, t represents the frame index at time t, $SNR_{prio}(k)$ is the *a priori SNR* of the k^{th} frequency component, and N_k represents the template components of the noise frequencies.

Defining local *a posteriori* and *a priori* SNRs by Eq. (S2) and Eq. (S3), respectively:

$$SNR^t_{post}(k) \triangleq \frac{\left|X^t_k\right|^2}{\left|N_k\right|^2} \tag{S2}$$

$$SNR^t_{prio}(k) \triangleq \frac{\left|X^t_k - N_k\right|^2}{\left|N_k\right|^2} = SNR^t_{post}(k) - 1. \tag{S3}$$

The right side of equation S3 is achieved due to the uncorrelated assumption between desired signal and noise. In this study, we modified and smoothed the *a priori* SNR using a weighted parameter α with the previous estimated *a priori* SNR, as presented in Eq. (S4):

$$SNR^t_{prio}(k) = (1-\alpha) \times \max\left(SNR^t_{prio}, 0\right) + \alpha \times \left|G^{t-1}(k)\right|^2 \times SNR^{t-1}_{prio}(k) \tag{S4}$$

where the max argument was designed to constrict the prior SNR to be positive, and α was chosen arbitrarily to be equal to 0.99 in order to refine the changes. After applying the suppression to the frames' magnitude frequencies ($\tilde{X}^t_k = X^t_k \times G^t(k)$), reconstruction of the signal was performed using the modified frequencies' magnitude and the corresponding unchanged phases.

Event detection and segmentation

In this study, we developed an event detection module for the purpose of detecting any acoustic/energetic event that could be a snore candidate according to its energy threshold and event duration rule. Moreover, the module was designed to achieve high sensitivity for detecting any energetic event including very low intensity snores.

Figure S1 presents the block diagram of the event detector module.

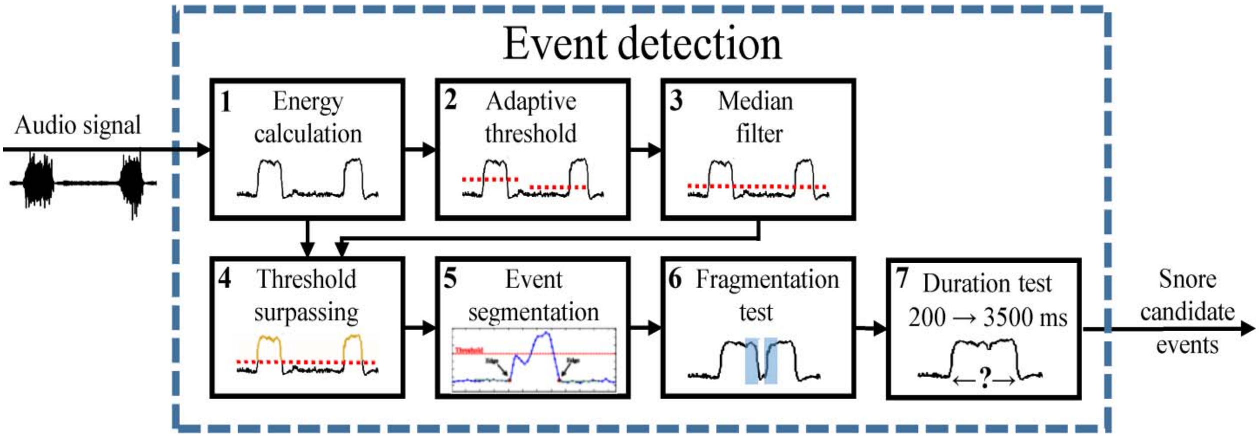

Figure S1 – Block diagram of the event detection module.

Block 1: The full-night audio signal was divided into one-minute sections. For every section, an energy vector was calculated using energy frames (frame size: 60 ms and 75% overlap).

Block 2: A section-related energy threshold (adaptive threshold) e_{th} was calculated using a histogram of the energy vector $hist_{energy}(e)$. Since the prevalence of stationary background noise frames was greater relative to the audio events (snore/non-snore), the energy value that is related to the peak of the histogram e_{max} was located in the low energy scale:

$$e_{max} = \arg\max_{e} \left\{ hist_{energy}(e) \right\}. \tag{S5}$$

The energy threshold ($e_{th} > e_{max}$) was set to the energy value corresponding to one-tenth of the peak amplitude:

$$hist_{energy}(e_{th}) = 0.1 \times hist_{energy}(e_{max}) \, . \tag{S6}$$

See the example in Fig. S2B.

Block 3: A five-order median filter was applied to the whole-night threshold values (vector) to smooth outliers.

Block 4: Applying the thresholds to the corresponding energy signal sections, suspected events are emerging, leading to starting and ending points of each suspected event.

Block 5: *Event segmentation* – In order to find the exact event boundaries (edges), the time edges of each audio event were calculated using an estimated slope technique. An illustration of the segmentation process is shown in Fig. 2 (in the main text). This process included the estimation of a slope from ten consecutive energy frames (150 ms window) – a linear regression fitting line was calculated from the consecutive energy frames in order to estimate its slope. This process was repeated and progressed outside the event boundaries one frame at a time as long as the slope did not change its sign.

Block 6: *Fragmentation test* – In case the detected audio events are too close to each other (< 200 ms), they were suspected to be one fragmented event (such as split snores). This fragmentation test involved a spectral similarity measure for the 100 ms adjacent windows of these events (the ending part from the first event and the initiating part from the following one). In case of similarity, the events were merged to form a single event.

Block 7: *Event duration test* – Only 200 ms to 3500 ms events were used in this study since we noticed that the duration of >99% of the manually labeled events fell in this range. Fig. 3 (in the main text) shows snore statistics based on the manual labeling of snoring events.

Figure S2 presents key steps in the event detection process. Panel A represents the energy signal associated with a one-minute segment. Panel B represents the corresponding histogram of the energy signal. Panel C represents the surpassed energy signal using the filtered threshold. Note that this panel is prior to event segmentation, fragmentation, and duration tests. Panel D represents a section within Panel C after all the tests and rules were applied, i.e., the final outcome.

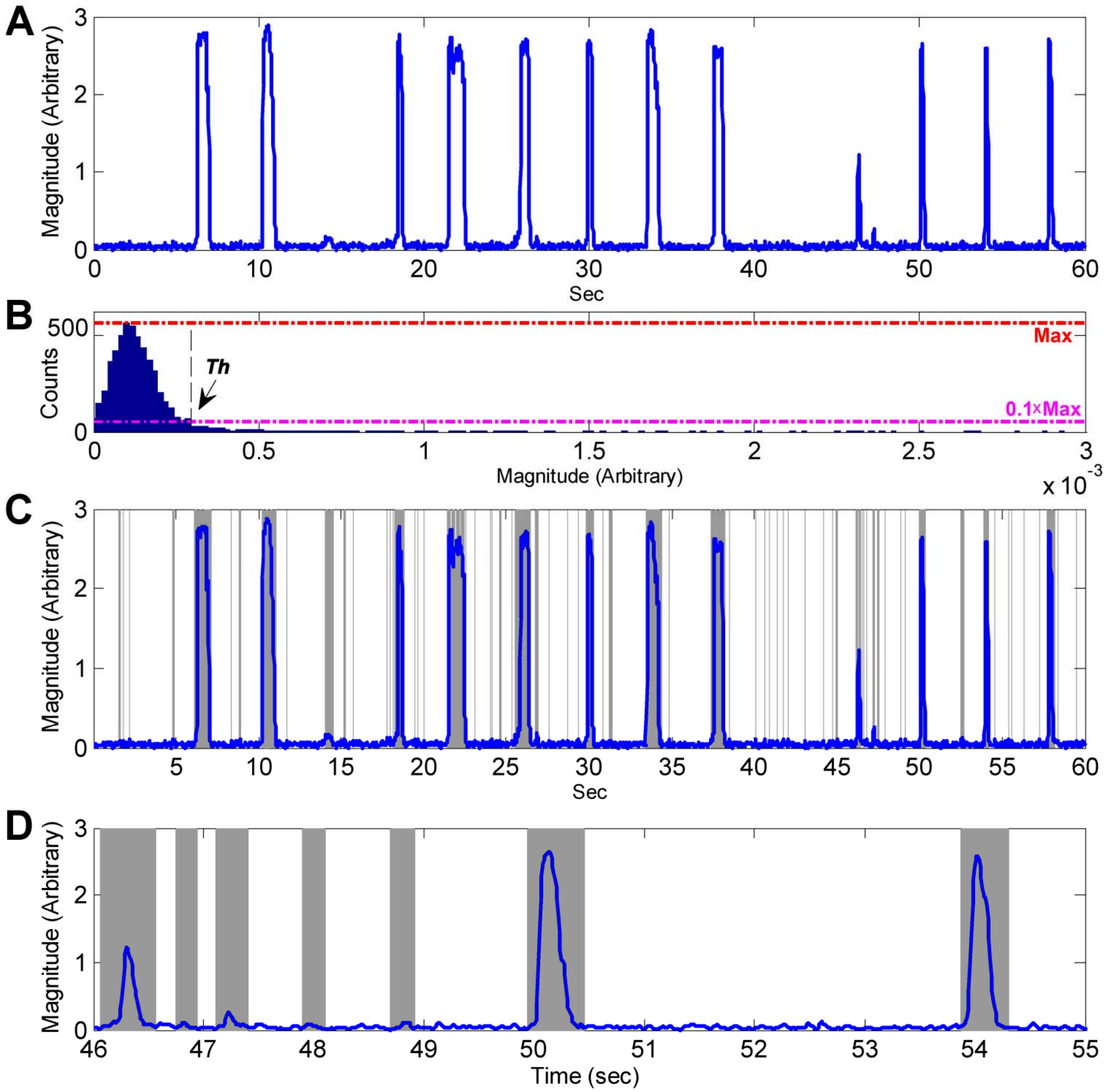

Figure S2 – Example of key steps in the event detection process. A) Energy calculation of a one-minute segment. B) The corresponding energy value histogram. The threshold was calculated according to Eq. (S6). C) The surpassed signal according to the filtered threshold. The grey background represents the event boundaries. Note that at this stage there was very high false alarm detection. D) The final detection output with zoom in at the corresponding C panel. Note that the remaining events surpassed every test and rule.

In order to validate our event detection module, we arbitrarily analyzed a total of four hours and ten minutes of recordings taken from 25 subjects (10 minutes from the middle of the recording for each subject from the design set).

The analysis process included manually marking each detectable audio event. The events were detected by listening and visually observing the energy and spectrogram of each suspected signal section. In total, we manually marked 3429 events, 137±66 per subject.

We automatically detected 592±171 snores per subject, resulting in *TP*=100% (positive detection) of manually detected events and with positive predictive value *(PPV)* of 23.1%, (×4 more false alarms).

Agreement between scorers

Manual labeling of audio events was an essential step for designing and evaluating the snore detection algorithm. Therefore, an *ad hoc* graphical user interface (GUI) for manual event classification based on visual and acoustic perception of the event itself and its surrounding context was designed, and research assistants (scorers) were rigorously and uniformly trained (see main text). We used Cohen's kappa coefficient [E2] to estimate the agreement between the three scorers. The following confusion matrices (CM) between each pair of the three scorers were obtained:

$$CM_{1,2}=\begin{pmatrix}0.9955 & 0.0045\\ 0.0173 & 0.9827\end{pmatrix},\quad CM_{1,3}=\begin{pmatrix}0.9986 & 0.0014\\ 0.0156 & 0.9844\end{pmatrix},\quad CM_{2,3}=\begin{pmatrix}0.9965 & 0.0035\\ 0.0209 & 0.9791\end{pmatrix}.$$

Very high agreement κ_{12}=97.4%, κ_{13}=97.9%, and κ_{23}=97.0% corresponding to that between scorers 1 and 2, scorers 1 and 3, and scorers 2 and 3, respectively, was achieved.

Feature extraction

Table S1 summarizes all the features that were extracted based on time and spectra-related domain.

Table S1. Features pool.

Feature	Symbol*	Count
I. Time related (Inter- & Intra-events)	T	**25**
a) Periodicity features (Inter-events)	$Ta_\bullet$ *	**10**
1. Rhythm period (±6 sec)	Ta_1	1
2. Rhythm period (±12 sec)	Ta_2 τ_p	1
3. Rhythm intensity (±6 sec)	Ta_3	1
4. Rhythm intensity (±12 sec)	Ta_4 R_I	1
5. Relative energy prior to event	Ta_5 E_P	1
6. 10 sec after (event's normalized area)	Ta_6	1
7. 10 sec area differences	Ta_7	1
8. 10 sec area division	Ta_8	1
9. 10 sec before & after period ratio	Ta_9	1
10. 10 sec before & after correlation	Ta_{10}	1
b) Duration and sample scattering (Intra-events)	$Tb_\bullet$	**4**
1. Duration	Tb_1	1
2. Duration trimmed (95%)	Tb_2	1
3. ZCR	Tb_3	1
4. Entropy	Tb_4	1
c) Energy (Intra-events)	$Tc_\bullet$	**11**
1. Intensity (dB)	Tc_1	1
2. SNR (dB)	Tc_2	1
3. Total area beneath energy envelop	Tc_3	1
4. Normalized area beneath energy envelop	Tc_4	1
5. Volume density rate (VDR)	Tc_5	1
6. Ratio of areas before & after the peak	Tc_6	1
7. Skewness of amplitudes	Tc_7	1
8. Skewness of envelop formation	Tc_8	1
9. Kurtosis of amplitudes	Tc_9	1
10. Kurtosis of envelop formation	Tc_{10}	1
11. Slope to 1st peak	Tc_{11}	1

Feature	Symbol	Count
II. Spectra-related (Intra-events)	S	**102**
a) Spectra models	$Sa_\bullet$	**68**
1. 20-MFCC (model coefficients)	$Sa_{1\#1:20}$	20
2. 20-LPC (model coefficients)	$Sa_{2\#1:20}$	20
3. 8-subband-frequency distribution	$Sa_{3\#1:8}$	8
4. MFCC (4 moments of coefficients)	$Sa_{4\#1:4}$	4
5. LPC (4 moments of coefficients)	$Sa_{5\#1:4}$	4
6. LP residuals (4 moments of residuals)	$Sa_{6\#1:4}$	4
7. DFT (4 moments of freq. distribution)	$Sa_{7\#7:4}$	4
8. DFT (4 moments of amp. distribution)	$Sa_{8\#1:4}$	4
b) Bio-characteristic frequency	$Sb_\bullet$	**10**
1. 3-first formants (frequency)	$Sb_{1\#1:3}$	3
2. 3-first formants (magnitude)	$Sb_{2\#1:3}$	3
3. F3-F1 (difference in frequency)	Sb_3	1
4. Pitch	Sb_4	1
5. Pitch intensity	Sb_5	1
6. Pitch density	Sb_6	1
c) Dynamic frequency	$Sc_\bullet$	**24**
1. Δ-MFCC	$Sc_{1\#1:20}$	20
2. Dynamic MFCC	Sc_2	1
3. Spectra flux	Sc_3	1
4. Centroid movement	Sc_4	1
5. MelCepstability	Sc_5	1

* The simplified symbols used in the paper body.

For convenience, the code name for each feature is composed from 3 symbols in its form: Xy_{num}, where "X" represents the domain {T=Time, S=Spectra}, "y" represents the domain subgroup {a,b,c}, and "$_{num}$" represents the index within subgroup y. For example, the code name for Pitch is Sb_4, and for the 10th MFCC coefficient, it is $Sa_{1\#10}$.

Time-domain set

Twenty-five features were included in this domain, categorized into three groups: a) Periodicity features, b) Duration and sample scattering, and c) Energy.

a) **Periodicity features** – Periodicity features are inter-event features based on a tested event's surrounding context. In fact, these features are derived from the energy signal corresponding to the interval that is being tested.

   $\boldsymbol{Ta_1}$ and $\boldsymbol{Ta_2}$ are features that measure the period of the rhythm detected in a 12- and 24-second interval, respectively, when the tested event is in the middle. The period was calculated via auto-correlation over the energy signal associated with the tested interval (see Fig. 5 in the main text).

   $\boldsymbol{Ta_3}$ and $\boldsymbol{Ta_4}$ are the corresponding intensities of the detected rhythm of Ta_1 and Ta_2. They were calculated using Eq. (3) in the main text.

   $\boldsymbol{Ta_5}$ and $\boldsymbol{Ta_6}$ are the normalized area (relative to the tested event) preceding and following the event, respectively; basically these features measure the equally existing events prior to or after the event.

   $\boldsymbol{Ta_7}$ and $\boldsymbol{Ta_8}$ are scores calculated over $\boldsymbol{Ta_5}$ and $\boldsymbol{Ta_6}$ simultaneously using subtraction or division of the two.

   $\boldsymbol{Ta_9}$ is the ratio of periods calculated for the 10 sec prior to the event and 10 sec after the event; this feature is essential in detection of apneic snores.

   $\boldsymbol{Ta_{10}}$ is a feature that measures the correlation coefficient between the 10 sec prior to the event and the 10 sec after the event.

b) **Duration and sample scattering –** This sub-group contains four features: two that measure the duration of the tested event and two that measure its sample scattering.

   $\boldsymbol{Tb_1}$ is the duration (in sec) of the entire event (from start to end), while $\boldsymbol{Tb_2}$ is the shortest duration in seconds (within the event) that holds 95% of the event's total energy.

   $\boldsymbol{Tb_3}$ is the zero crossing rate (ZCR) of the event samples. $\boldsymbol{Tb_4}$ is the entropy of the event samples measured as in Eq. (S7):

$$Tb_4 = -\sum_{i=1}^{M} P_i \log(P_i) \quad \text{(S7)}$$

where P_i is the probability of the amplitude to be quantified to bin i out of M=100 bins quants.

c) Energy (Intra-events) is the third sub-group within the time domain features. It contains features calculated regarding both event-based and frame-based energy features.

$\boldsymbol{Tc_1}$ and $\boldsymbol{Tc_2}$ are event-based energy features that measure the event's total intensity and the SNR of the event (both on the dB scale), respectively.

$\boldsymbol{Tc_3,\ldots,Tc_{11}}$ are frame-based energy features that measure parameters regarding the formation of the event's frames.

$\boldsymbol{Tc_3}$ is the total area beneath the event's energy and $\boldsymbol{Tc_4}$ is the normalized area beneath the event's energy, where the rectangle that contains the event is equal to 1.

$\boldsymbol{Tc_5}$ is the volume density rate (VDR). It is similar to the SNR score but calculated as [(max-min)/max] of the energetic frames.

$\boldsymbol{Tc_6}$ is the ratio between the areas located prior to and after the maximum peak location of the energetic frames.

$\boldsymbol{Tc_7}$ is the skewness (3^{rd} moment) of the frame's magnitude distribution.

$\boldsymbol{Tc_8}$ is the skewness (3^{rd} moment) of the frame's formation along time.

$\boldsymbol{Tc_9}$ and $\boldsymbol{Tc_{10}}$ are the same as $\boldsymbol{Tc_7}$ and $\boldsymbol{Tc_8}$ but calculate the kurtosis (4^{th} moment).

$\boldsymbol{Tc_{11}}$ is the slope of the line connecting $E_{t=0}$ and $E_{t=peak}$. The slope is calculated as: $1/(t_{peak}-t_0)$.

Spectral-domain set

One-hundred-and-two features were included in this set, comprising three sub-groups: a) Spectra models, b) Bio-characteristic frequencies, and c) Dynamic frequencies.

a) Spectra models – This category includes coefficients of different spectra models and four moments of the distribution of their coefficients.

DFT_k denotes a 128-coefficient DFT of the event's signal.

Sa$_1$ is the 20th order MFCC model [E3] containing 20 coefficients as 20 individual features.

Sa$_2$ is the 20th order LPC model [E3]. It also contains 20 coefficients as 20 individual features.

Sa$_3$ represents 8 sub-bands of the event's DFT content,

$$S_i = \frac{\sum_{k=8i}^{8i+7} |DFT_k|}{\sum_{k=0}^{127} |DFT_k|} \tag{S8}$$

Sa$_4$ represents the four moments of the MFCC coefficient (**Sa$_{1\#1}$,..., Sa$_{1\#20}$**) distribution.

Sa$_5$ represents the four moments of the LPC coefficient (**Sb$_{1\#1}$,..., Sb$_{1\#20}$**) distribution.

Sa$_6$ represents the four moments of the LP residuals (the residual of the signal when applying the LPC model).

Sa$_7$ represents the four moments of the frequency distribution of the absolute DFT.

Sa$_8$ represents the four moments of magnitude of the absolute DFT distribution.

b) Bio-characteristic frequencies – This category includes features regarding models and parameterization of the human vocal tract presented in the event.

Sb$_1$ are three features that estimate the frequencies of the first three formants.

Sb$_2$ are three features that estimate the amplitude of the corresponding first three formants.

Sb$_3$ is the difference between the third and the first formants.

Sb$_4$ is the detected pitch within the event.

Sb$_5$ is the intensity of the detected pitch (i.e., the periodicity of the event).

Sb$_6$ is the pitch density [E4].

c) Dynamic frequencies – This category includes features that measure and quantify frequency changes through time.

Sc$_1$ are the delta-MFCC [E3]. They represent the first derivative over each coefficient through time (samples).

Sc$_2$ is the dynamic MFCC feature, which measures the MFCC's variance along time Eq.(S9):

$$Sc_2 = \frac{1}{20}\sum_{k=1}^{20} VAR\left[MFCC(\mathrm{k},\mathrm{n})\right]. \tag{S9}$$

Sc_3 is the spectra flux feature; it is measured as Eq. (S10):

$$Sc_3 = \frac{1}{8}\sum_{k=1}^{8}\frac{1}{N}\sum_{n=1}^{N-1}\left[\log\left(\left|DFT_{k,n+1}\right|\right) - \log\left(\left|DFT_{k,n}\right|\right)\right]^2 \tag{S10}$$

where $DFT_{k,n}$ represents the DFT in frequency sub-band k and at the frame index n. N is the total number of frames of the event.

Sc_4 is the frequency's centroid transitions in event, which measures the distance traveled of the frequency center of mass calculated in a mel-scale as shown in Eq. (S11)

$$Sc_4 = \frac{1}{N}\sum_{n=1}^{N-1}\left|MelCenter_{n+1} - MelCenter_n\right| \tag{S11}$$

where $MelCenter_n$ represents the center of mass of the frequencies in mel-scale at frame index n.

Sc_5 is the MelCepstability feature [E4].

Feature selection

Table S2 presents the selected features that discriminate between snore and non-snore events according to the forward feature selection. Note that the contribution of the features to this separability is presented in descending priority order (left to right).

Table S2. Selected features.

#	Symbol	#	Symbol	#	Symbol	#	Symbol
1	Ta_5	10	$Sa_{1\#2}$	19	$Sa_{1\#6}$	28	$Sa_{2\#4}$
2	Ta_4	11	$Sa_{7\#1}$	20	Sc_2	29	$Sa_{4\#1}$
3	$Sb_{1\#1}$	12	$Sa_{1\#13}$	21	$Sa_{1\#16}$	30	$Sa_{3\#4}$
4	Tc_8	13	$Sa_{5\#2}$	22	Sc_3	31	Ta_1
5	Tc_4	14	Ta_2	23	Sb_6	32	Tc_6
6	$Sa_{4\#3}$	15	$Sa_{5\#1}$	24	$Sa_{3\#7}$	33	Sc_4
7	Sc_5	16	Ta_8	25	$Sa_{7\#4}$	34	$Sb_{2\#1}$
8	$Sa_{1\#5}$	17	$Sa_{2\#6}$	26	Sb_5		
9	Tb_4	18	Ta_9	27	$Sa_{1\#11}$		

References

E1. Scalart P (1996) Speech enhancement based on a priori signal to noise estimation. Conf Proc IEEE International Conference on Acoustics, Speech, and Signal Processing 2: 629-632.

E2. Cohen J (1960) A coefficient of agreement for nominal scales. Educational and psychological measurement 20: 37-46.

E3. Deller JR, Hansen JHL, Proakis JL (2000) Discrete-time processing of speech signals. New York: Institute of Electrical and Electronics Engineers Press.

E4. Ben-Israel N, Tarasiuk A, Zigel Y (2012) Obstructive apnea hypopnea index estimation by analysis of nocturnal snoring signals in adults. Sleep 35: 1299-1305C.

Supplementary information for paper 3

Sleep-wake evaluation from whole-night non-contact audio recordings of breathing sounds

Dafna Eliran, Tarasiuk Ariel, and Zigel Yaniv.

PloS one 10.2 (2015): e0117382.

ONLINE SUPPORTING INFORMATION S1 DATASET

Sleep-wake evaluation from whole-night non-contact audio recordings of breathing sounds

Eliran Dafna, Ariel Tarasiuk, Yaniv Zigel

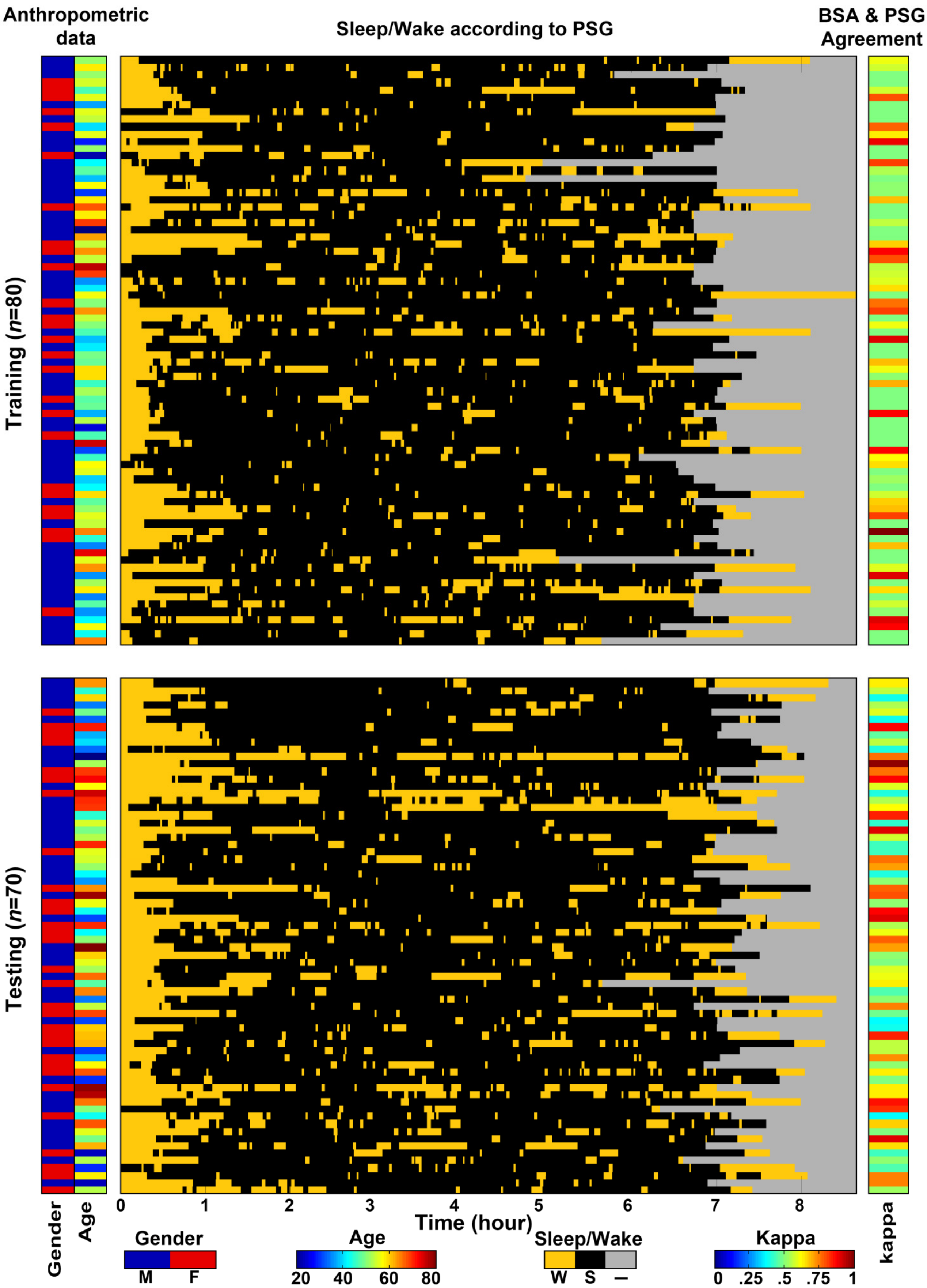

Figure A – Individual big-data visualization for the study design (training, *n*=80) and validation (testing, *n*=70): design dataset – upper panels; validation dataset – lower panels. Each horizontal line represents one individual's data. Sleep/wake activity pattern was manually annotated epoch-by-epoch using polysomnography (PSG) scoring criteria. Note the large individual differences in sleep-wake pattern, especially the sleep latency (from time zero to the first black mark of sleep) and the large individual variability of awakening during sleep (mustard colors between black regions). The onset of the gray area indicates study termination for each individual. Cohen's kappa (epoch-by-epoch sleep/wake) agreement score for each subject was calculated comparing our proposed breathing sound analysis (BSA) system and the PSG scoring. For study protocol, see main body of the manuscript.

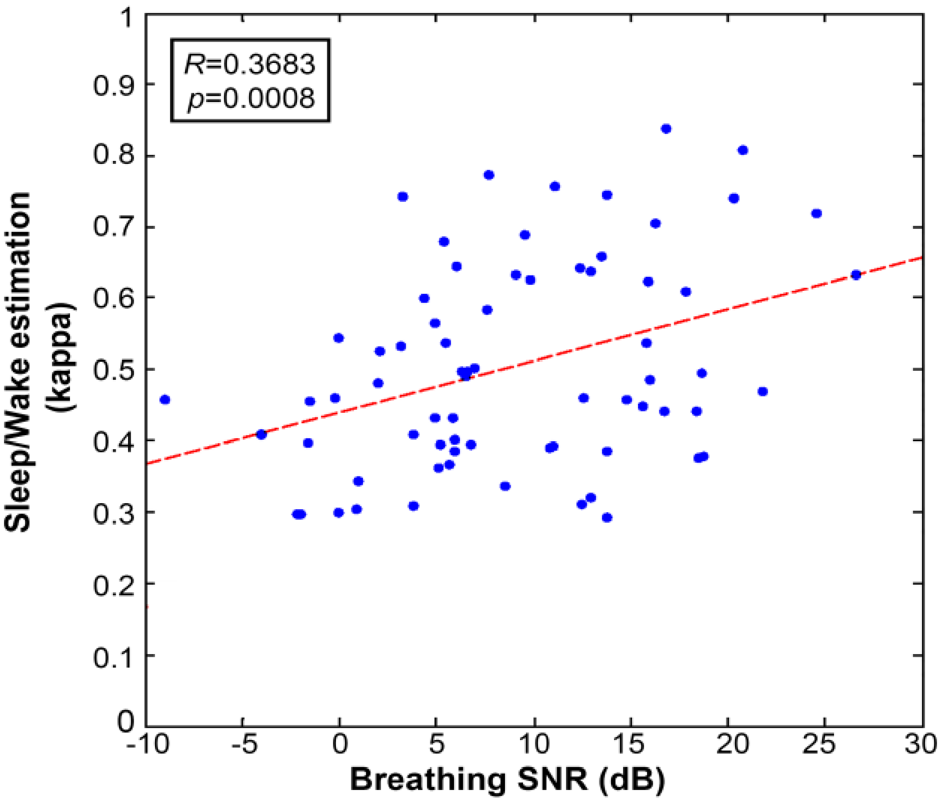

Figure B – The correlation between sleep-wake estimation performances (using kappa score) and subject's breathing sound recording quality (signal to noise ratio, SNR). Each dot represents one individual from the validation (testing) dataset (*n*=70).

תקציר

פוליסומנוגרפיה היא גישת הזהב לשערוך תפקוד השינה והפרעותיה. בדיקה זו מצריכה שהיה של לילה במעבדת שינה, בה מחובר הנבדק למספר רב של חיישנים הבודקים את תפקוד השינה, לב ומערכת הנשימה. פענוח בדיקת השינה מצריך טכנאי ומומחה להפרעות שינה המייקרים את הבדיקה. בשנים האחרונות מושקעים מאמצים לחפש חלופה נוחה וזולה לשערוך שינה והפרעותיה, אשר יגביר הנגישות לאבחנת הפרעות שינה.

השערת המחקר היא שניתן לשערך פעילות של שינה-ערות באמצעות ניתוח אותות שמע מקולות הנשימה. קולות הנשימה מושפעים משינויים בקצב הנשימה ומתנגודת דרכי האוויר העליונות. מטרות המחקר: 1) לפתח אלגוריתם המבוסס על אנליזה של קולות הנשימה אשר יוכל להבדיל בין מצב שינה וערות תוך שימוש בטכנולוגיה ללא מגע. 2) לשערך באופן אמין מדדים לשערוך טיב השינה כגון: זמן שינה כולל, הזמן מרגע שכיבה במיטה ועד להירדמות, יעילות שינה, זמן ערות מתוך הלילה ואינדקס התעוררות לשעה. 3) לבחון ולהשוות את המערכות המוצעת אל מול הבדיקה המקובלת פוליסומנוגרפיה.

במחקר זה השתתפו 150 פציינטים שהופנו למעבדה לחקר הישנה שבמרכז הרפואי-אוניברסיטאי סורוקה. קולות נשימה ליליים הוקלטו במהלך בדיקת שינה שיגרתית בעזרת מיקרופון (RODE NTG1) שהותקן בחדר השינה של הפציינטים.

מחקר זה מציג גישה חלוצית לשערוך תבניות שינה-ערות תוך שימוש באותות שמע שהוקלטו ללא מגע בפציינט. אנו פיתחנו מערכת לזיהוי קולות הנשימה מאות שמע מלילה שלם. מערכת זו אומנה ונבדקה על מאגר מידע גדול במטרה להשיג זיהוי אמין ומדוייק של נשימות. תוך שימוש במאפיינים אקוסטים שחושבו הן במישור הזמן והן במישור התדר, השגנו אחוז דיוק לזיהוי של למעלה מ-98%.

חקרנו את הקשר שבין קולות הנשימה למגוון רחב של מדדים הקשורים במצבי השינה ובנתונים פיזיולוגיים של הנבדקים וזאת במטרה ללמוד את הקשר האמיתי של קולות הנשימה למצבי השינה השונים. מצאנו כי אנליזה של אותות השמע יכולה לספק אבחנה אמינה ומדוייקת של מדדים לאיכות השינה. אחוזי הדיוק לזיהוי שינה-ערות ברזולוציה של 30 שניות הינה 83.3%, עם רגישות של 92.2% (שינה כשינה) וספציפיות של 56.6% (ערות כערות). השוואה של מדדי טיב שינה בין המערכת המוצעת לבין הפוליסומנוגרפיה הראו שגיאות ממוצעות של 16.6 דקות, 35.8 דקות, 29.6 דקות ו-8% עבור זמן ערות עד לשינה, זמן שינה כולל, זמן ערות מרגע הרדמות ויעילות שינה, בהתאמה.

מחקר זה ממחיש את הפוטנציאל הקיים בניתוח קולות נשימה לשערוך שינה לצרכי מחקר וכן לצורך קליני-רפואי.

מילות מפתח: ניתוח אותות שמע, נשימה, שינה, מערכות לומדות, עיבוד אותות.

<u>הערכת שינה והפרעות שינה באמצעות טכנולוגיות ללא מגע</u>

מחקר לשם מילוי חלקי של הדרישות לקבלת תואר "דוקטור לפילוסופיה"

מאת

דפנה אלירן

הוגש לסינאט אוניברסיטת בן גוריון בנגב

תאריך עברי
יא' באדר תשע"ז

תאריך לועזי
09.03.2017

באר שבע

הערכת שינה והפרעות שינה באמצעות טכנולוגיות ללא מגע

מחקר לשם מילוי חלקי של הדרישות לקבלת תואר "דוקטור לפילוסופיה"

מאת

דפנה אלירן

הוגש לסינאט אוניברסיטת בן גוריון בנגב

אישור המנחה המנחה ד"ר יניב ציגל 9.3.2017

אישור דיקן בית הספר ללימודי מחקר מתקדמים ע"ש קרייטמן ____________________

תאריך עברי
יא' באדר תשע"ז

תאריך לועזי
09.03.2017

באר שבע

דף פנימי בעברית

העבודה נעשתה בהדרכת

ד"ר יניב ציגל

במחלקה להנדסה ביורפואית

בפקולטה למדעי ההנדסה

<u>הצהרת תלמיד המחקר עם הגשת עבודת הדוקטור לשיפוט</u>

אני החתום מטה מצהיר/ה בזאת: (אנא סמן):

_**X**_ חיברתי את חיבורי בעצמי, להוציא עזרת ההדרכה שקיבלתי מאת מנחה/ים.

_**X**_ החומר המדעי הנכלל בעבודה זו הינו פרי מחקרי <u>מתקופת היותי תלמיד/ת מחקר</u>.

_**X**_ בעבודה נכלל חומר מחקרי שהוא פרי שיתוף עם אחרים, למעט עזרה טכנית הנהוגה בעבודה ניסיונית. לפי כך מצורפת בזאת הצהרה על תרומתי ותרומת שותפי למחקר, שאושרה על ידם ומוגשת בהסכמתם.

תאריך __**09.03.2017**__ שם התלמיד/ה __**אלירן דפנה**__ חתימה ___________

הצהרה

המאמר העונה לשם "מאפייני קולות נשימות ונחירות במהלך שינה במבוגרים" נכתב על ידי, על ידי עמיתי אסף לברטובסקי מהפקולטה למדעי החיים, אוניברסיטת בן-גוריון בנגב, ובעזרת המנחים האקדמים שלנו ד"ר יניב ציגל ופרופ' אריאל טרסיוק.

במאמר זה, הראינו כי בעזרת גלאי נשימות/נחירות, ניתן לבדוק באופן אובייקטיבי את מאפייני קולות הנשימה/נחירה במהלך השינה. בנוסף, חקרנו את השפעת גורמים פיזיולוגים נוספים כגון מגדר, גיל ואינדקס מדד מסת גוף (BMI) על תכונות הנשימה, וכן שינויים בפרמטרים אלו במהלך זמן השינה.

תרומתי במאמר זה: איסוף ואירגון של מאגר שינה/נשימות אשר היה בשימוש במחקר זה. פיתחתי גלאי לקולות נשימה אשר מהווה בסיס לעבודת המחקר (מאמר 1). בעזרת גלאי זה, חילצתי אלפי אירועי נשימות/נחירות ממאות נבדקים. עבור כל אירוע קול נשימתי, חישבתי/תיכננתי מספר מאפייני נשימות על מנת לחקור וללמוד את השפעת פרמטרים פיזיולוגיים שונים על מאפייני קולות הנשימה. כמו כן, הייתי מעורב בניתוח הסטטיסטי של המאגר, עיצוב גרפי של האיורים ובכתיבת המאמר.

תרומת אסף: אירגון מאגר המידע, ניתוח הסטטיסטי של המאגר, עיצוב גרפי של איורים וטבלאות ובכתיבת המאמר.

יניב ציגל ואריאל טרסיוק: בתור המנחים האקדמים שלנו, הם הובילו ותמכו בנו לאורך כל תהליך המחקר. הידע הרב, התובנות והניסיון שלהם ללא ספק שיפרו את השערת המחקר וכן את יעדי המחקר על מנת לקבל תוצאות בעלות משמעותיות סטטיסטית וחדשניות. בנוסף, הם תרומו רבות בכתיבת המאמר.